2018

An Integrated Closed Convergent System for Optimal Extraction of Head-Driven Tidal Energy

Michelle Ann Vieira
University of North Florida, michelleavieira@gmail.com

AN INTEGRATED CLOSED CONVERGENT SYSTEM FOR OPTIMAL EXTRACTION OF HEAD-DRIVEN TIDAL ENERGY

Michelle A. Vieira

B.S Mechanical Engineering UNF, 2003

A thesis submitted in partial fulfillment of the requirements

for the degree of Master of Science with a Major in Coastal and Port Engineering

The University of North Florida

College of Computing, Engineering, and Construction

October 2018

Sponsored by

Taylor Engineering Research Institute / TERI

Chairperson of the Supervisory Committee:

Professor Don Resio

Department of Civil Engineering

Members of the Supervisory Committee:

Professor Brian Kopp

Department of Electrical Engineering

Professor Cigdem Akan

Department of Civil Engineering

Thesis entitled “An Integrated Closed Convergent System for Optimal Extraction of Head-Driven Tidal Energy” by Michelle Vieira is approved:

_____ _____

Committee Chair: Don Resio

_____ _____

Committee Member 1: Brian Kopp

_____ _____

Committee Member 2: Cigdem Akan

Accepted for the School of Engineering:

_____ _____

Department Chair: Dr. Osama Jadaan

Accepted for the College of Computing, Engineering and Construction:

_____ _____

College Dean: Dr. Chip Klostermeyer

Accepted for the University:

_____ _____

Dean of the Graduate School: Dr. John Kantner

ABSTRACT

As the demands for energy increased with the global increase in population, there is a need to create and invest in more clean and renewable energy sources. Energy derived from the movement of the tides is an ancient concept that is currently being harnessed in a handful of large tidal range locations. However, the need to move from fossil fuel driven energy sources to those that are clean and non-polluting is a priority for a sustainable future.

Globally, hydropower potential is estimated to be more than 16,400-Terawatt hours annually. Given that the electricity consumption worldwide was at 15,068-Terawatt hours in 2016, if properly utilized, hydropower could supply a substantial percentage of current demand.

Most of the current hydropower supply is drawn from well-established dams and tidal barrage systems. However, tidal power plants that harness the change in water height and flow along the coast (i.e. using tidal energy) have the potential to push these figures even higher. Although there is no exact number for lengths of global coastlines, there are estimates that put that number between 220,000 and 880,000 miles of coasts. These opportunities in tidal energy technologies that harness energy from the sea may one day be the key to solving our energy crises.

This research explored in detail a closed, convergent system for optimal extraction of head-driven tidal energy with minimal adverse environmental effects. The long-term goal of this project is to create a system that is viable in low tidal range locations traditionally not considered for locations of tidal energy systems, therefore increasing the overall global tidal energy portfolio. By implementing a closed system of ‘bladders’ and convergent nozzles to optimize the flow rate of the contained fluid, the proposed system can 1) derive tidal energy in low tidal range geographies

2) avoid typical hazards like system biofouling, marine life propeller impacts, and 3) allow for ease of installation, operation, and maintenance.

ACKNOWLEDGMENTS

I'd like to thank the University of North Florida's School of Engineering, College of Computing, Engineering and Construction (CCEC). In addition, I would like to thank the Taylor Engineering Research Institute (TERI) for making this research and coursework under the Coasts and Ports Engineering program possible. My genuine appreciation to professors Don Resio, Brian Kopp, William Dally, and Cigdem Akan for all the efforts they have offered during this research. It's necessary to thank all the students in the TERI lab who offered their help for many parts of this project. Thank you, Abdallah Elsafty, Ashley Norton, Amanda Tritinger, Dorukhan Ardag, Patrick Cooper, Nikole Ward, William Fletcher, Mathew Davies, Christian Matemu, and Sergio Pena. Also, thank you to the University of North Florida Graduate School and Dr. John Kantner for assisting the tidal energy system research from the beginning.

TABLE OF CONTENTS

LIST OF FIGURES

LIST OF TABLES

LIST OF APPENDISES

1. INTRODUCTION

The objective of this research was to develop a renewable tidal energy capture system that eliminates many or all obstacles that traditional tidal systems, i.e.: tidal barrage, tidal lagoon, and tidal stream, have not been able to overcome. The overall goal was to design a system that eliminates system biofouling, minimizes or eliminates negative interference with marine life and local ecology, and offers easy of system deployment and maintenance.

Another important objective of this tidal system research was to create a system that, unlike traditional tidal barrages and tidal lagoons, can be utilized in low tidal range regions such as the east coast of Florida. This coast borders the Atlantic Ocean and experiences a semidiurnal tidal cycle with an average tidal range that is less than 2 meters. Traditional systems currently worked on a 'head differential' and therefore require a tidal range with lower limits around 7 to 8 meters. Creating a system that can harness the potential tidal energy in these low tidal range regions would tremendously increase the renewable energy potential available across the globe.

The hypothesis that drove this research was that by creating a closed convergent tidal energy capture system that utilizes optimized nozzles to accelerate the contained fluid as it approaches the turbine/turbines, we can achieve the following: 1) tidal energy driven by the potential energy of the weight of the water column that is then converted to kinetic energy as the contained fluid is forced through a nozzle that optimizes fluid velocity; 2) a closed system that eliminates biofouling by avoiding exposure to water with high levels of salinity i.e. seawater; 3) a closed system that eliminates potential propeller impact on marine life; 4) on land turbine housing that allows for ease of operation and maintenance.

In order to achieve this goal, the proposed research was aligned with the following plan of action: First, a proof of concept experiment was conducted using a small-scale physical model of the proposed tidal energy system. This allowed for testing the hypothesis that a fluid can be driven against gravity in a closed system. The next test conducted utilized small-scale tests using a physical model to test the effect of convergent pipes and nozzles for optimizing fluid velocity through the proposed system. Following this, a simplistic numerical model of the tidal system was created to estimate its behavior and investigate theoretical fluid velocity and associated power output. An economic study of the system was then conducted to estimate the Levelized Cost of Energy (LCOE) to predict the economic viability and compare it to other renewable energy systems. As an important component of this work, Provision and Utility Patents were drafted and submitted through the University of North Florida's Office of Sponsored Research to protect the intellectual property be investigated. As a final step, part of the potential transition to an operational system, intermediate scale testing of the system was conducted.

2. BASIC CONCEPTS AND LITERATURE REVIEW

This research was predominantly focused on the creation of a closed convergent tidal energy system that utilizes convergent flow to optimize fluid velocities in order to capture an optimized amount of tidal energy. This literature review provides background information of ocean tidal movements to allow for a basis of background knowledge of physics that drive tidal range globally and provide understanding for the vast amount potential energy available from the tidal changes. In addition, a review of historical tidal energy systems, both successful and unsuccessful was researched to allow for an understanding of challenges and breakthroughs in the industry.

2.1 Basic Tidal Concepts

Tides are the result of the interaction of the gravity of the sun, earth, and moon. The rise and fall of the tides creates potential energy in the form of 'head differential' or tidal range. The flows of coastal waters due to flood and ebb currents creates kinetic energy. Both forms of energy can be harvested by tidal energy technologies as renewable energy. The movement of the tides can be explained by a variety of gravitation forces that act on the earth and the oceans contained on it. At the center of mass of the earth-moon system, the centripetal acceleration provided by the gravitational attraction between the moon and the earth exactly equals the centrifugal acceleration due to the rotation about the common center of mass. The period of rotation about this common center of mass is 27.32 days. Everywhere else on the earth, there is an imbalance between the centripetal and centrifugal accelerations. The centrifugal acceleration is approximately equal everywhere on the earth, but the gravitational force due to

the moon varies over the surface of the earth depending on location. This imbalance results in a force that creates the tides, or tide-generating force.

At the spot on the earth exactly under the moon or sub-lunar point and the spot on the earth exactly opposite that, or antipode, the tide-generating force is in the same direction as

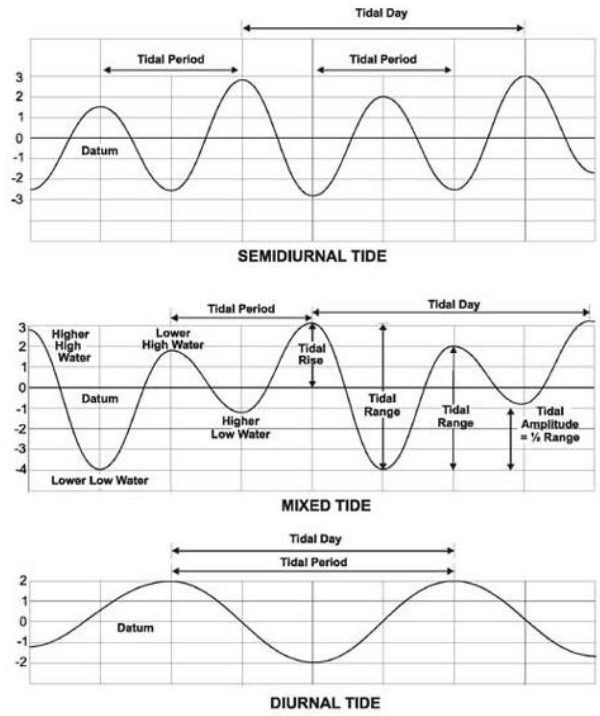

Figure 1: Tidal Phase and Frequency (Department of Oceanography, Naval Postgraduate School, 2017)

earth's gravity. Therefore, this force has little effect since its magnitude is significantly much less than gravity. This horizontal component, of the tide-generating force, is called the tractive force. The equilibrium tide would result from the tide-generating forces if the earth was completely covered by water and responded instantly to the changing forces and friction forces were not applied. Because of these tractive forces, the equilibrium tide has two bulges, one on either side of the earth. For this reason, you see two high tides and two low tides per lunar day. This condition is known as the semidiurnal lunar tidal constituent and has a period of 12.42

hours. The lunar day or tidal day is a total of 24.84 hours. The moon's orbit and associated tidal bulges are tilted relative to the earth's equator. This results in the two high waters per lunar day not being equal. This is known as the diurnal inequality of the lunar semidiurnal tide and results in diurnal tides.

The shape of the ocean basin is a major factor in determining whether the tide in a particular area is semidiurnal, diurnal or a mixture of the two. The sun also plays a role in influencing the movement of the tides. This interplay gives rise to another semidiurnal constituent. The summation of the lunar and solar semidiurnal tides is known as beating. When the sun and moon are at right angles to each other a neap tide condition is created. These neap tides deliver relatively small tidal ranges. In opposition are spring tides. These spring tides occur when the sun and moon are lined up and deliver relatively large tidal ranges. Various other parameters of the moon's orbit around the earth and the earth's orbit around the sun give rise to other tidal constituents that add complexity to the tidal signal. This research relies on a basic understanding of tidal constituents and uses a localized semidiurnal average for investigation (Department of Oceanography, Naval Postgraduate School, 2017).

2.2 Untapped Global Potential of Hydropower

Hydropower uses water as its fuel in a manner roughly analogous to how a traditional coal-fired power plant uses coal to fuel its turbines. However, unlike coal, this fuel is not reduced or used up in the process. Because the motions in a tidal cycle are part of a constantly recharging system, hydropower is a renewable energy. When flowing water is captured and turned into electricity, it is called hydroelectric power or hydropower (Energy Efficiency & Renewable Energy, 2017)

Tidal energy is a form of hydropower that converts the energy of the cyclical movement of tides into electricity or other useful forms of power. Since the tides are governed by the earth, moon, and sun interactions as outlined above, they are entirely predictable and can be modeled years and decades into the future. This makes tidal energy a completely reliable and predictable energy source (Kim Rutledge, 2011).

Hydropower is currently the most harnessed form of renewable energy and plays a vital role in global power generation. Worldwide, the total installed hydro capacity was reported at 1,246 Gigawatts in 2015, bringing the total energy generation for 2016 to an estimated 4,102-Terawatt hours (International Hydropower Association, 2017). This total represents the greatest contribution of energy from a renewable source estimated to date. These current hydropower figures are equivalent to approximately 16% of global electricity generation. These existing hydropower plants also provide at least 50% of the total electricity supply in more than 35 countries (International Renewable Energy Agency, 2015).

Globally, hydropower potential is estimated to be more than 16,400-Terawatt hours annually, although the estimates vary and are dependent on the source (U.S. Energy Information Administration, 2017),. Independent research that utilized both calculations based on theoretical methods of tidal dynamics and also the use of 2D hydrodynamic numerical models resulted in results that are consistent with published proposed tidal energy values. The proposed Severn Tidal Barrage in the United Kingdom was taken as a case study by Junqiang Xia, Roger Falconer, Binliang Lin, and Guangming Tan. These two aforementioned approaches were then applied to estimate the potential annual tidal energy output. The results show that the estimated tidal energy output for the barrage would range from 13 to 16 Terawatt hours per annum, which is similar to

the value of 15.6 Terawatt hours in reports published by the International Energy Agency and Department of Energy and Climate Change (Junqiang Xia1, 2015).

The second method provides a more accurate estimate of the total annual energy output from a barrage, but more detailed information on the barrage and turbine parameters is required for more accurate results. The model predictions from the second approach also indicated that the energy output from the Severn Barrage could be increased with technological advances in the sluice gate and turbine performance. It was predicted that the total annual energy output could be increased to 15.3 Terawatt hours with a higher discharge coefficient, and to 15.1 Terawatt hours with an improved turbine performance. It was also estimated that the annual output could be increased to 16.6 Terawatt hours if the performance of both sluices and turbines could be improved to match ideal conditions. Again, projected potential annual energy output corresponds to figures published in reports by climate and energy authorities (Junqiang Xia1, 2015).

It's important to note that these studies project values of tidal barrage potentials over coastal regions that experience a given tidal range. There are also vast amounts of dynamic tidal or tidal stream energy that is left out of these figures and models that could potentially change these projections by a factor of two or more. Given that electricity consumption worldwide was at 15,068-Terawatt hours in 2016, if properly utilized, hydropower could supply a hefty percentage of current demand (Enerdata, 2018). Most of the current hydropower figures are drawn from well-established dams and tidal barrage systems. However, tidal power plants that harness the change in water height and flow along the coast (i.e. using tidal energy) have the potential to swing these figures even higher. Although there is no exact number for lengths of global coastlines, there are estimates that put that number between 220,000 and 880,000 miles of coasts. These tidal energy

technological interfaces between the land and sea may one day be the key to solving our energy crises (Egbert, 2002).

2.3 Understanding the Future of Tidal Energy Systems Through the Past

Harnessing power from water or hydropower has been used throughout human history. Perhaps dating back to the prehistoric times, humans realized the utility of putting fast-moving river currents to work with the aid of a paddle-equipped wheel linked up to a spindle or rotor. The water wheel dates back at least to ancient Greece, where Grecian millers used this rudimentary form of hydropower to grind wheat into flour (Shere, 2013).

In the late 19th century, hydropower became a primary source for generating electricity in many parts of the United States. The first hydroelectric power plant was built at Niagara Falls in 1879. In 1881, street lamps in the city of Niagara Falls were powered by hydropower (Kim Rutledge, 2011).

The past century of hydropower has seen many advancements that have helped it become an integral part of the renewable energy mix in the United States and the global economy. Hydropower is no longer just the venerable water wheel but shows up as a variety of machinery used to capture the energy present in rivers, changes in tide, currents, and waves (Energy Efficiency & Renewable Energy, 2017).

2.4 Existing Tidal Energy Capture Systems

Currently, there are two types of systems that derive energy from the cyclical movement of the tides. Tidal range systems use the vertical difference in height known as ‘head differential’ or ‘tidal range’ between the high tide and the succeeding low tide. Artificial tidal barrages, in the form of a dam, lagoon, or other barrier, may be constructed to capture the tide. Turbines in the

barrier or lagoon generate electricity as the tide floods into the reservoir. This water is retained and can then be released through turbines, generating electricity once the tide outside the barrier has receded (Ruud Kempener, 2014).

There are several large commercial scale tidal power plants in operation around the world. Sihwa Lake Tidal Power Station is the largest tidal power station in the world was commissioned in South Korea in 2011. This power station has a maximum generating capacity of 254 MW and is an interesting construction because of its design that utilized an existing seawall and then retrofitted it with ten 25.4 MW submerged turbines to produce electricity from the tidal flows. The next largest is a 240 MW bulb turbine plant at the mouth of La Rance estuary in France. This power station site generates enough power to supply electricity to a city of 300,000 people. The Annapolis Royal Generating Station is another high energy producing barrage, located on the Annapolis River in Nova Scotia, Canada. This power station was commissioned in 1984 and has a generating capacity of 20MW. The Annapolis Station has the capability to power around 4500 houses in the area. Others barrage systems include Kislaya Guba Tidal Power Station in Russia with a capacity of 1.7 MS, Jianxia Tidal Power Station in China at 3.2 MW, and Uldolmok Tidal Power Station in South Korea at 1.5 MW (Tidal Power, 2017)

Tidal stream technologies, or dynamic tidal systems, are the second class of tidal power generation schemes. They act much like underwater wind turbines, generating power from the kinetic energy of fast-flowing tidal currents. Tidal Stream systems capture the flow of water as the tide ebbs and floods, manifesting as tidal current. Tidal stream devices extract energy from this kinetic movement of water, much like wind turbines extract energy from the movement of air. The

currents created by the movement of the tides are often magnified where water is forced to flow through narrow channels or around headlands (Tidal Power, 2017).

The generators are generally sunk between twenty to thirty meters below the surface of the water and can be situated anywhere that possesses a strong tidal flow. However, developing a successful tidal current turbine has been more difficult than simply dropping a wind turbine in the ocean. Because water is about 800 times denser than air, tidal stream turbines must be built to be much more robust than their terrestrial counterparts. The advantage of the greater density of water is that relatively large amounts of power can be produced with relatively small rotor diameters. For example, rotors with a diameter of 10-15 meters can generate as much as 700 kilowatts of power, whereas a 600 kilowatt wind turbine requires a rotor diameter of up to 45 meters. Current designs of tidal turbines function best at flow rates of 7-11 kilometer per hour (Tidal Power, 2017).

Tidal stream technologies are still in its infancy and have experienced many innovations as well as setbacks along the way. For this reason, there are many companies forging the path forward in this field, but none have proved a concept that can stand the test of the battering currents and environmental exposure. Almost 40 new devices have been tested in the last few years with a few making it to full-scale testing. So far, most of the development of this technology is taking place in Canada, China, France, Ireland, Japan, South Korea, Spain, the United Kingdom, and the United States. Most of these countries have at least one open sea test site. The European Marine Energy Centre (EMEC), based in Scotland, is one of the longest running sites where tidal current turbines have been tested since 2005. In the USA, the Verdant turbine was tested in the East River of New York City and Ocean Renewable Power Company is demonstrating its vertical axis turbines near Eastport in Maine (Ruud Kempener, 2014).

2.5 Global Research in Tidal Energy Capture Systems

Looking toward the future, innovative scientists and engineers have proposed several novel tidal range alternatives to the barrage. One of the most promising being the tidal lagoon. Tidal lagoons would not be attached to the shoreline at all, but rather be artificially created pools in the sea that would let water in and out while generating power similar to the way tidal barrages operate. These proposed lagoons would offer with greater efficiency without isolating ecologically sensitive inter-tidal areas. As of early 2016, the first tidal lagoon project was under construction off the coast of the Welsh city of Swansea, enclosing around 11 km^2 of water. It is projected to produce 320 Megawatts of power for 14 hours a day. This is enough energy to power 155,000 homes and will make it the largest tidal energy facility in the world. The Swansea Tidal Lagoon is scheduled for completion in 2019, if successful, it will be the first of six proposed tidal lagoon projects to be built on Britain's west coast (Tidal Power, 2017)

The Dutch-designed Dynamic Tidal Power system is an even more radical and promising tidal range proposal. A large T-shaped pier would be built up to 60 km straight out from the coast, blocking tides that move parallel to the coast and cause enough head differential to could produce tremendous amounts of electricity, while possibly avoiding many of the economic and environmental problems of other tidal range technologies. No such projects have been built yet, but teams from China and the Netherland are moving forward with planning on such projects (Tidal Power, 2017).

Tidal stream technologies have seen huge advances in the last decade, with many companies around the world working to recreate the success of wind turbines on land in the underwater realm. Yet the technology is far less mature than wind power, and tidal stream

technologies are just now leaving the prototype and demonstration phase. Companies around the world are pioneering a large variety of different designs, recently totaling around 40 unique prototypes. Most function on the same principles as horizontal axis wind turbines, however, there are a collection of more novel designs. These include vertical-axis turbines, rotating screws, tidal kites, and paddlewheels. Further research is necessary in this field, the most critical is creating turbines that can survive the hostile and saline conditions of the ocean. A recent test in Nova Scotia resulted in a tidal stream turbine failing as the rotors were ripped off by the immense tidal forces experienced in the Bay of Fundy. In addition, the corrosive salt water encountered in the marine environments also takes a serious toll on equipment. Experiments are also ongoing on the best method for mooring the turbines to the seafloor. Concrete bases on the seabed are the most common of mooring system being utilized. However, other mooring designs include turbines mounted on towers and floating systems that are tethered to the seabed. Research is also being conducted on overcoming the challenges of connecting the power grid (Tidal Power, 2017).

2.6 Predictable and Reliable Tides

Tidal energy outperforms all other renewable energies when it comes to predictability. Unlike the amount of sun-filled days or the available wind velocity, the tides are well understood and can be modeled to optimize an energy generation system for years to come. Because of this, the power generation as a percent of the installed capacity of tidal systems far outperforms wind and solar, reaching up to 90% of the installed or nameplate capacity for a system. Where nameplate capacity is the design intended full-load sustained output of a facility. Power generating systems with an output consistently near their nameplate capacity have a high capacity factor.

These capacity factors as compared to nameplate capacity are important factors when comparing renewable energy across economic performance. For example, wind turbines under 100-kilowatt on average cost between $3000 to $8000 per kilowatt of nameplate capacity. At the utility scale, this initial construction cost is between $1.3-$2.2 million per Megawatt of nameplate capacity. It is important to note that the nameplate capacity of wind turbines and other energy-producing plants is then scaled back by the above-mentioned capacity factor. Wind has an average capacity factor of 25% to 33%, meaning that wind farms will only achieve their nameplate capacity rating of 1/4 to 1/3 of their runtime. This is due to inconsistent wind speeds, variability in wind directions, and time periods when no wind is present (Poyry, 2017).

2.7 Current State Hydropower and Tidal Energy

Historically, hydropower has proven to be a cost-effective and reliable electricity source. It offers high efficiency and low operating and generation costs, though its upfront investment cost is relatively high. The capital costs of large hydropower projects are dominated by the civil works and equipment costs. These can represent between 75% and as much as 90% of the total investment costs. These initial investment costs are highly site-specific as each project is designed for a particular location. Proper site selection and hydro scheme design are therefore key challenges. Annual operations and maintenance costs are often quoted as a percentage of the investment cost per kilowatt per year, or as USD per kilowatts per annum. Typical values range from 1% to 4% of the total system cost. The International Energy Agency (IEA) assumes 2.2% for large and 2.2% to 3% for smaller hydropower projects, with a global average of around 2.5%. Other studies indicate that fixed operation and maintenance costs represent 4% of the total capital cost. This figure may be appropriate for small-scale hydropower plants, however large hydropower

plants will have significantly lower values. An average value for operation and maintenance costs of 2% to 2.5% is considered the acceptable average for large-scale projects, which is equivalent to average costs of between USD 20 per kilowatt per annum and USD 60 per kilowatt per annum for the average project by region in the IRENA Renewable Cost Database. (Agency, 2015)

There are a limited amount of established tidal power plants to derive long-term cost and return from. Because of this, tidal range power generation study is dominated by two large plants in operation, the La Rance Tidal Barrage in France and the Sihwa Tidal Plant in South Korea. The construction costs for La Rance were around USD 340 per installed kilowatt (2012 value, originally commissioned in 1966), while the Sihwa barrage was constructed for USD 117 per installed kilowatt in 2011. The latter used an existing dam for the construction of the power generation technology. The construction cost estimates for proposed tidal barrages range between USD 150 per installed kilowatt in Asia to a much higher USD 800 per installed kilowatt in the UK but are very site specific. Again, the typical systems are high in installation cost but yield a good return with a low cost of electricity production. For example, electricity production costs for La Rance and Sihwa Dam are EUR 0.04 per kilowatt-hour and EUR 0.02 per kilowatt-hour respectively (International Renewable Energy Agency, 2015).

2.8 Current Competitive Renewables: Wind and Solar

Other renewable energy capture devices, such as wind turbines, photovoltaic cells and solar concentration plants play an important role in the long-term power generation portfolio. Currently, wind energy and their corresponding turbines offer a technology that is effective in high sustained-wind regions but cannot be implemented in many coastal areas. The same can be said about solar which relies heavily on solar exposure and is often unpredictable.

However, the proposed tidal system can add another avenue of energy collection in regions where these other technologies are not optimal or even viable. If used in harmony with each other, we could move to a future that moves away from a dependence on fossil fuels and completely renewable power generation portfolio.

Currently, solar photovoltaic cells are an important component of the global renewable portfolio. These systems are easily scaled, either too large solar farms for commercial use or down to rooftop solar for residential use. However, these systems experience a large amount of variability due to weather conditions and unavailable solar energy generation during the sundown hours. In addition, solar technologies face intermittency issues, large energy storage costs, have a limited lifetime of photovoltaic cells with cell efficiency diminishing each year after being manufactured. The cost of utility-scale installation comes in around $3-$3.5 million per Megawatt (SunRun, 2018). When the capacity factor in introduced to these cost figures, the cost jumps to $20-$30 million per actual Megawatt.

Energy harnessed from the wind currently contributes an important piece of the total renewable energy portfolio. Wind turbines offer a technology that is highly effective in regions that experience high sustained winds. However, these turbines cannot be implemented in many coastal areas that experience intermittent winds and high-intensity storms. Wind farms also create concerns over effects on surrounding ecology, noise level concerns, and complaints about visual clutter of the affected geographies. These systems require a high cost to manufacture, install, as well as, operation and maintenance (Windustry Resource Library, 2012). The present cost of these system average at $1.3-$2.2 million per Megawatt for utility scale installation. When the capacity factor for wind is introduced, this figure jumps to $5.2-$8.8 million per Megawatt.

3. MOTIVATION FOR

The motivation behind this research was to develop a renewable energy tidal system that builds on the previous research and history of this field while moving forward with a system that can overcome many of the traditional obstacles that past system have and presently encounter. If able to achieve this, our system will be able to contribute another resource in the renewable portfolio of clean energy systems helping to gain more global independence from fossil fuels as a primary energy source.

Current tidal barrage systems and the proposed tidal lagoon and tidal stream systems encounter are exposed to biofouling conditions because the mechanical parts interface with the harsh and high salinity waters of the tidal systems that they must operate within. This increases the amount of system maintenance that is required. The direct contact with turbine propellers with the surrounding ecosystem also means there is the possibility of impacts with local marine life as it passes through the system. The proposed system aimed to eliminate the interaction of both biofouling waters to the mechanical system the mechanical impacts to local marine life.

In addition, this research into a novel tidal system aimed to develop a system that can be deployed in coastal regions with low tidal ranges that would not typically be considered for tidal energy capture systems such as the tidal barrage or tidal lagoon.

Finally, this system may also offer unique uses in the area of disaster relief, remote location energy production, remote or emergency military operations, and possible use for powering desalination projects.

4. PROPOSED TIDAL ENERGY SYSTEM

This section of work begins with an outline of an innovative, closed convergent tidal energy system. The proposed system allows for scalable energy generation from tides, even in areas with relatively small tidal ranges, while avoiding many of the traditional pitfalls of existing technologies, such as bio-fouling, harm to marine ecosystems, damages to turbines due to debris in the water and wear on moving parts due to sediment and other suspended materials in the water. This system has the flexibility to be used in residential and commercial energy production applications. Additionally, the need for system maintenance is greatly reduced by placing the turbines on land for easy accessibility, which also permits easier access to the energy grid.

Figure 2: Infographic illustrating the proposed closed convergent tidal system. The closed convergent tidal generator uses two compliant flexible bladders, one offshore and the other offshore to derive energy from the tidal range. The onshore option of generator placement allows for easy of installation and maintenance. The closed system eliminates biofouling and interactions with local ecology.

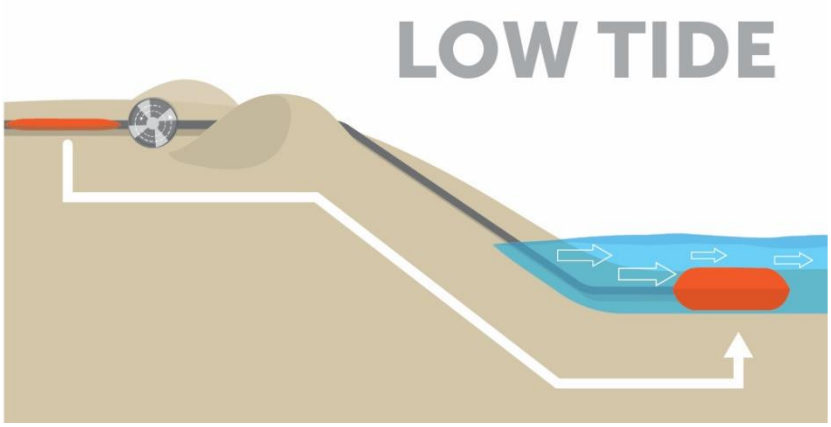

Figure 5: Low tide infographic of proposed tidal system. As the ebb tide forces the tidal waters to recede, the onshore bladder releases its fluid. Gravitational forces pull the fluid through the turbine and toward the offshore bladder.

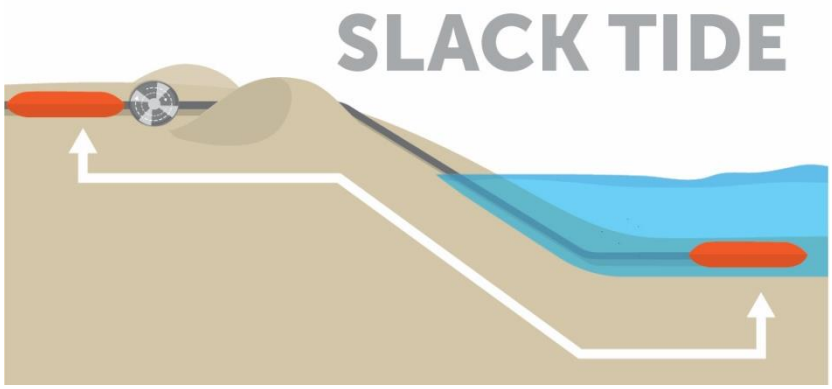

Figure 4:Slack tide infographic of proposed tidal system. During this portion of the tidal cycle, the tidal waters are free from forces in either direction. At this time, a sluice gate or valve will be closed in order to hold the potential energy of the system while the tide moves to the optimum position.

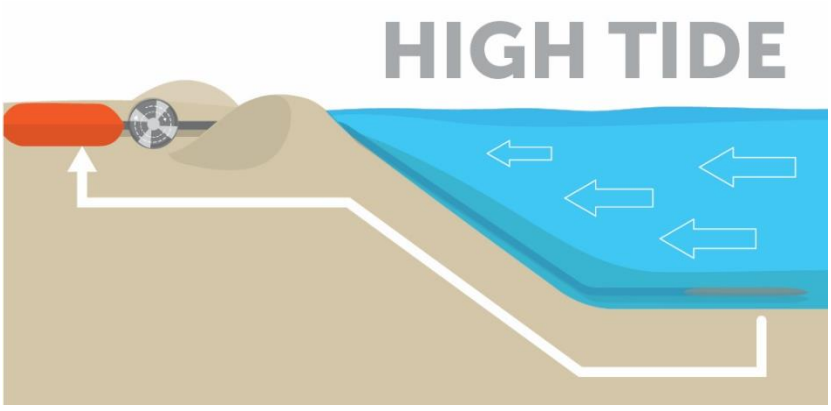

Figure 3: High tide infographic of proposed tidal system. As the flood tide pushes in towards high tide, the tidal waters apply pressure to the full offshore bladder and force the contained fluid through the turbine(s) toward the onshore bladder.

Coastal regions along most of the East and Gulf Coasts of the United States, and many other areas around the world, are located where (1) topographic slopes are very low for substantial distances inland, (2) wind speeds are quite low, and (3) tidal energy is presently not considered economically feasible. Thus, coastal regions are typically only able to utilize solar photovoltaic sources to generate renewable energy. The proposed system has the potential to solve this long-felt but unresolved need and provide these coastal regions with much needed additional options for renewable power generation.

The current proposed tidal energy concept is a closed system that utilizes closed bladders in an offshore tidal area, where closed bladders are used on both ends of the head-driven system. Using a closed system containing a specific volume of liquid within connected, symbiotic onshore-offshore, compliant bladders that include a hydropower turbine located between them, the system captures potential energy within the "head differentials" over a tidal cycle. These compliant bladders can be scaled from small, residential-sized systems up to commercial applications to accommodate local needs and meet a diverse set of applications. They can also be designed to conform to specific local environmental conditions and constraints.

The onshore bladder location lends itself to being placed in a shallow excavated basin to allow for multiple land uses above it (e.g., parking garage, pier, port offloading area, etc.). In addition to the on-land, in-water setup, the system can use bladders that both reside under the surface of the water as long as sufficient "head differential" exists between the locations. Pressure-sensing valves can be included within such a cyclic system to optimize flow rates. Site selection will be an important aspect of the overall construction costs and minimizing adverse environmental impacts related to land loss.

The current tidal system can include bladder designs that are oversized such that each can contain at least the total volume of fluid in the entire system. The onshore system should be located at local mean sea level and allow for the variation of local sea level on scales longer than typical tidal cycles. The extra material allows each bladder to expand upward and contract downward at appropriate rates, maximizing utilization of the pressure differential. The tidal system further includes connections between the onshore and offshore containers, which include a number high-efficiency hydro-turbines.

The system can further include a network of valves and convergence to increase the flow rate from the available head (typically less than about 1-2 feet at any given tide phase) to the flow rate of an equivalently much higher natural head. This flow rate is optimized to allow maximum power to be generated by any specific hydro-turbine system for a specific volume of water passing through the system. Increasing the available energy density enables the application of this system to include locations with low tidal ranges.

Overall, the control system can accelerate flows to optimal velocities, as will be particularly important for applications in areas with relatively small tidal ranges. The extra compliant material in each bladder allows water to flow in and out of the system with minimal lost energy from the head-differential.

It is an object of the current proposed design to provide a closed volume tidal power generation system that minimizes many of the ecological concerns and system biofouling issues that arise when mechanisms are exposed to harsh saltwater conditions. Because the mechanical hardware is kept in a controlled fluid environment, the life of these parts can be prolonged much longer than those exposed to a natural environment. To avoid biofouling and maintenance

problems, the system concept should use water from which all organisms and debris have been removed and which has been de-salinized to prevent the occurrence of significant corrosion. This provides both improved maintainability and environmental compatibility.

An example of the mechanics of the current system is now discussed herein. Starting at zero tide level on a rising tide, the water level above the offshore bladder is allowed to increase until the pressure differential is capable of generating optimal power from flow through the generator. At that time (expected to be less than about 1 hour from the zero-differential time), the shutoff valve is automatically opened, and head-driven flow will flow through the generator. These bladders are designed manifold/converging sections on each side of the generator that greatly increase the flow velocity as the generator is approached. This control system maintains flow rates in the optimal velocity range for a given hydropower turbine, enabling maximum energy extraction within the design constraint of the contained volumes – even in areas small tidal ranges.

When the offshore tide begins to fall, the pressure differential eventually drops below the optimal value for power generation; and the cutoff valve will again be closed, until the lowering water above the offshore bladder attains a potential pressure differential capable of producing the optimal negative flow for power generation in the offshore direction (again expected to be less than about a 1-hour duration). In this operation, semi-diurnal tides typical along the East Coast of the United States can generate dependable, optimal power for about 4 hours out of every ~6 hours of available time.

The proposed system can include but is not limited to the following: 1) A tidal energy system, substantially as shown and described herein. 2) A system for optimal extraction of head-driven tidal energy with minimal or no adverse environmental effects, substantially as shown and

described herein. 3) A method of generating tidal energy from tides, substantially as shown and described herein. 4) A closed tidal energy system, comprising: a) a closed, compliant onshore bladder located at a local mean sea level; b) a closed, compliant offshore bladder in communication with the onshore bladder; c) a turbine housing disposed between the onshore bladder and the offshore bladder; d) a high-efficiency hydropower turbine disposed within the turbine housing, wherein the turbine captures head differentials over a tidal cycle between the onshore bladder and the offshore bladder; e) a generator in communication with the hydropower turbine; f) a pressure-sensing shut-off valve in communication with the offshore bladder, wherein the shut-off valve is opened when a pressure differential of a water level above the offshore bladder is sufficient to generate optional power from the flow through the generator, wherein opening the shut-off valve permits head-driven flow to flow through the generator, wherein the offshore and onshore bladders include manifolds on each side of the generator to cause flow velocity to increase as the flow approaches the generator; g) a control system, optionally including the manifolds, that maintains the flow velocity in an optimal velocity range for the hydropower turbine, thus enabling maximum energy extraction, wherein the shut-off valve is closed when the pressure differential above the offshore bladder reduces to a value that is insufficient for optimal power generation, wherein the shut-off valve remains closed until the lowering water above the offshore bladder attains a potential pressure differential capable of producing optimal negative flow for power generation in the offshore direction.

This work initiated the work to test the hypothesis that the proposed system is both physically and economically viable as a new source of renewable energy.

5. METHODOLOGY

This research was comprised of the following steps in order to test the given hypothesis for the proposed tidal capture energy system: 1) a proof of concept experiment was conducted using a small-scale physical model of the proposed tidal energy system. This allowed for testing the hypothesis that a fluid can be driven against gravity in a closed system. 2) small-scale tests using a physical model to test the effect of convergent pipes and nozzles for optimizing fluid velocity through the proposed system. 3) a simplistic numerical model of the tidal system was created to estimate its behavior and investigate theoretical fluid velocity and associated power output. 4) an economic study of the system was conducted to estimate the Levelized Cost of Energy (LCOE) to predict the economic viability and compare it to other renewable energy systems. 5) Provision and Utility Patents were created and submitted through the University of North Florida's Office of Sponsored Research to protect the intellectual property be investigated. 6) as part of the potential transition to an operational system, intermediate scale testing of the system was conducted.

6. TIDAL ENERGY CONCEPTS

As previously noted, because water is 800 times denser than air, you can expect greater energy output for lower velocities in tidal power applications. Therefore, at low speeds, they have kinetic energy per unit area comparable to that of winds of speed nearly an order of magnitude higher. Because of this physical property, tidal currents contain an enormous amount of energy that can be captured.

This cubic relationship between velocity and power is the same as that for the power curves relating to wind turbines, but there are practical limits to the amount of power that can be extracted from tidal streams. Some of these limits relate to the design of the tidal stream turbines and the characteristics of the underwater resource (Using the Power of Tidal Streams to Generate Electricity , 2017)

6.1 Governing Equations for Proposed Tidal System

In 1920, A. Betz predicted the ideal frictionless efficiency of a propeller windmill using a simulation shown in the figure below. Because incompressible flow was assumed, we can transfer these concepts from horizontal axial wind turbines to those used in a comparable manner in the tides.

The propeller is represented by an actuator disk, which creates a pressure discontinuity across the plane of the propeller. These values are represented by area A and local velocity V. The wind or tidal stream is represented by a stream tube of approach velocity V_1 and a slower downstream wake velocity V_2. The pressure rises to p_b at the point before the disk and drops to p_b at the point just after the disk, and then returning to free-stream pressure in the far wake.

A control-volume horizontal momentum relationship can be applied to relate sections 1 and 2 and gives:

$$\sum F_x = -F = \dot{m}(V_2 - V_1)$$

A similar relation for a control volume encompassing points just before and after the disk gives:

$$\sum F_x = -F + (p_b + p_a)A = \dot{m}(V_a - V_b) = 0$$

Equating these above relationships will yield the propeller force:

$$F = (p_b - p_a)A = \dot{m}(V_1 - V_2)$$

Using the assumption of ideal flow within the system, the pressures can be found by applying the incompressible Bernoulli relation up to the disk:

$$p_\infty + \frac{1}{2}\rho V_1^2 = p_b + \frac{1}{2}\rho V^2$$

$$p_a + \frac{1}{2}\rho V_2^2 = p_\infty + \frac{1}{2}\rho V_2^2$$

Subtracting these equations and noting that $\dot{m} = \rho AV$ through the propeller, then $p_b - p_a$ can be substituted into the above propeller force equation to yield:

$$p_b - p_a = \frac{1}{2}\rho(V_1^2 - V_2^2) = \rho V(V_1 - V_2)$$

Which can be simplified to:

$$V = \frac{1}{2}(V_1 + V_2)$$

Continuity and momentum require that the velocity V through the disk equal the average of the wind/tidal and far-wake speeds. Therefore, the power extracted by the dick can be rewritten in terms of velocities V_1 and V_2 by the combination of the above simplified equation and the original propeller force equation to obtain:

$$P = FV = \rho A V^2 (V_1 - V_2) = \frac{1}{4}\rho A (V_1^2 - V_2^2)(V_1 + V_2)$$

For a given wind or tidal speed V_1, we can find the maximum possible power by differentiating P with respect to V_2 and setting this equal to 0, which results in:

$$P = P_{max} = \frac{8}{27}\rho A V_1^3$$

at

$$V_2 = \frac{1}{3}V_1$$

The maximum available power to the propeller is the mass flow through the propeller times the total kinetic energy of the wind or tide:

$$P_{available} = \frac{1}{2}\dot{m}V_1^2 = \frac{1}{2}\rho A V_1^3$$

or

$$P = \frac{1}{2}\rho A V^3$$

Where ρ is the water density that interacts with the turbine (fresh water in our tidal design specifications), A is the rotor area and V is velocity that acts on the rotor.

However, for reasons such as the Betz limit, rotor design, blade profile, and losses, only a percentage of this power can be retrieved by any converter. This maximum possible efficiency of an ideal frictionless system is usually stated in term of the power coefficient. As found here:

$$C_P = \frac{P}{\frac{1}{2}\rho A V_1^3}$$

Which then yields:

$$C_{p,max} = \frac{16}{27} = 0.593$$

This number is called Betz limit and is a theoretical upper limit on the ability of turbine technology to convert raw energy into useful electrical output energy. This limiting factor is referred to as the power coefficient C_p, and is estimated to be 59.3%. The use of a power coefficient C_p is necessary to consider for these factors inherent to the conversion of energy from mechanical to electrical. This power equation then becomes:

$$P = \frac{1}{2}C_p\rho A V^3$$

The efficiency, η, of the system turbine, must also be included in this equation to give:

$$P = \frac{1}{2} C_p \eta \rho A V^3$$

(Manhar Dhanak, 2016), (White, 2008)

6.2 Governing Equations for Fluid in Pipes

In order to study flow through pipes, we first assume frictionless flow and utilize the Bernoulli Equation:

$$\int_1^2 \frac{\partial V}{\partial t} ds + \int_1^2 \frac{dp}{\rho} + \frac{1}{2}(V_2^2 - V_1^2) + g(z_2 - z_1) = 0$$

To evaluate the two remaining integrals, one must estimate the unsteady effect $\frac{\partial V}{\partial t}$ and the variation of density with pressure. At this time, we consider only steady $\frac{\partial V}{\partial t} = 0$ which implies incompressible flow or a fluid with a constant density. With these assumptions, the equation then becomes:

$$\frac{p_{2-}p_1}{\rho} + \frac{1}{2}(V_2^2 - V_1^2) + g(z_2 - z_1) = 0$$

$$\frac{p_1}{\rho} + \frac{1}{2}(V_2^2 - V_1^2) + g(z_2 - z_1) = 0$$

Under the assumptions of an incompressible fluid with negligible viscosity, Bernoulli's principle states that:

$$\frac{V^2}{2} + gh + \frac{p}{\rho} = constant$$

where v is fluid speed, g is the gravitational acceleration 9.81 m/s^2, h is the fluid's height above a reference point, p is pressure, and ρ is density. Define the opening to be at h=0. At the top of the tank, p is equal to the atmospheric pressure. v can be considered 0 because the fluid surface drops in height extremely slowly compared to the speed at which fluid exits the tank. At the opening, h=0 and p is again atmospheric pressure. Eliminating the constant and solving gives:

$$gh + \frac{p_{atm}}{\rho} = \frac{V^2}{2} + \frac{p_{atm}}{\rho}$$

Solving for v gives Torricelli's idealization of efflux from a hole in the side of a tank.

$$V^2 = 2gh$$

$$V = \sqrt{2gh}$$

For a parallel flow case, consider three pipes diverging at point A and converging back at point B, the pressure drop is the same in each pipe and the total flow is the sum of the individual flows:

$$\Delta h_{A \to B} = \Delta h_1 = \Delta h_2 = \Delta h_3$$

$$Q = Q_1 + Q_2 + Q_3$$

(Frank M White, Fluid Mechanics)

This is the most ideal case; however, we must take head losses throughout the system. Care must be given to the design of the system entrance, any convergence or divergence, pipe bends, valves, and inner pipe walls, and length since these will all affect the head losses experienced by the system. If an inlet consists of sharp corners, flow separation can occur at this location and vena contracta is formed.

7. INITIAL EXPERIMENT OF TIDAL SYSTEM USING A PHYSICAL MODEL

The proposed tidal energy system aimed to deploy a system of closed compliant bladders to contain a fluid that will move onshore and offshore with the ebb and flood tides. With the onshore bladder emptying by the force of gravity and the offshore bladder emptying by the force of the water column increasing above and forcing this contained fluid up to the elevation of the onshore bladder.

A small-scale test was created to test the concept that conservation of mass will allow for an equal return of the fluid as the pressure in the form of a water column is applied to the offshore portion of the system. Note: Throughout the experimental discussion the onshore bladder will refer to the higher elevation bladder while the offshore bladder will refer to the one at a lower elevation.

To simulate the system on a very simplified and small scale, two 250-gallon portable water containment bladders from "HUSKY" brand with part number BT-250V30 were utilitzed. These water containment bladder tanks are also referred to as pillow tanks and area widely used in the following industries: agricultural, industrial, commercial, marine, oil, and military and are

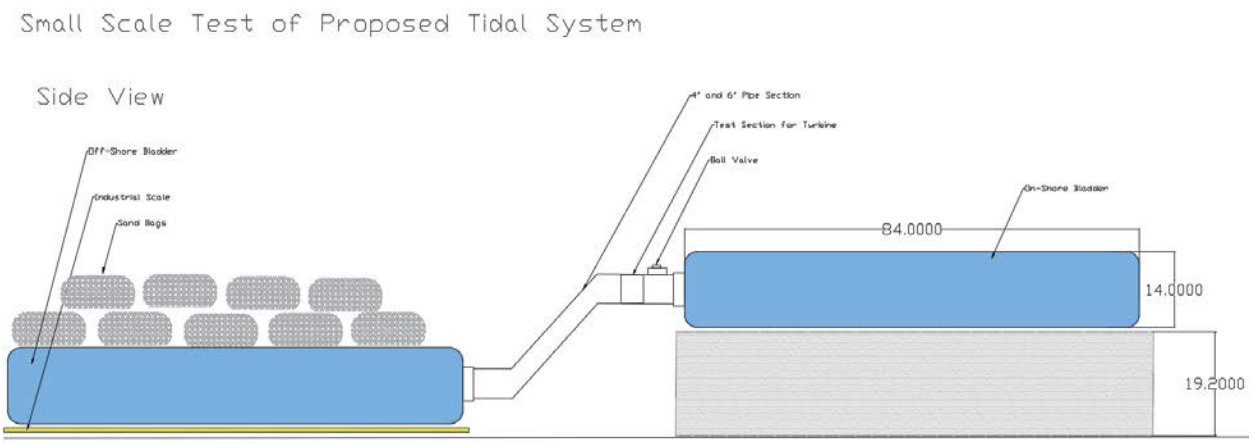

Figure 6: Small Scale Physical Model AutoCAD Drawings (Side View)

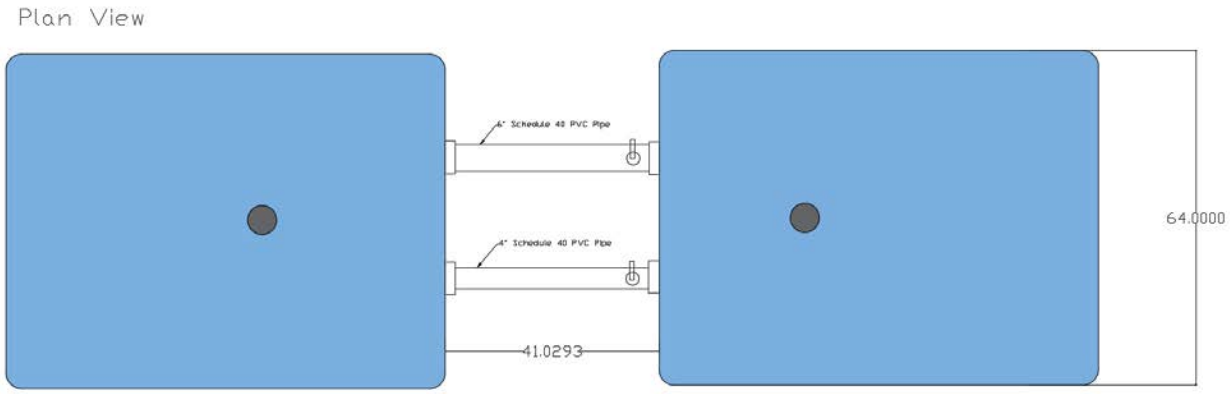

Figure 7: Small Scale Physical Model AutoCAD Drawings (Plan View)

available at www.huskyportable.com. The bladder tanks are constructed out of urethane with PVC connections. The two tanks utilized for this small-scale physical model experiment measured 60 inches by 84 inches by 14 inches. These bladders represented the onshore and offshore systems. The onshore bladder was raised on a platform to an elevation of 19.2 inches while the offshore bladder was placed on an industrial scale at ground level. These bladders were then connected via PVC flange and pipes to each other. One round of testing allowed the fluid to pass back and forth through an unobstructed pipe, while a second test implemented the use of a turbine and generator to test the viability of the concept with this addition.

To initiate testing, the onshore bladder was filled with water with the exit valve closed. The scale was initialized and then the valve was opened. By using the industrial scale and the pipe geometries within the system, the volumetric flow rates and velocities could be determined through the pipes from one bladder to another. Once the onshore bladder was empty, the valve was closed and the scale reset.

The next step consisted of applying ten 60-pound sand bags to the top of the offshore bladder to simulate the applied tidal range to the system. This applied weight of 600 pounds would

be roughly equivalent to 71.90 gallons or 9.61 ft^3 of water to simulate the column of water since one gallon of water weighs approximately 8.3454 pounds and $1ft^3$ is equivalent to 7.48 gallons. Once the weight was fully applied, the scale was initialized, and the valve between the bladders was opened allowing the fluid to flow from the offshore bladder to the onshore bladder. Again, the change is volume of the offshore bladder was recorded in order to calculate the velocity and flow rate through the system.

The following equations govern the proposed design of the closed system for optimal extraction of head-driven tidal energy. Since the system is first limited by bladder volume, it is important to create parameters using the following equations to define geometry:

$$A_B = L_B W_B \qquad V_B = A_B H_B$$

Where A_B is the bladder area, L_B length, W_B is width, H_B height, and V_B volume of bladder. For simplification of design, a rectangular cross-sectional area has been used. It is important to note that the bladder shape can be designed to fit any environment.

In order to optimize available power capture, it is necessary to select pipe and convergent nozzle dimensions that increase velocity of constrained fluid while reduces losses that the system experiences during convergence.

$$A_p = \pi r_p^2 \qquad A_n = \pi r_n^2$$

Where A_p is the cross-sectional area of the pipe, r_p is the exit pipe radius, A_n is the cross-sectional area of the convergent nozzle at the exit, and r_n is the radius of the convergent nozzle at the exit.

$$U_p = \sqrt{2g(H_{L,t} - H_{L,t+\Delta t})} \qquad Q = A_p U_p \qquad H_{L,t+\Delta t} = H_{L,t} - \frac{Q\Delta t}{A_B}$$

$$U_p = \sqrt{2g(H_{W,t} - H_{W,t+\Delta t})} \qquad Q = A_p U_p \qquad H_{L,t+\Delta t} = H_{L,t} - \frac{Q\Delta t}{A_B}$$

(White, 2008)

7.1 Analysis of Initial Experimental Results of Tidal System Physical Model

The outlined steps were repeated multiple times for the physical model of the system with and without a turbine applied to the pipes that connect the bladders. The results from this experimental testing are as follows:

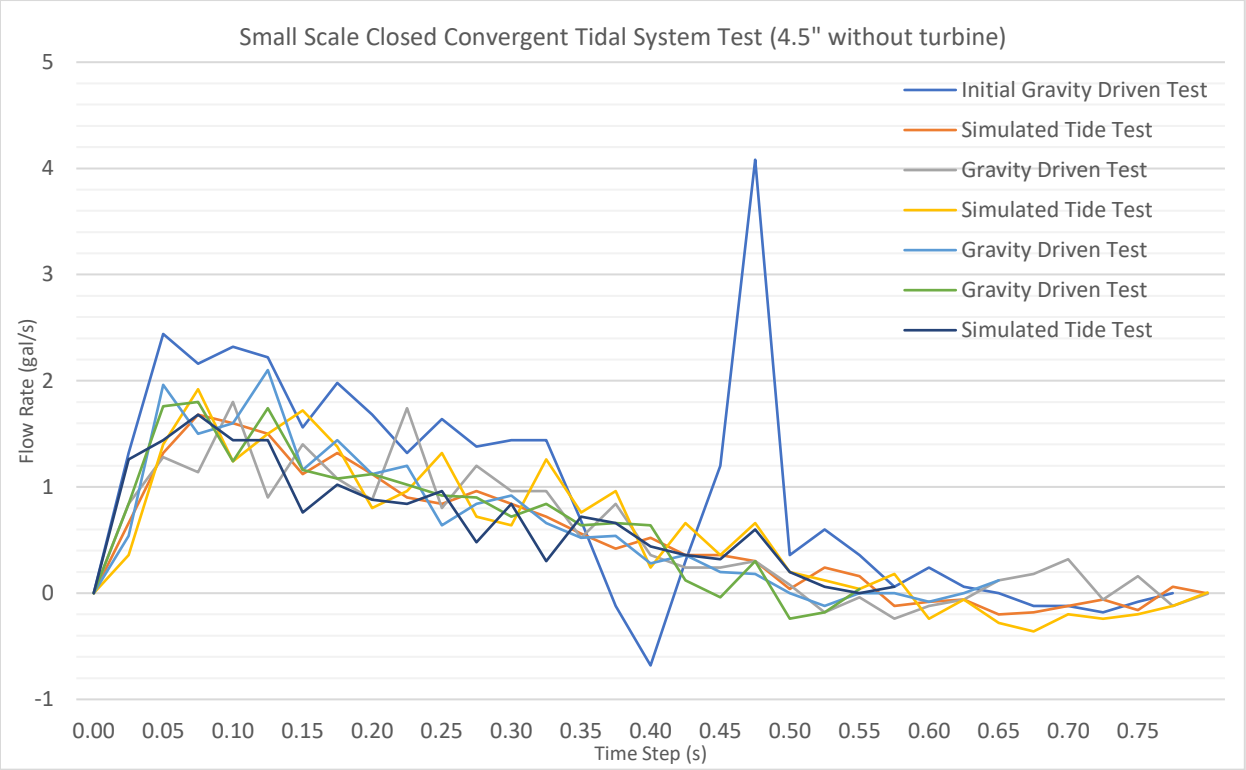

Figure 8: Small Scale Closed Convergent Tidal System Experimental Testing Without Turbine Results

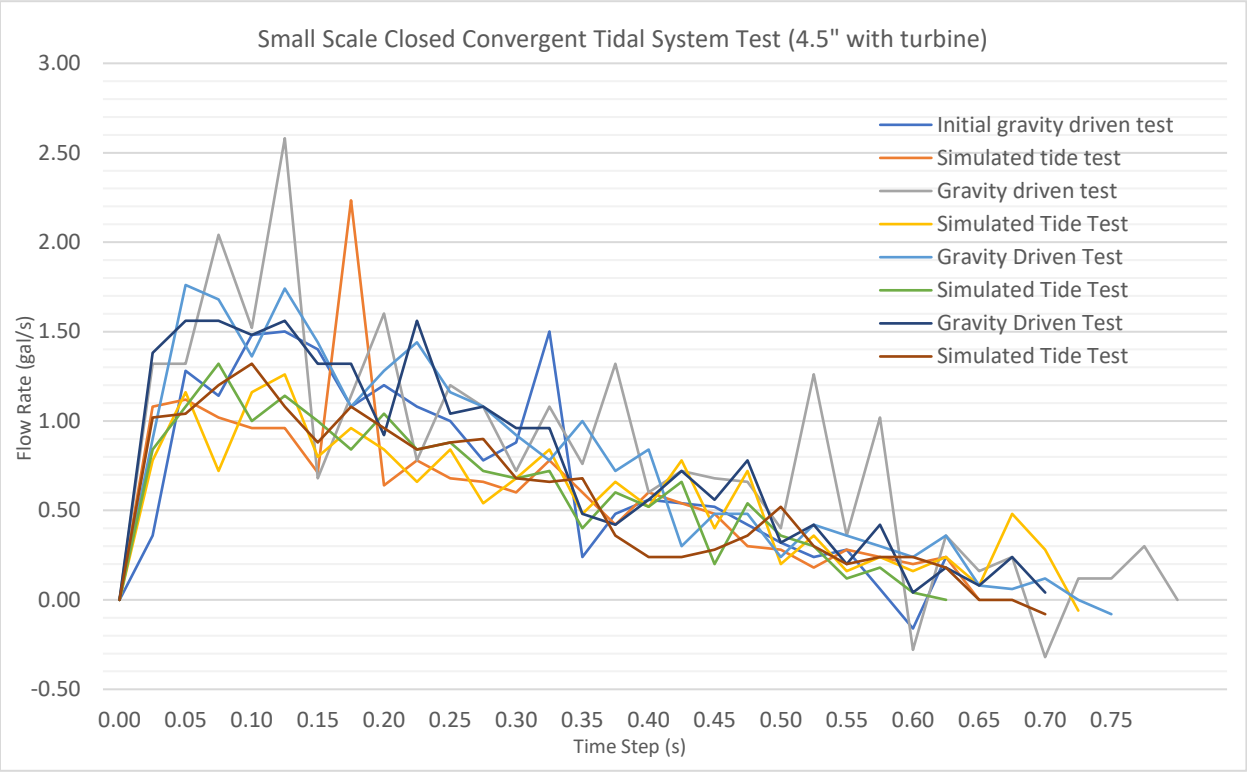

Figure 10: Small Scale Closed Convergent Tidal System Experimental Testing W Turbine Results

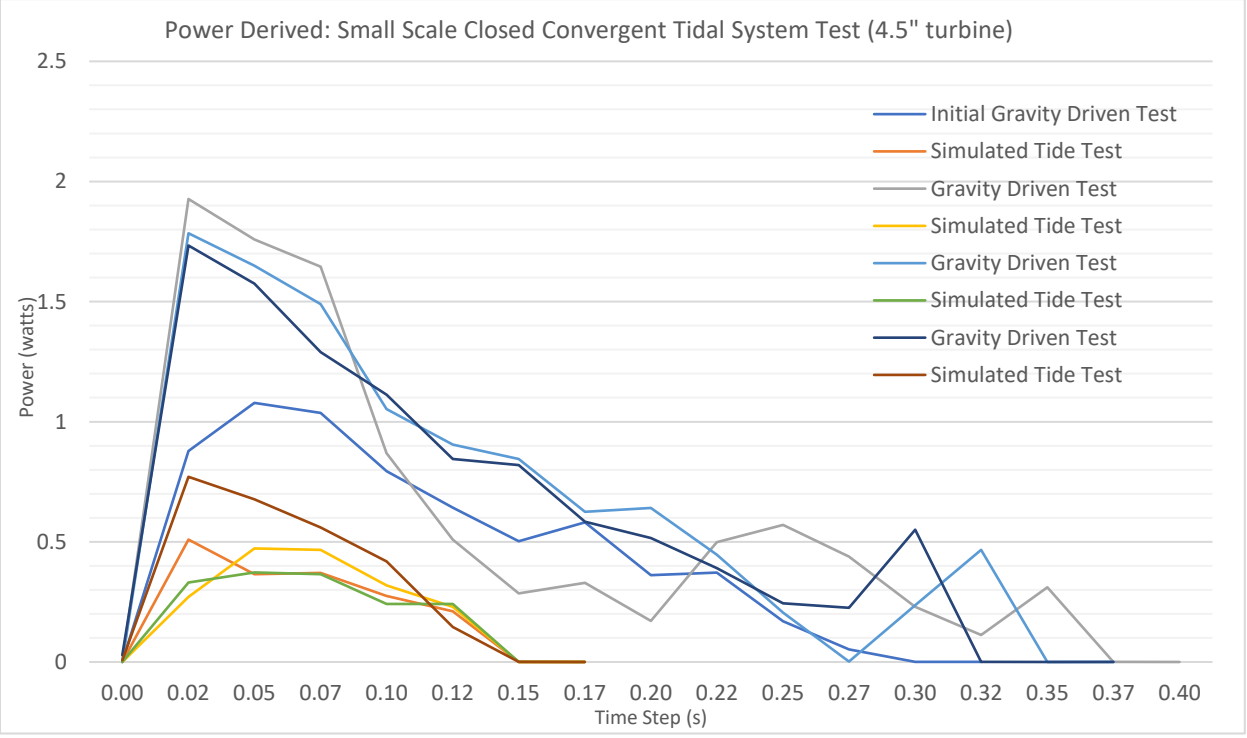

Figure 9: Small Scale Closed Convergent Tidal System Experimental Testing Power Derived

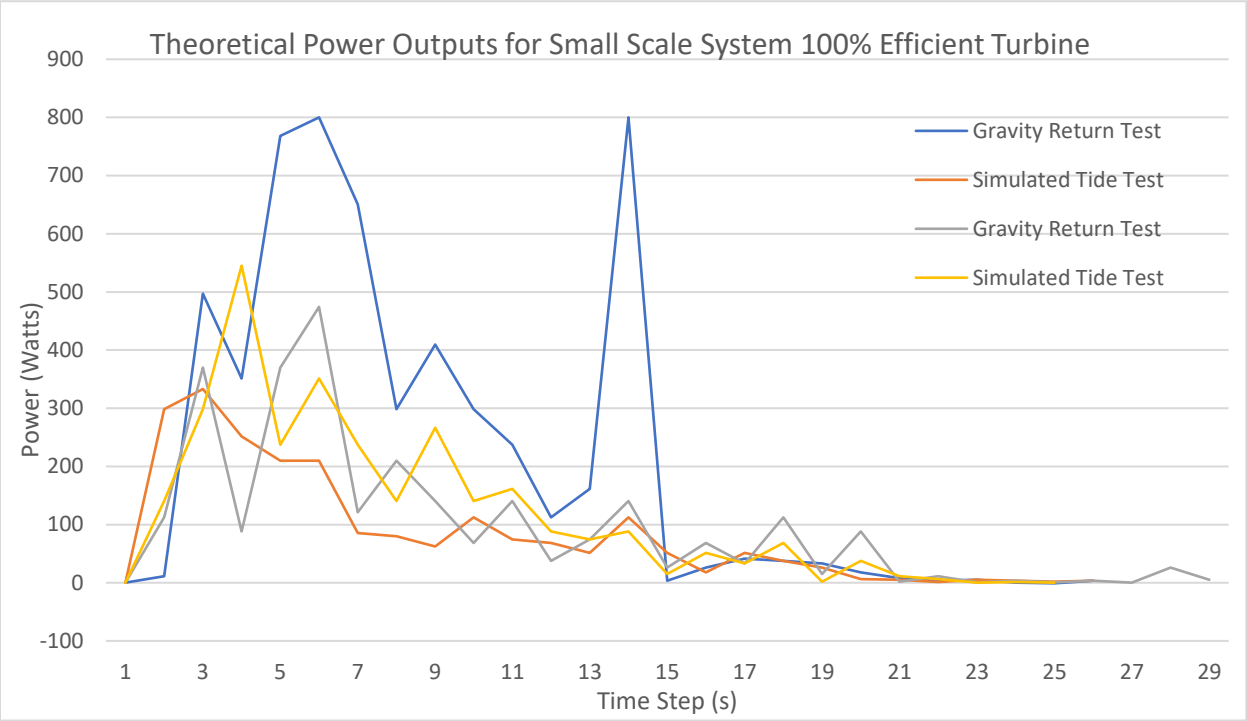

Figure 11: Theoretical power outputs for fluid velocity present in small scale experiment

By utilizing this simplistic physical model to mimic the proposed system at a micro scale, we were able to conclude the following: 1) Utilizing sandbags to model the weight of a water column did apply enough force to push the fluid contained within the bladders against gravity and up to a higher elevation. 2) We can assume that water weight will create the same effects on the system. 3) Power can be derived from a closed system such as the one modeled in the experiment.

During this experiment at a small scale, we were able to observe some events that can be considered a learning experience and collected as we move into larger scale systems. These observations include: 1) Creating a seal between a compliant urethane bladder and rigid PVC flange connection and valve proved very difficult. In larger experiments and builds, these

connection points need to be considered. 2) When the valves were opened the fluid velocity within the system crenates a wave of momentum within the bladder that creates a reflection of water on the backside of the receiving bladder. As the system is designed to be larger, this wave may also grow and could overwhelm the system. 4) The use of 'fabric' nozzles for convergence from the bladder to the turbine rotor was overwhelmed by the reduction in pressure within the system as the velocity increased. This pressure drop caused the unrigid nozzle to fail.

8. CONVERGENT PIPES AND NOZZLES FOR AMPLIFIED FLUID VELOCITY

An important component of the proposed tidal energy capture technology was the application of the conservation of momentum through the use of convergent pipes and or nozzles to increase and optimize the fluid velocity through the turbine sections of the systems. The hypothesis that drives this portion of experimental data is the equation:

$$Q_{in} = Q_{out} = AV$$

Where Q is the volumetric flow rate in and out of the system or pipes, A is the effective area the fluid passed through within the pipe, and V is the fluid velocity. In addition, for the case of pipes in parallel flow the equation:

$$Q_{total} = Q_1 + Q_2 + Q_3 + \cdots Q_n$$

Can be utilized to solve for an idealized flow rate for a system of convergent pipes (White, 2008).

It should be noted that to decrease frictional losses within the exit of the system as the flow is contracted, the reducer or nozzle was constructed using a gradual contraction from entrance diameter to exit diameter. Utilizing this gradual contraction can substantially decrease the energy loss experienced in the system. As the proposed tidal system scales, it will be of importance to monitor and reduce frictional losses where possible.

This experiment tested the hypothesis that the fluid velocity within the pipes could simply be amplified by converging pipes and/or constricting the flow rate using a nozzle. First, the idealized flow rates were calculated using the simplistic equation that states the volumetric flow rate into the system must be equal to the volumetric flow rate out of the system. The planned experiment compares eight different cases of convergence: 1) one pipe with no nozzle, 2) two convergent pipes with no nozzle, 3) three convergent pipes with no nozzle, 4) four convergent

pipes with no nozzle, 5) one pipe with nozzle, 6) two convergent pipes with nozzle, 7) three convergent pipes with nozzle, and 8) four convergent pipes with nozzle. The pipes used for the experiment were 2-inch Schedule 40 PVC, 2-inch WYE connectors, and a manufactured nozzle with gradual slope to minimize turbulence and losses at this connection.

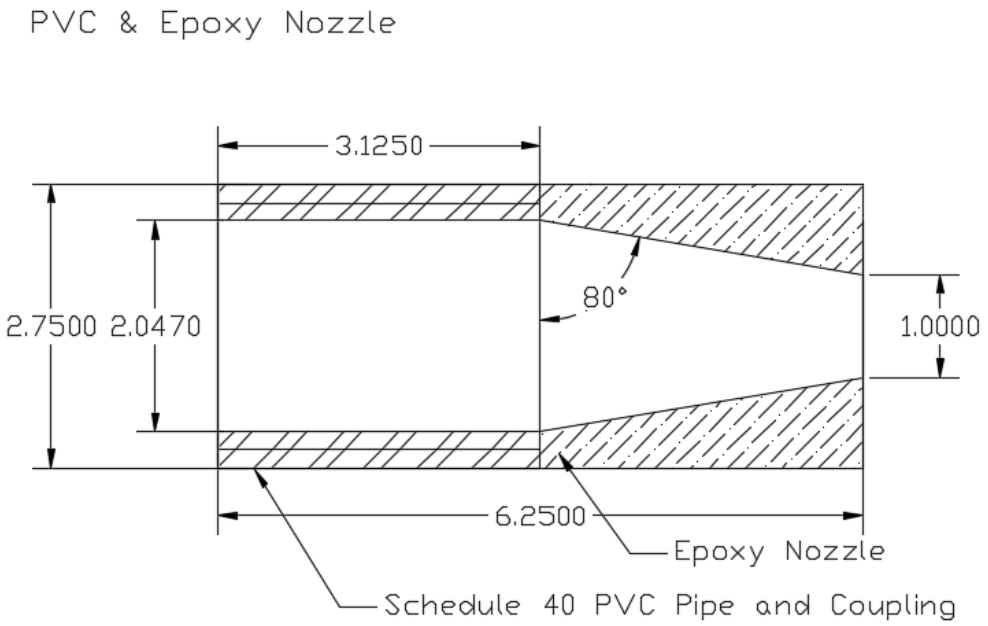

Figure 13: Manufactured PVC and Resin Epoxy Nozzle for Convergence Experiment

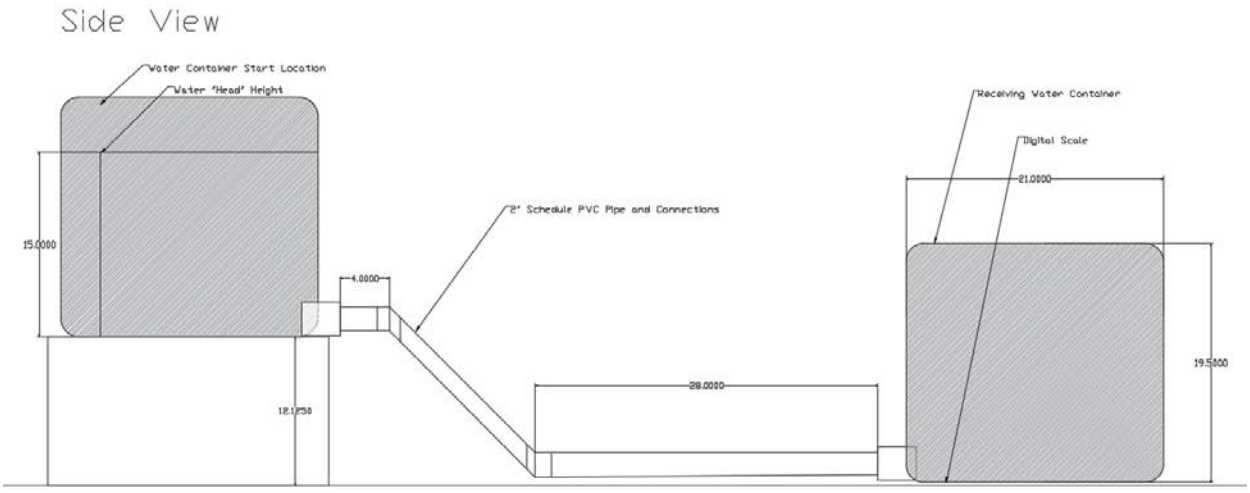

Figure 12: Convergent Flow Experiment Set Up (Side View)

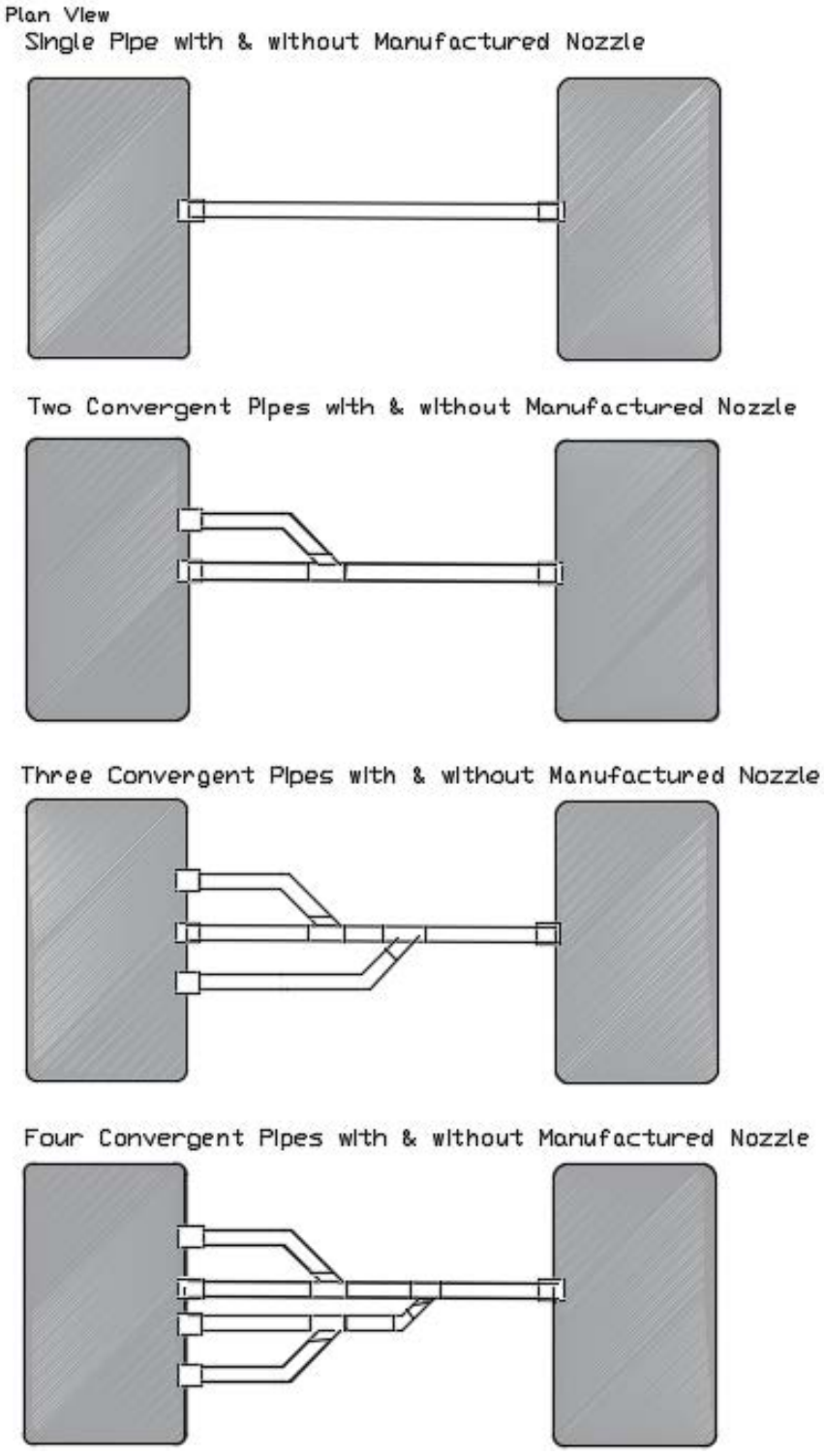

Figure 14: Convergent Flow Experiment Set Up (Plan View)

8.1 Analysis and Results of Convergent Pipes and Nozzle for Amplified Fluid Velocity

The following graph shows the expected theoretical outcomes for the experiment:

As expected, the condition that yields the highest fluid velocity is the four convergent pipes with a nozzle, since this relationship simply relies on the conservation of mass.

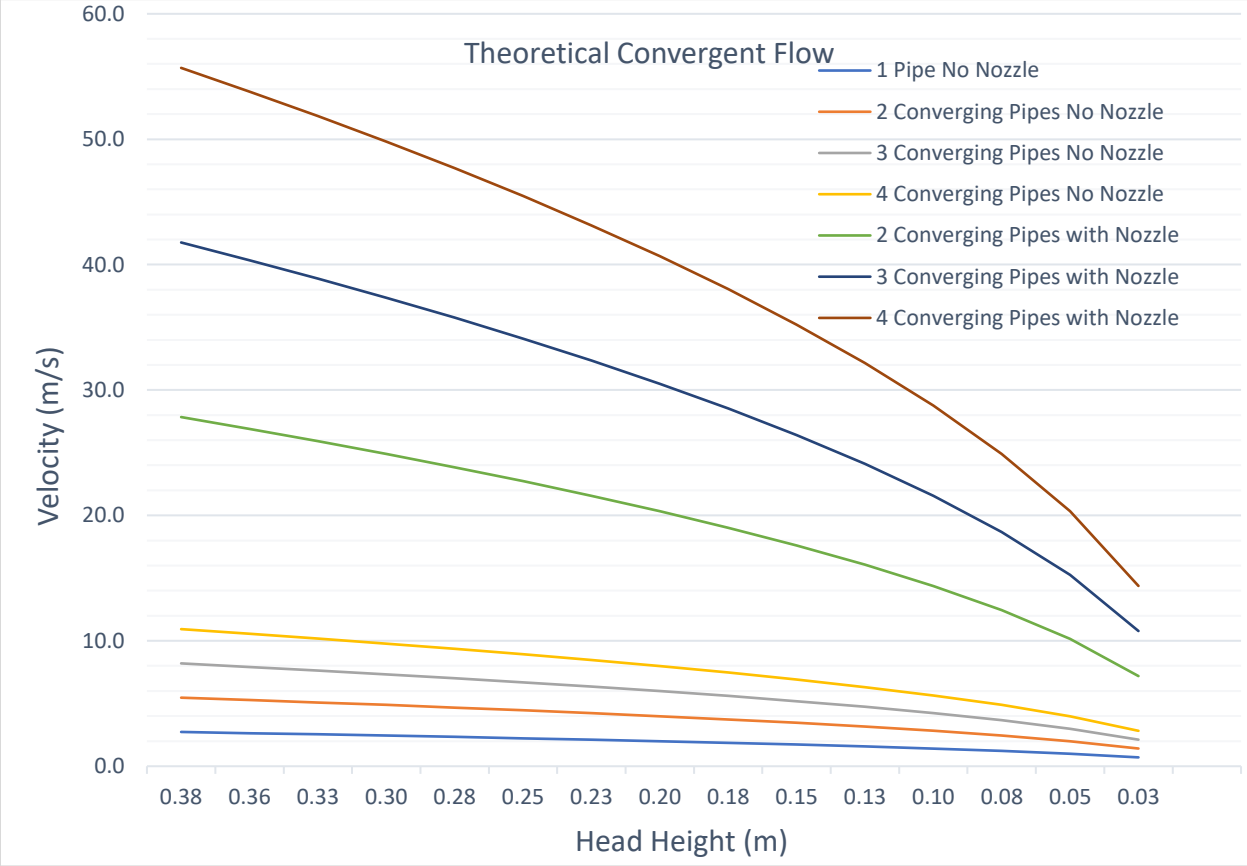

Figure 15: Expected theoretical fluid velocities through the experimental convergent system

However, during experimental application, losses within the flow due to sharp edges of the pipe at the fluid exits, joints, contraction, and friction along the pipe walls were expected. The experiment aimed to determine how loss affects the rate of convergence within the system.

To test this, a simple experiment was designed using the previously mentioned series of pipes. These pipes were the connection point between two containers of fluid. One container was filled while the pipes were closed using sluice valves at each open orifice. Once the container was filled to the test height with fluid, the valves were opened allowing the fluid to move from the higher head container, through a pipe or serious of pipes, and a nozzle or open pipe into the lower head receptacle. A scale was placed under this lower receptacle to measure the change of weight of water in the container over time. This data was then used to calculate the volumetric flow rate experienced by the system and converted into fluid velocity at the entrance point of the lower receptacle.

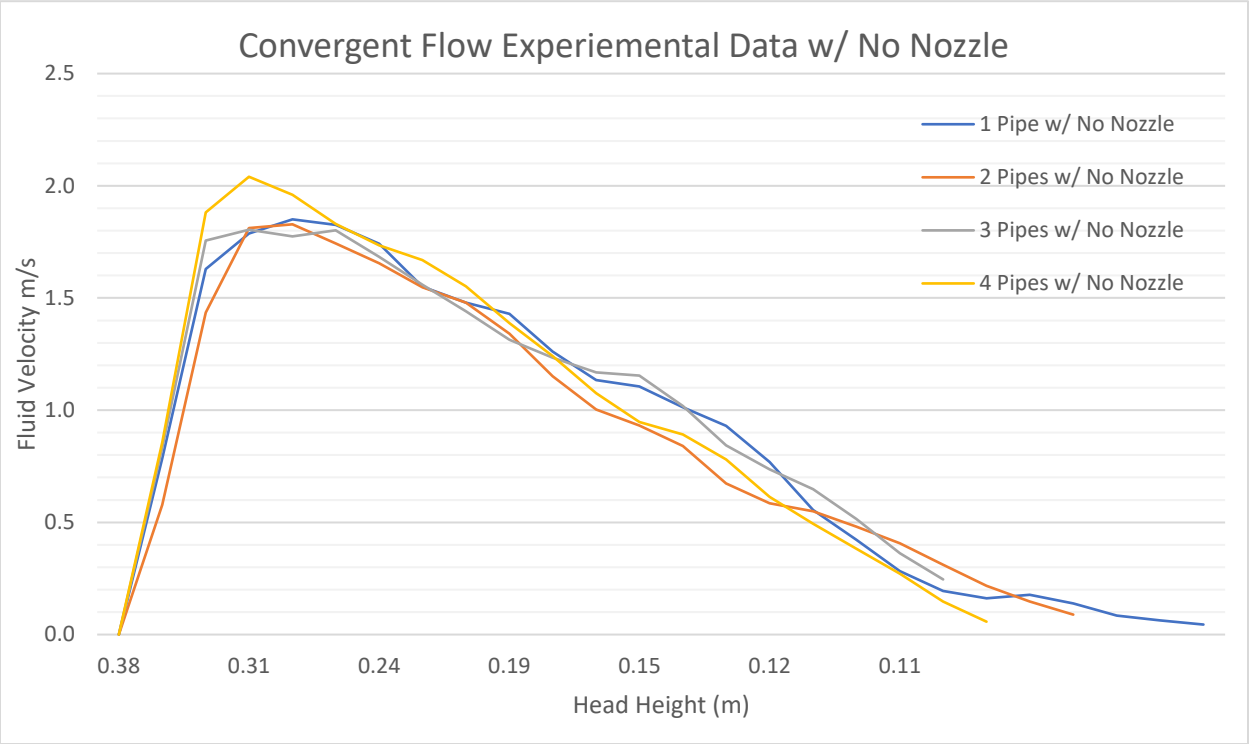

Figure 18: Convergent flow experimental data without nozzle

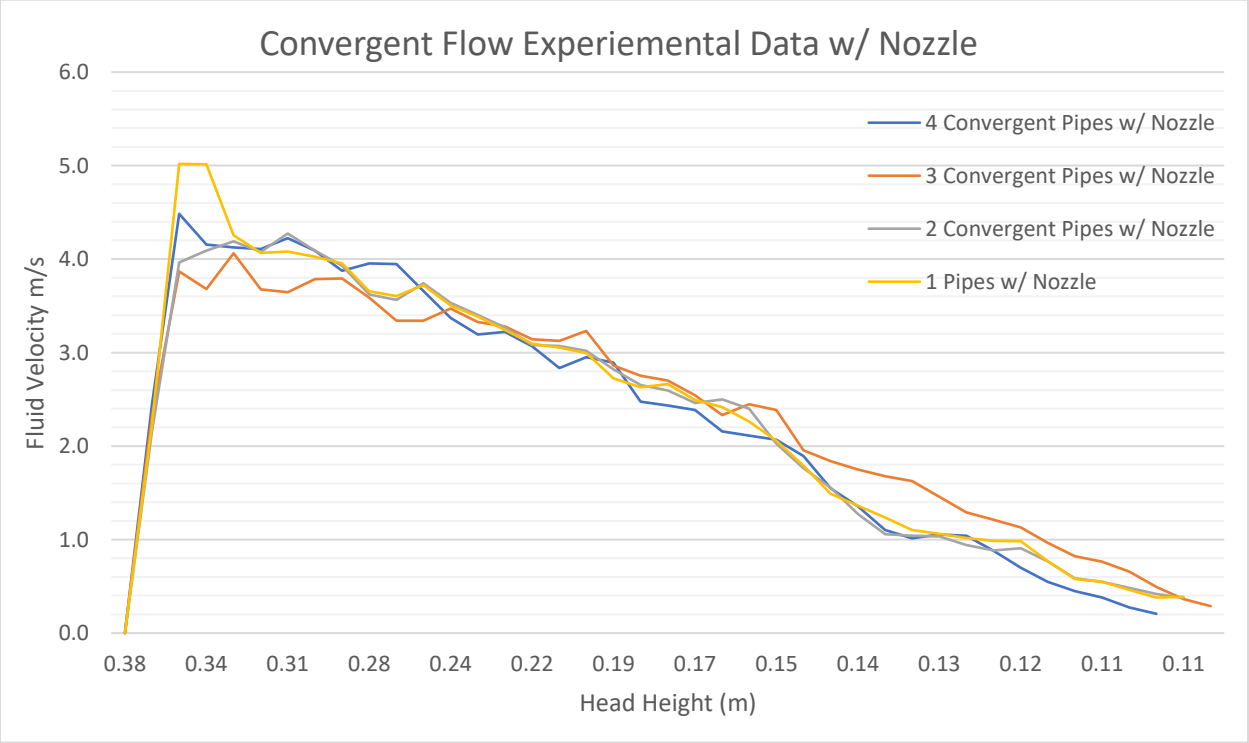

Figure 17: Convergent flow experimental data with nozzle

9. NUMERICAL MODEL SIMULATION OF TIDAL ENERGY SYSTEM

In order to understand how the proposed tidal energy capture system performs at a larger scale, a numerical simulation was created in MATLAB to model a simplistic version. The model takes advantage of the laws of conservation of the volume of fluid and conservation of fluid momentum. In addition, since the tides are being considered for powering the system, a simple relationship of the tidal constituent was be implemented:

$$Y(t) = Hcos(\omega t - \phi)$$

where H is the amplitude, ω is the speed of rotation, t is the time elapsed since the selected starting point and ϕ is the phase lag. It is important to note that in a specific system model, the tidal relationship would require a more detailed analysis that takes into consideration mean spring tides and mean neap tides and multiple tidal constituents for the focus location (Sean Petley, 2015)

The design length, width, and height of the compliant bladders were treated as system inputs as well as the tidal amplitude. The system also allowed for design inputs for pipe diameter and nozzle diameter to optimize the fluid velocity through the turbine(s) within the system. The number of pipes and turbines can also be adjusted within the model to create the desired power output. After the design components were applied, the system ran over the period of one half of a semidiurnal tidal cycle that encompasses a high and low tide peak within 12.41 hours or 44,676 seconds. It is important to note that semidiurnal, diurnal, and mixed semidiurnal tidal conditions can be presented in varying regions (NOAA, 2017).

The simulation then returns the corresponding fluid velocities within the pipe(s) and through the nozzle section(s) along with a power output curve over the high and low tide conditions.

These results are used later in this research to analyse the economic viability of the system compared to other available renewable energy systems.

In order to use data that is specific to the areas of low tidal range, the east coast of Florida, specifically Jacksonville was investigated to use as tidal inputs for the numerical model of the system. Off the coast of Northeast Florida, the tide ranges from approximately 2 meters at high tides and approximately -0.3 meters at low tide. In order to approximate the effective tidal range on the proposed closed convergent system that is being modeled, a tidal range of 1m will be

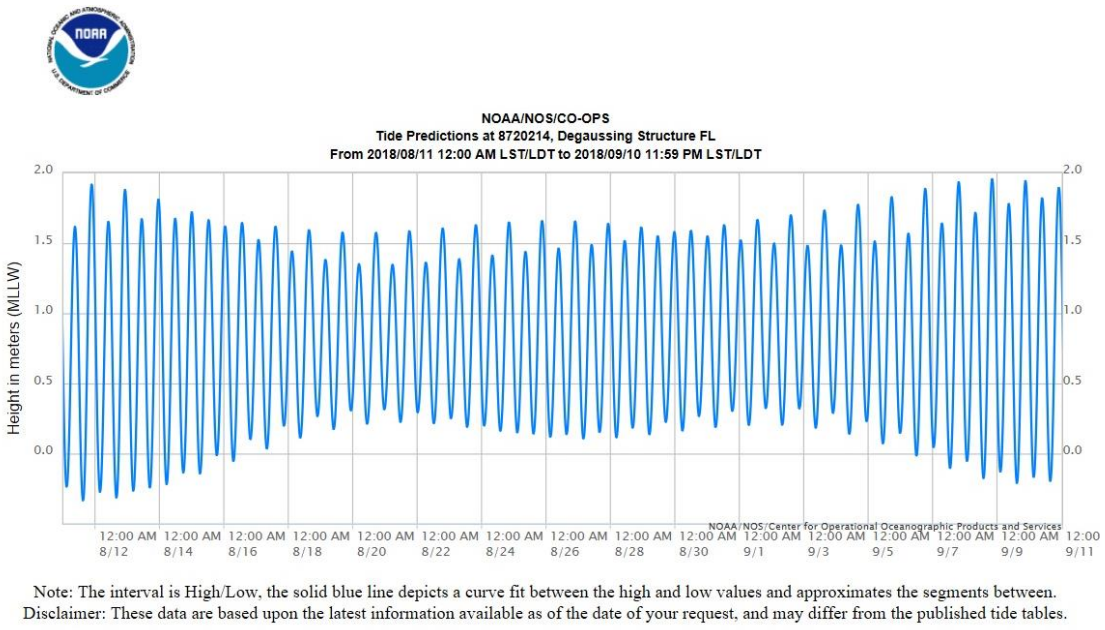

Figure 19: Figure 20: Tidal range data from NOAA station 8720214 (National Oceanic and Atmospheric Administration (NOAA), 2018)

assumed in the model runs for this research. However, the model can be used in future research to determine fluid velocities and power outputs for a variety of tidal ranges.

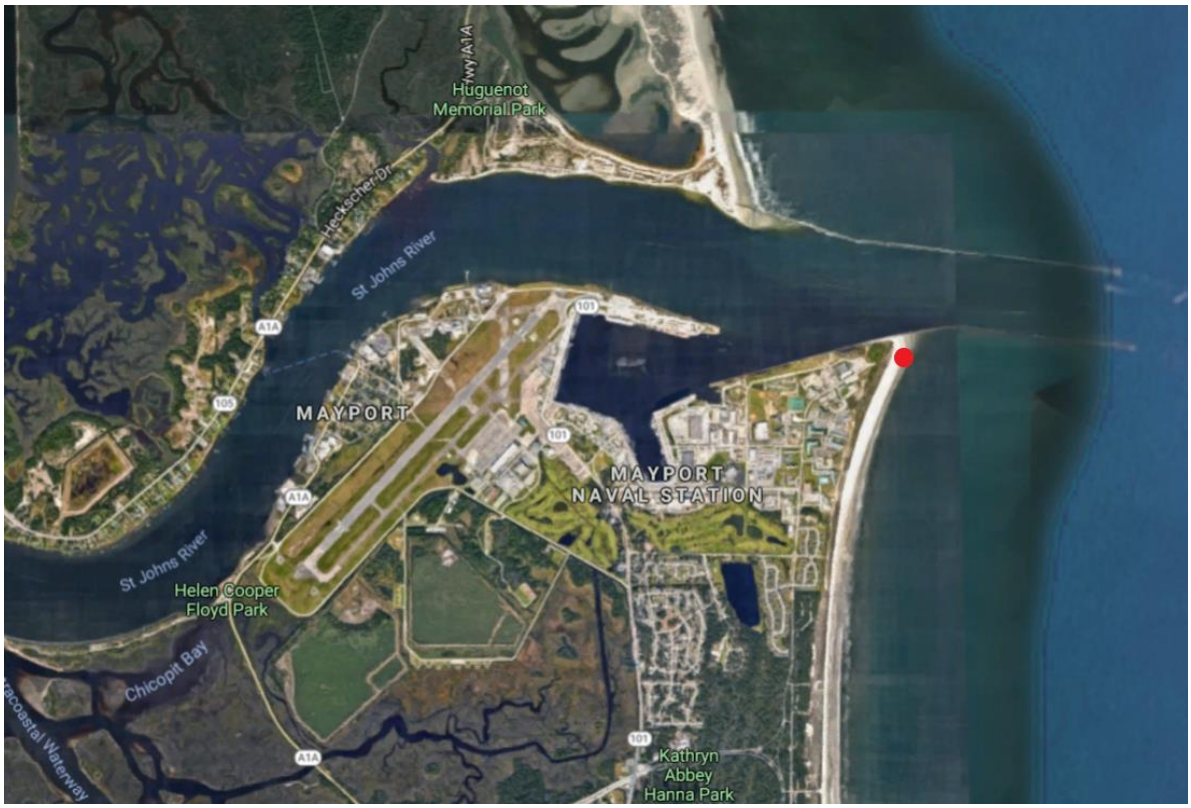

Figure 21: Google map location of NOAA station 8720214 (Google, 2018)

9.1 Analysis and Results and Numerical Model Simulation

The following results were derived from a running a MATLAB numerical simulation of the proposed system:

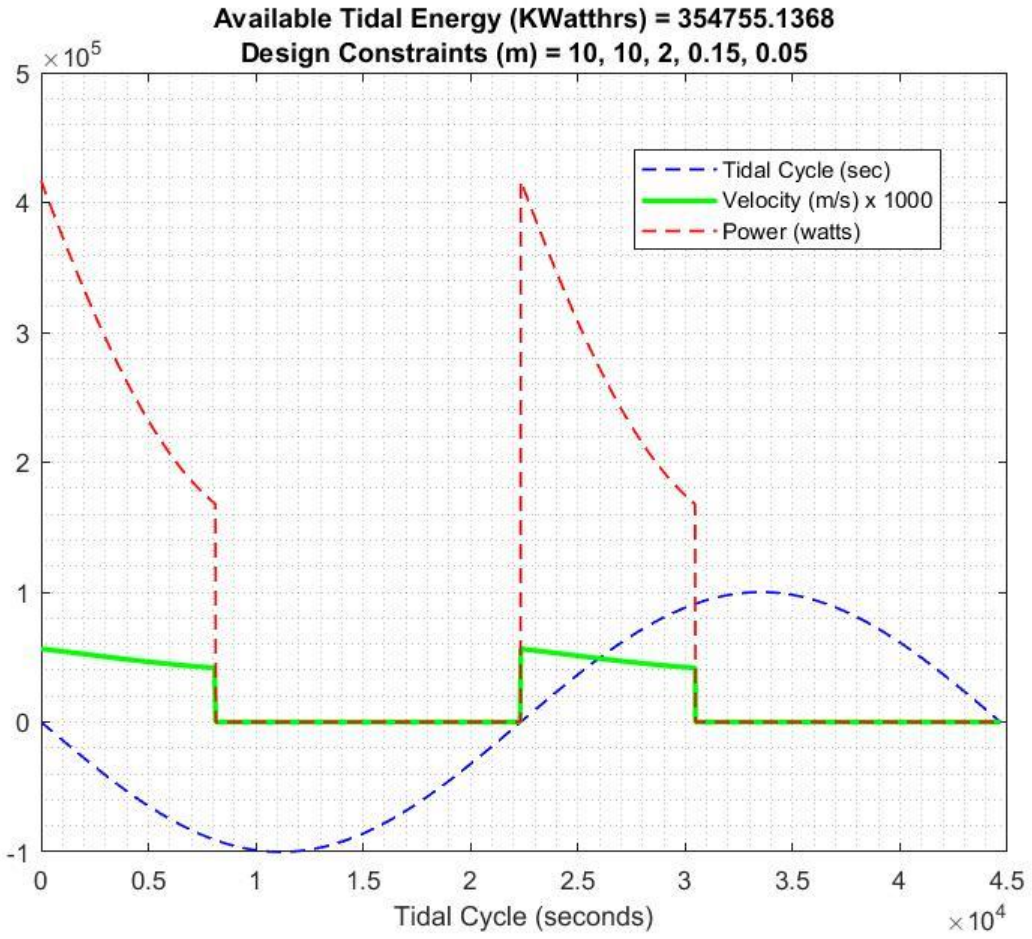

Figure 22: MATLAB Simulation of the proposed tidal system (1)

The above graph illustrates the behavior of a small scale closed convergent tidal system with bladder dimensions 10 m length, 10 m width, and 2 m heights. The nozzle radiuses were 0.2 m and 0.1 m respectively. The tidal amplitude was 1 m and there was 1 turbine in the system. Over the period of a tidal cycle, the system theoretically would produce 354,755 Kilowatt hours or 354 Megawatt hours.

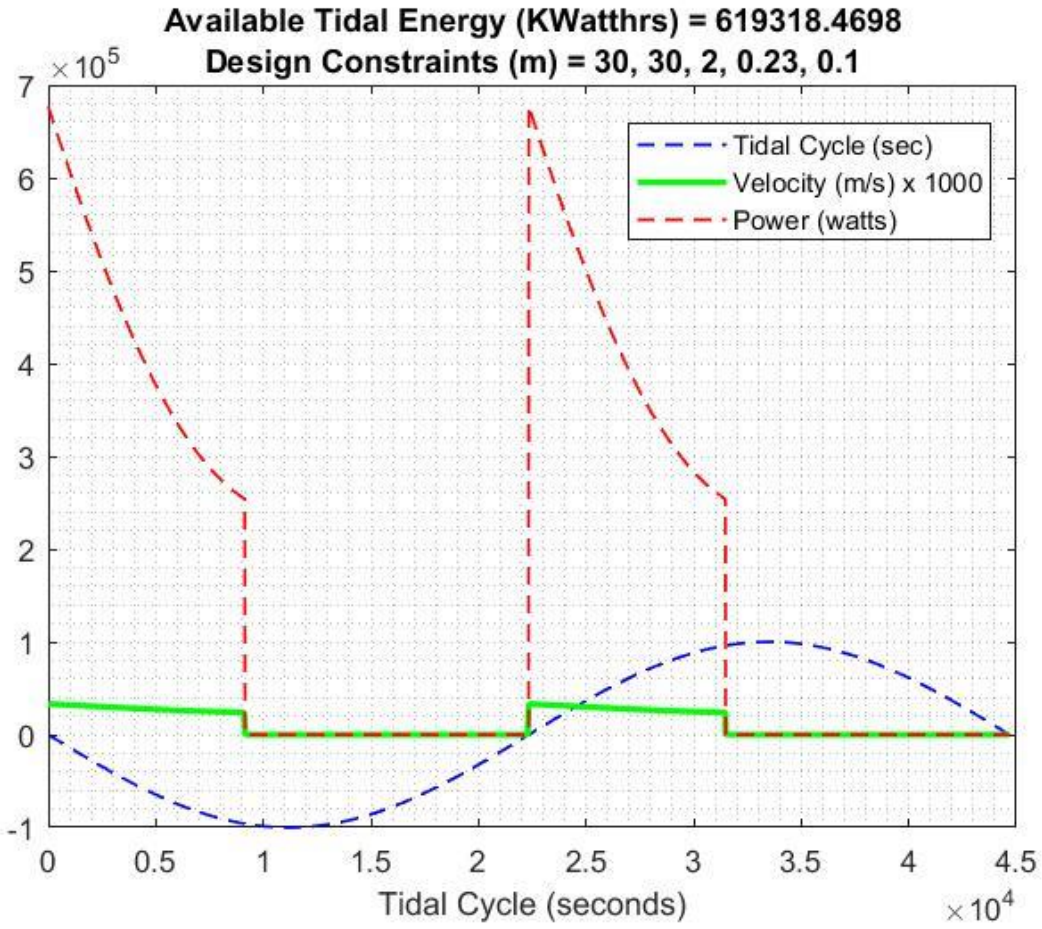

Figure 23: MATLAB Simulation of the proposed tidal system (2)

The above graph illustrates the behavior of a small scale closed convergent tidal system with bladder dimensions 30 m height, 30 m width, and 2 m heights. The nozzle radiuses were 0.23m and 0.1 m respectively. The tidal amplitude was 1 m and there were 2 turbines designed in the system. Over the period of a tidal cycle, the system theoretically would produce 619,318 Kilowatt hours or 619 Megawatt hours.

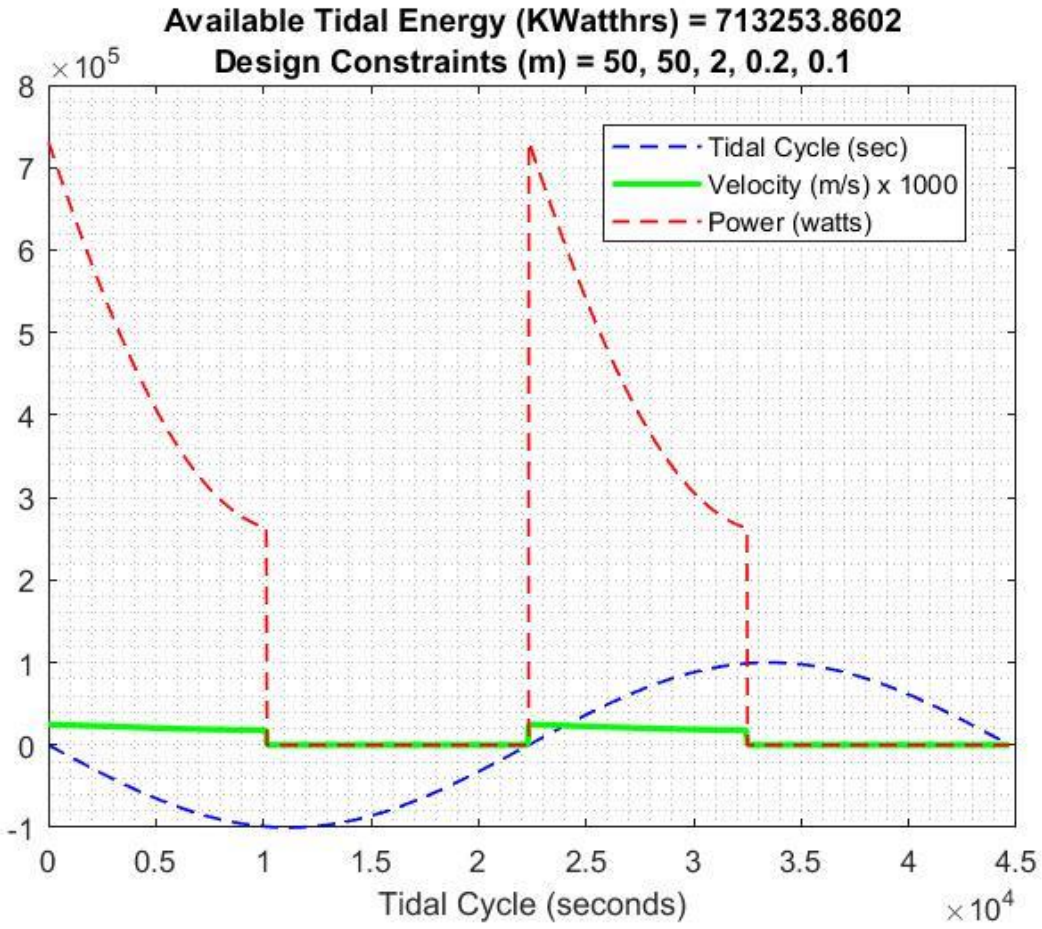

Figure 24: MATLAB Simulation of the proposed tidal system (3)

The above graph illustrates the behavior of an intermediate scale closed convergent tidal system with bladder dimensions 50 m height, 50 m width, and 2 m heights. The nozzle radiuses a were 0.2 m and 0.1 m respectively. The tidal amplitude was 1 m and there were 5 turbines designed in the system. Over the period of a tidal cycle, the system theoretically would produce 713,253 Kilowatt hours or 713 Megawatt hours.

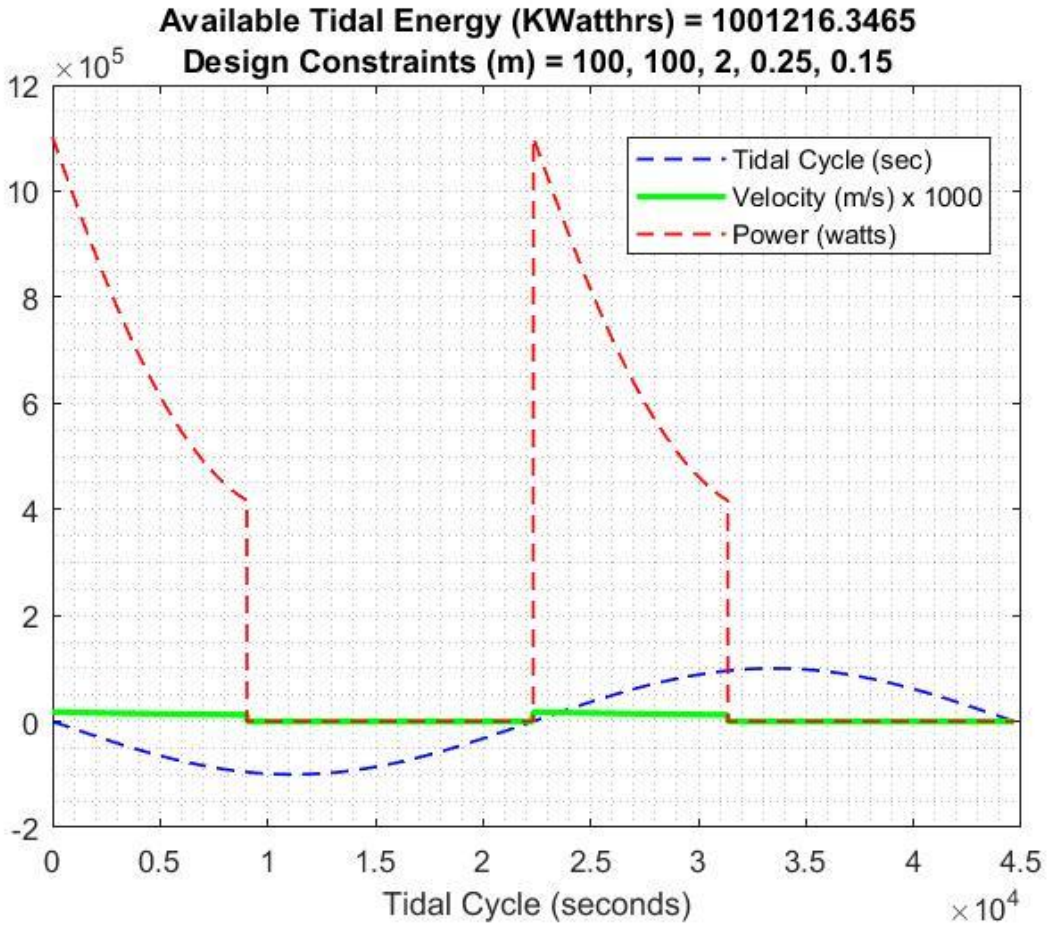

Figure 25: MATLAB Simulation of the proposed tidal system (4)

The above graph illustrates the behavior of an intermediate to large scale closed convergent tidal system with bladder dimensions 100 m height, 100 m width, and 2 m heights. The nozzle radiuses were 0.25 m and 0.15 m respectively. The tidal amplitude was 1 m and there were 10 turbines designed in the system. Over the period of a tidal cycle, the system theoretically would produce 1,001,216 Kilowatt hours or 1,001 Megawatt hours.

It is important to note that this is the first version of a simplistic model to estimate power potentials of the proposed system. The current numerical model assumes an ideal case with turbine efficiency at 100%. When a turbine is selected for an actual system, these values can be added to

the model. In addition, major and minor friction losses are not accounted for in this model. Again, as a system is being designed, this specific data can be calculated, and the power output can be adjusted.

10. ECONOMIC ANALYSIS OF PROPOSED TIDAL SYSTEM

Although many factors must be assessed when determining the viability of a possible new source of electric, the factor that typically governs the success of a system long term is cost. Using the equation below for the Levelized Cost of Electricity or LCOE, an estimated average cost of electricity can be calculated over a lifetime of a system.

$$LCOE = \frac{Sum\ of\ Cost\ Over\ Lifetime}{Sum\ of\ Electricity\ Over\ Lifetime} = \frac{\sum_{t=1}^{n} \frac{I_t + M_t + F_t}{(1+r)^t}}{\sum_{t=1}^{n} \frac{E_t}{(1+r)^t}}$$

Where I_t is the investment expenditures in the year t, M_t are the operation and maintenance expenditure in year t, Ft are the fuel expenditures in the year t (not that with renewable technologies the fuel expenditures are zero, Et is the electrical energy generated in the year t, r is the discount rate applied to the technology, and n is the expected lifetime of the system (U.S. Energy Information Administration, 2017).

10.1 Analysis and Results of Economic Analysis of Proposed Tidal System

This estimated LCOE of the proposed closed convergent tidal system was estimated using figures from the numerical simulation. These values were then scaled down by estimated appropriate turbine efficiencies and capacity factors to determine an estimated annual energy output for a semidiurnal tidal region. These calculations were then estimated over several tidal ranges to account for the different possible applications of the renewable energy system. The initial costs to the system were also estimated and include fabric, turbines, and installation. A more

Table 1: Economic analysis of proposed tidal energy system

Length (m2)	Width (m2)	Foot Print (m2)	Height	Volume (m^3)	Surface Area (m^2)	Fabric Cost ($/$m^2$)	Estimated Turbine Cost	Estimated Installation Cost	Total Estimated Cost	Potential Power (KWhr) .59 Betz Limit	Number of Turbines	Diurinal (MWhr)	Turbine 80%	Capacity Factor 90%
10	10	100	1	100	480	2,400	1,358	20,000	23,758	26.97	1	9.84	7.88	7.09
20	20	400	1	400	1,760	8,800	3,221	30,000	42,021	63.97	1	23.35	18.68	16.81
30	30	900	1	900	3,840	19,200	7,247	40,000	66,447	143.94	1	52.54	42.03	37.83
40	40	1,600	1	1,600	6,720	33,600	12,883	50,000	96,483	255.89	1	93.40	74.72	67.25
50	50	2,500	1	2,500	10,400	52,000	17,708	60,000	129,708	351.74	1	128.39	102.71	92.44
60	60	3,600	1	3,600	14,880	74,400	23,007	70,000	167,407	456.99	1	166.80	133.44	120.10
70	70	4,900	1	4,900	20,160	100,800	30,696	80,000	211,496	609.72	1	222.55	178.04	160.23
100	100	10,000	1	10,000	40,800	204,000	49,723	20,000	273,723	987.64	1	360.49	288.39	259.55
500	500	250,000	1	250,000	1,004,000	5,020,000	99,462	200,000	5,319,462	1975.61	2	721.10	576.88	519.19
1,000	1,000	1,000,000	1	1,000,000	4,008,000	20,040,000	149,193	500,000	20,689,193	2963.42	3	1081.65	865.32	778.79
									AVERAGE	783.59	1.30	286.01	228.81	205.93

Length (m2)	Width (m2)	Foot Print (m2)	Height	Volume (m^3)	Surface Area (m^2)	Fabric Cost ($/$m^2$)	Estimated Turbine Cost	Estimated Installation Cost	Total Estimated Cost	Potential Power (KWhr) .59 Betz Limit	Number of Turbines	Diurinal (MWhr)	Turbine 80%	Capacity Factor 90%
10	10	100	2	200	560	2,800	5,700	20,000	28,500	113.22	1	41.32	33.06	29.75
20	20	400	2	800	1,920	9,600	16,526	30,000	56,126	328.25	1	119.81	95.85	86.26
30	30	900	2	1,800	4,080	20,400	37,183	40,000	97,583	738.56	1	269.57	215.66	194.09
40	40	1,600	2	3,200	7,040	35,200	66,103	50,000	151,303	1313.01	1	479.25	383.40	345.06
50	50	2,500	2	5,000	10,800	54,000	103,286	60,000	217,286	2051.57	1	748.82	599.06	539.15
60	60	3,600	2	7,200	15,360	76,800	148,732	70,000	295,532	2954.26	1	1078.30	862.64	776.38
70	70	4,900	2	9,800	20,720	103,600	202,441	80,000	386,041	4021.08	1	1467.69	1174.16	1056.74
100	100	10,000	2	20,000	41,600	208,000	320,562	20,000	548,562	6367.33	1	2324.08	1859.26	1673.33
500	500	250,000	2	500,000	1,008,000	5,040,000	641,124	200,000	5,881,124	12734.66	2	4648.15	3718.52	3346.67
1,000	1,000	1,000,000	2	2,000,000	4,016,000	20,080,000	961,686	500,000	21,541,686	19101.99	3	6972.23	5577.78	5020.00
									AVERAGE	4972.39	1.30	1814.92	1451.94	1306.74

Length (m2)	Width (m2)	Foot Print (m2)	Height	Volume (m^3)	Surface Area (m^2)	Fabric Cost ($/$m^2$)	Estimated Turbine Cost	Estimated Installation Cost	Total Estimated Cost	Potential Power (KWhr) .59 Betz Limit	Number of Turbines	Diurinal (MWhr)	Turbine 80%	Capacity Factor 90%
10	10	100	3	300	640	3,200	13,096	20,000	36,296	260.12	1	94.94	75.96	68.36
20	20	400	3	1,200	2,080	10,400	41,374	30,000	81,774	821.82	1	299.96	239.97	215.97
30	30	900	3	2,700	4,320	21,600	93,093	40,000	154,693	1849.10	1	674.92	539.94	485.94
40	40	1,600	3	4,800	7,360	36,800	165,498	50,000	252,298	3287.29	1	1199.86	959.89	863.90
50	50	2,500	3	7,500	11,200	56,000	258,591	60,000	374,591	5136.39	1	1874.78	1499.83	1349.84
60	60	3,600	3	10,800	15,840	79,200	372,370	70,000	521,570	7396.40	1	2699.69	2159.75	1943.77
70	70	4,900	3	14,700	21,280	106,400	506,837	80,000	693,237	10067.32	1	3674.57	2939.66	2645.69
100	100	10,000	3	30,000	42,400	212,000	722,591	20,000	954,591	14352.84	1	5238.79	4191.03	3771.93
500	500	250,000	3	750,000	1,012,000	5,060,000	1,445,183	200,000	6,705,183	28705.69	2	10477.58	8382.06	7543.86
1,000	1,000	1,000,000	3	3,000,000	4,024,000	20,120,000	2,167,775	500,000	22,787,775	43058.54	3	15716.37	12573.09	11315.78
									AVERAGE	11493.55	1.30	4195.15	3356.12	3020.51

Table 2: Economic analysis of proposed tidal energy system (cont.)

acity r 90%	Annual Energy Production Semidiurnal (MWhr)	Annual Energy Production Semidiurnal (kWhr)	Turbine 80%	Capacity Factor 90%	Turbine 60%	Capacity Factor 80%	Estimated Cost per kWh	Scaled Estimated Cost Per KWh	Scaled Estimated Cost Per KWh
7.09	19.7	19688.1	15.8	14.2	11.8	9.5	0.048268	0.067039	0.100559
16.81	46.7	46698.1	37.4	33.6	28.0	22.4	0.035993	0.049991	0.074986
37.83	105.1	105076.2	84.1	75.7	63.0	50.4	0.025295	0.035131	0.052697
67.25	186.8	186799.7	149.4	134.5	112.1	89.7	0.02066	0.028695	0.043042
92.44	256.8	256770.2	205.4	184.9	154.1	123.2	0.020206	0.028064	0.042096
20.10	333.6	333602.7	266.9	240.2	200.2	160.1	0.020073	0.027879	0.041818
60.23	445.1	445095.6	356.1	320.5	267.1	213.6	0.019007	0.026398	0.039598
59.55	721.0	720977.2	576.8	519.1	432.6	346.1	0.015186	0.021092	0.031638
19.19	1442.2	1442195.3	1153.8	1038.4	865.3	692.3	0.147538	0.204914	0.307371
78.79	2163.3	2163293.3	1730.6	1557.6	1298.0	1038.4	0.38255	0.531319	0.796979
05.93	572.02	572019.64	457.62	411.85	343.21	274.57	0.073	0.102	0.153

acity r 90%	Annual Energy Production Semidiurnal (MWhr)	Annual Energy Production Semidiurnal (kWhr)	Turbine 80%	Capacity Factor 90%	Turbine 60%	Capacity Factor 80%	Estimated Cost per kWh	Scaled Estimated Cost Per KWh	Scaled Estimated Cost Per KWh
29.75	82.6	82647.2	66.1	59.5	49.6	39.7	0.013793	0.019158	0.028736
86.26	239.6	239622.5	191.7	172.5	143.8	115.0	0.009369	0.013013	0.019519
34.09	539.1	539148.8	431.3	388.2	323.5	258.8	0.00724	0.010055	0.015083
45.06	958.5	958497.3	766.8	690.1	575.1	460.1	0.006314	0.00877	0.013155
39.15	1497.6	1497646.1	1198.1	1078.3	898.6	718.9	0.005803	0.00806	0.01209
76.38	2156.6	2156609.8	1725.3	1552.8	1294.0	1035.2	0.005481	0.007613	0.01142
56.74	2935.4	2935388.4	2348.3	2113.5	1761.2	1409.0	0.005261	0.007306	0.010959
73.33	4648.2	4648150.9	3718.5	3346.7	2788.9	2231.1	0.004721	0.006557	0.009835
46.67	9296.3	9296301.8	7437.0	6693.3	5577.8	4462.2	0.025305	0.035146	0.052719
20.00	13944.5	13944452.0	11155.6	10040.0	8366.7	6693.3	0.061793	0.085823	0.128735
06.74	3629.85	3629846.47	2903.88	2613.49	2177.91	1742.33	0.015	0.020	0.030

acity r 90%	Annual Energy Production Semidiurnal (MWhr)	Annual Energy Production Semidiurnal (kWhr)	Turbine 80%	Capacity Factor 90%	Turbine 60%	Capacity Factor 80%	Estimated Cost per kWh	Scaled Estimated Cost Per KWh	Scaled Estimated Cost Per KWh
58.36	189.9	189887.6	151.9	136.7	113.9	91.1	0.007646	0.010619	0.015929
15.97	599.9	599928.6	479.9	431.9	360.0	288.0	0.005452	0.007573	0.011359
85.94	1349.8	1349843.0	1079.9	971.9	809.9	647.9	0.004584	0.006367	0.00955
63.90	2399.7	2399721.7	1919.8	1727.8	1439.8	1151.9	0.004205	0.005841	0.008761
49.84	3749.6	3749564.7	2999.7	2699.7	2249.7	1799.8	0.003996	0.00555	0.008325
43.77	5399.4	5399372.0	4319.5	3887.5	3239.6	2591.7	0.003864	0.005367	0.00805
45.69	7349.1	7349143.6	5879.3	5291.4	4409.5	3527.6	0.003773	0.005241	0.007861
71.93	10477.6	10477573.2	8382.1	7543.9	6286.5	5029.2	0.003644	0.005062	0.007592
43.86	20955.2	20955153.7	16764.1	15087.7	12573.1	10058.5	0.012799	0.017777	0.026665
15.78	31432.7	31432733.5	25146.2	22631.6	18859.6	15087.7	0.028999	0.040276	0.060414
20.51	8390.29	8390292.16	6712.23	6041.01	5034.18	4027.34	0.008	0.011	0.016

in-depth cost analysis would be necessary in the future that includes land, and land development, operation and maintenance.

This initial estimation of the LCOE of the proposed closed convergent tidal energy system was estimated to show there is a great possibility that the technology could compete with other renewable energy systems and even fossil fuels. The graph below is a representation of energy costs across the sector and gives an approximation on where the proposed system would rank among other competitors.

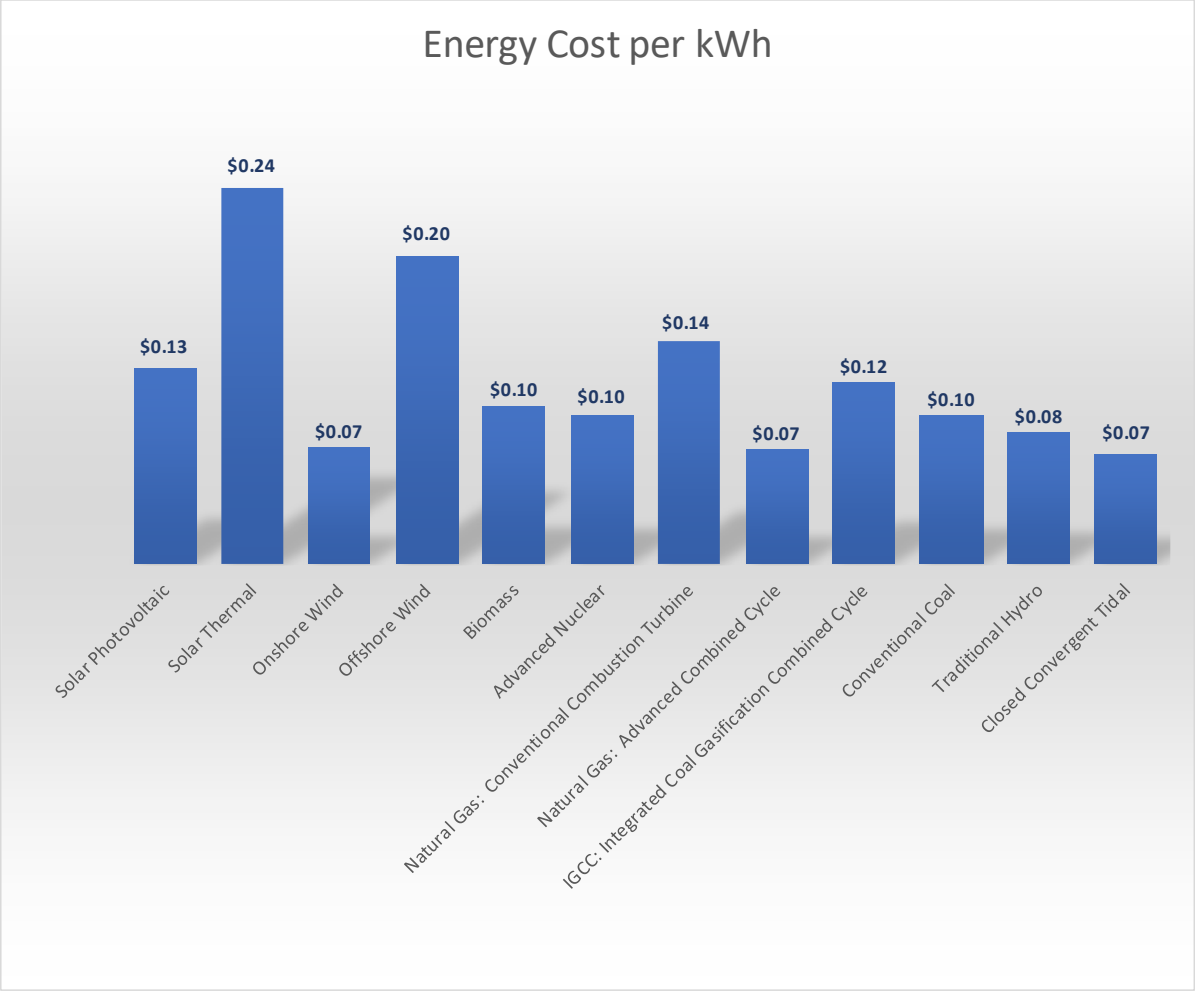

Figure 26: LCOE cost comparison of proposed tidal system to other energy systems (Institute for Energy Research, 2009)

Although the cost analysis is preliminary and would require years of energy production data and more site location costs included, the proposed tidal energy system appears to rank on par with conventional hydropower dams and even comes in as an equal to onshore wind and natural gas.

10 PROVISIONAL AND UTILITY PATENTS FOR PROPOSED ENERGY SYSTEM

The proposed closed convergent tidal energy system takes concepts that have been utilized in past systems and then incorporates novel ideas that allow it to be implemented in low tidal range

regions that would not be viable locations for traditional and current hydropower and tidal energy applications. In addition, the proposed system overcomes many of the pitfalls of present systems. For these reasons, it was necessary to protect the intellectual property being investigated through the creation of a Provision and then subsequent Utility Patent through the University of North Florida's Office of Sponsored Research.

This process included identifying the patentable ideas associated with the proposed tidal system and identifying how the system is different from the previous systems.

Although the patent has been submitted for international protection, it is not yet submitted to any nation's patent office for review. Until this process is complete, it is imperative for the patent draft to be kept from the public record. However, a confirmation of international submittal has been included for record in APPENDIX 21.

11 PLAN FOR INTERMEDIATE SCALE TESTING OF TIDAL SYSTEM

As a final step, of this body of work and part of the potential transition to an operational system, an intermediate scale testing of the system was designed, constructed and minimally tested. The aim of this last work was to initiate tests at a larger scale and inspire more research and investigation into specific pieces of the system that required in-depth study.

11.1 Intermediate Scale Testing Head-Driven Test

The following diagram illustrates an experiment that was created in order to test the effectiveness of a weight in the form of a column of water acting on a compliant structure.

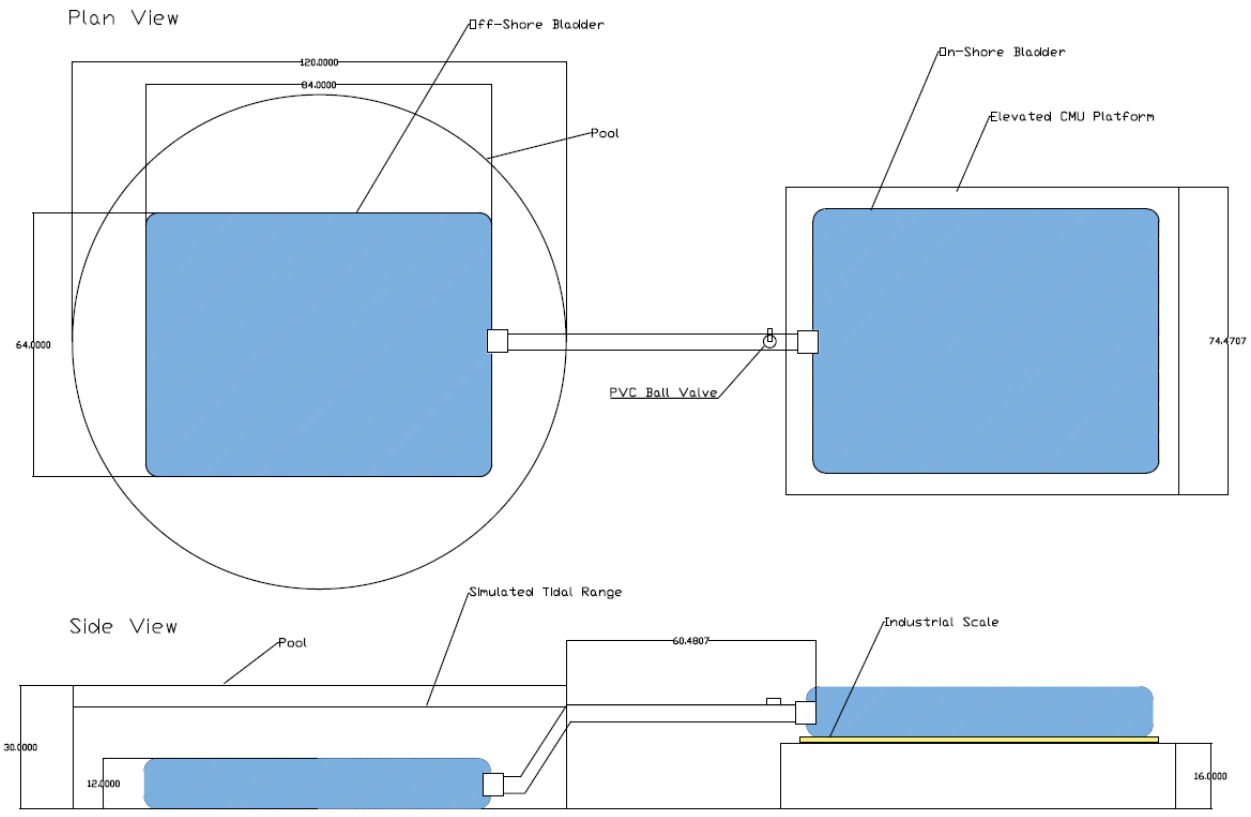

Figure 27: Intermediate testing experiment to demonstrate flow against gravity forced by water column

The aforementioned “HUSKY” brand bladders with part number BT-250V30 were again utilized in this experiment. In order to mimic a tidal head differential, the offshore bladder was placed inside of an above ground pool. This allowed the experimenter to manipulate the tidal head and then measure its effective forcing on the compliant structure. Again, an industrial scale was utilized under the onshore bladder. This allowed for measurements of change of weight of water over time and then results in a conversion to fluid velocity through the entrance pipe via these calculations. The setup also gave the experimenter the ability to change onshore bladder elevations and adjust the slope of the pipe to study the effects on the system.

11.2 Results and Analysis of Intermediate Scale Testing Head-Driven Test

The following data was collected after conducting one field test on the experimental set up with an approximate water of 36 inches from the bottom of the pool. The offshore bladder was filled with water to it approximate maximum fill height of 12 inches, resulting in an effective head height of 24 inches applying force to the bladder. Note that during this experiment, the buoyancy of the fabric bladder caused the bladder to rise to the top of the water column. To overcome this force, 4 ten-pound weights were attached to the top of the bladder. This experiment revealed the necessity for a well-designed mooring system when deployed that overcomes the system buoyancy forces.

Table 3: Initial results from head driven closed convergent tidal experiment

	4" Schedule 40 PVC Test Segment							
Time Step	Weight	Adj Wt	Weight	Flow Rate	Flow rate	Area of exit	Velocity =q/a	velocity
s	lb	lb	gal	gal/s	in3/s	in2	in/s	m/s
0.00	5	0	0.00	0.00	0.0	12.6	0.0	0.00
0.02	6	1	0.12	0.06	13.9	12.6	1.1	0.03
0.05	12	7	0.84	0.24	55.5	12.6	4.4	0.11
0.07	19	14	1.68	0.42	97.1	12.6	7.7	0.20
0.10	26	21	2.52	0.28	64.7	12.6	5.1	0.13
0.12	42	37	4.44	0.96	221.8	12.6	17.7	0.45
0.15	76	71	8.52	1.36	314.3	12.6	25.0	0.64
0.17	109	104	12.48	1.98	457.6	12.6	36.4	0.92
0.20	175	170	20.41	2.64	610.1	12.6	48.5	1.23
0.22	210	205	24.61	2.10	485.3	12.6	38.6	0.98
0.25	289	284	34.09	3.16	730.3	12.6	58.1	1.48
0.27	321	316	37.94	1.92	443.7	12.6	35.3	0.90
0.30	401	396	47.54	3.20	739.5	12.6	58.8	1.49
0.32	469	464	55.70	4.08	942.9	12.6	75.0	1.91
0.35	534	529	63.51	2.60	600.8	12.6	47.8	1.21
0.37	585	580	69.63	3.06	707.1	12.6	56.3	1.43
0.40	650	645	77.43	2.60	600.8	12.6	47.8	1.21
0.42	778	773	92.80	7.68	1774.8	12.6	141.2	3.59
0.45	875	870	104.44	3.88	896.6	12.6	71.4	1.81
0.47	927	922	110.68	3.12	721.0	12.6	57.4	1.46
0.50	995	990	118.85	2.72	628.6	12.6	50.0	1.27
0.52	1051	1046	125.57	3.36	776.5	12.6	61.8	1.57
0.55	1121	1116	133.97	2.80	647.1	12.6	51.5	1.31

As the data reveals, the forcing of the water column does indeed drive the fluid within the offshore bladder up to the onshore bladder against gravity. More experiments are required to understand the relationship between applied head height, pipe distance, pipe slope, and onshore bladder height differential and their effect on fluid velocity as it moves through the system. To limit variables, convergence is neglected in this experiment but could be added and studied more fully.

11.3 Intermediate Scale Test to Investigate Convergence on a Turbine

In an attempt to understand the effects of convergence of fluid and it interfaces with a turbine to produce electricity, one more experiment was created. This setup was created with the hopes of more research encompassing the specific physics of convergence on a turbine, how to maximize and optimize the effective fluid velocity, and how to minimize losses within the system at this point of convergence.

In this experimental setup, an above ground pool was utilized to mimic one of the system bladders. As pipe was fixed to the perimeter wall to allow water to flow out. This 12-inch Schedule 40 PVC connected to a 12 inch to 10-inch PVC pipe reducer. The purpose of the reducer is to lower the exit area and then, in turn, increase the fluid velocity as it meets the hydro turbine that is installed within the following 10-inch Schedule 40 PVC pipe. This final length of pipe empties into a catch pool that allows for the water to be recycled between experimental runs. The following diagram illustrates the experimental set up:

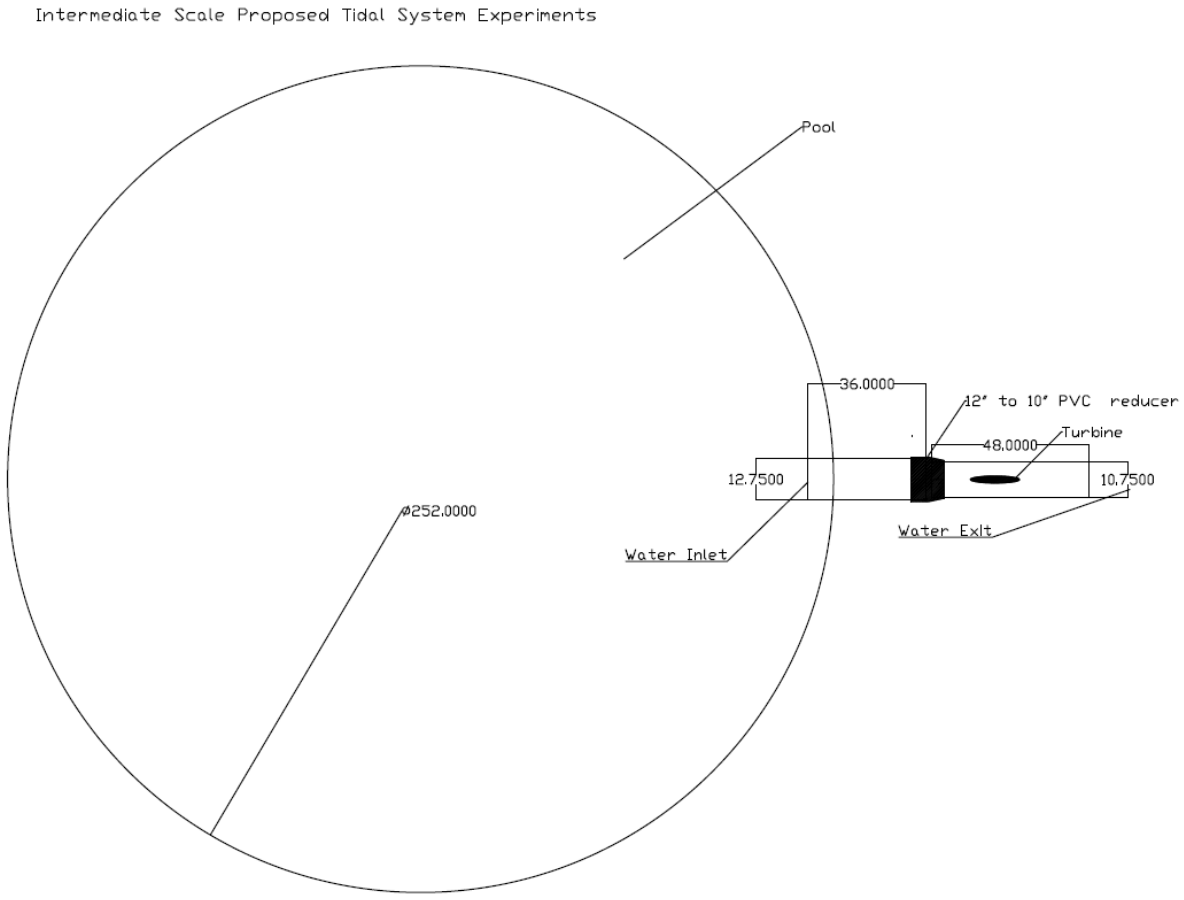

Figure 29: Intermediate scale test of convergence into a turbine (Plan View)

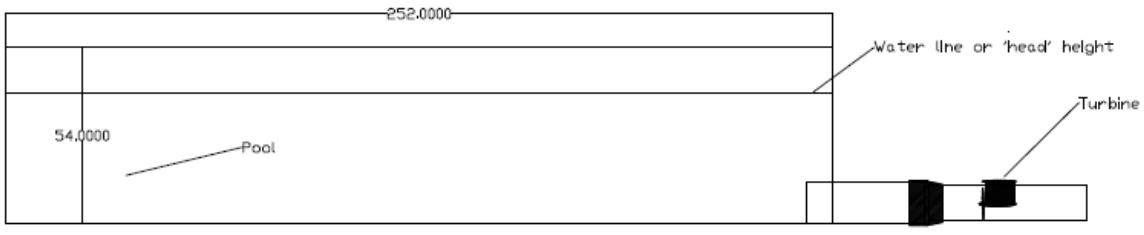

Figure 28: Intermediate scale test of convergence into a turbine (Side View)

To test possible power outputs from the system with a hydro turbine, an off the shelf model was selected that could work at the current experimental scale. The Watt & Sea brand POD 600 was selected for its size and available power outputs. More information about this and other available hydro generators can be found at www.wattandsea.com.

The associated power output curves were available for the Watt & Sea tubine and utilized for system optimization. The 240-millimeter propeller was selected in order to match the pipe inner diameter with the propeller diameter as closely as possible. This output curve implies that at a water velocity of 11 knots or 5.65 meters per second the turbine will deliver a power output of its maximum at 600 Watts.

The hydro turbine includes an alternating current (AC) generator with a permanent magnet attached to an optimum converter. For the experimental setup, the system will require an additional power source that is responsible for controlling the output voltage because the product is designed for power to be stored in a 12 Volt or 24 Volt battery. A current meter was required on the converter and the power supply to tell who is providing what power to the load. To match the load as it increases or decreases due to the fluid velocity impacting the rotors, three load diverters that could be activated according to speed were added to the electrical configuration. The finished product is illustrated in the figure below. Note that all electrical engineering was researched, designed, and built by Dr. Brian Kopp to ensure experiment safety and accuracy.

For a preliminary test of this system: 1) the system was set up will all electrical connections 2) a 10 inch PVC pipe was placed in the 10 to 12 inch reducer 3) a 12-inch pipe was valved using an inflatable plug 4) a water pump was then utilized to pump water from the onsite wave pool to

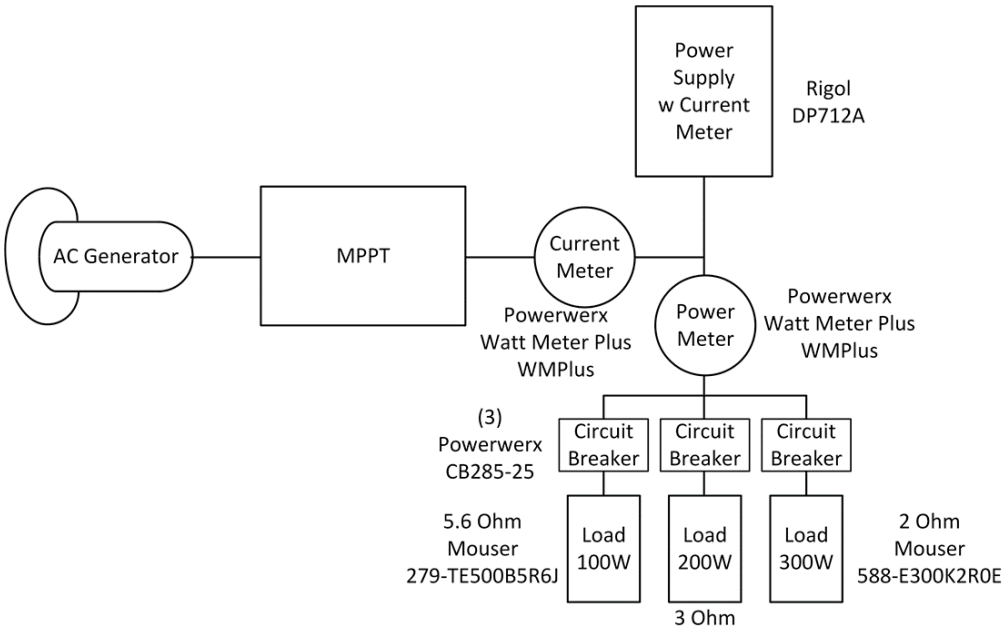

Figure 30: Electrical configuration of turbine interface (Kopp, 2018)

the tidal test pool, this process took up to an hour depending on desired water level in the tidal pool 5) once the water was at the desired level, one person was required to release the valve within the pool and another was necessary to read and adjust the turbine reading station and/or record the total empty time. These steps were repeated with a 10-inch test section that included the turbine as well.

11.4 Results and Analysis of Intermediate Scale Test to Investigate Convergence on a Turbine

The preliminary test results are as follows:

Table 4: Preliminary result from intermediate scale testing of proposed tidal system

12" to 10" Schedule 40 PVC Test Segment								
Turbine	Pool Radius	Fill Height	Pipe Exit Area	Empty Time	Pool Volume	Flow rate=ΔV/t	Velocity =Q/A	Theoretical Power
w or w/o	m	m	m^2	s	m3	m3/s	m/s	Watts
With Turbine	3.353	0.626618	0.05	234.84	22.13	0.094	1.869	97.60
Without Turbine	3.353	0.626618	0.05	176.18	22.13	0.126	2.491	231.14

The pool for both experimental runs was filled to a height of 0.626618 meters. In one case the 10-inch pipe without the turbine was tested and the next run the 10-inch pipe that houses the turbine was tested. To gauge the expected results, the numerical simulation of the proposed tidal system was tuned to the specific criteria of the experiment i.e.: length of bladder 5.0; width of bladder 5.0; height of bladder 0.72484, tidal amplitude 1, radius of pipe 0.1509903, radius of nozzle 0.1266952, and number of turbines 1. The model estimated that the maximum velocity at the pipe would be 3.7695 m/s and the maximum velocity at the nozzle 5.3534 m/s. It also yielded an estimated power output of 568 Watts maximum that includes an estimated efficiency of the Watt and Sea POD 600 of 0.1470 with a total expected run time of 190 seconds. It should be noted that while running the experiment with the turbine, the output of the electricity never rose above 24 Watts on the meter.

Unfortunately, the projected results of the experiments did not align with the initial data we pulled from the preliminary experiments. After taking a step back and investigating all of the variables that may be affecting the experiment, it has been determined that the following areas require more research to continue in the direction of intermediate scale testing: 1) nozzle geometry

was limited by available resources and because of its lack of gradation and quick transition from 12 inch to 10 inch the nozzle increased frictional losses during this transition that overwhelmed the system 2) limits on pipe sizing and challenges with working with large PVC pipes kept the experiment from using a greater step down in nozzle diameters, in future tests a larger step down in exit areas would be desired 3) performance of Watt and Sea turbine within a pipe requires more investigation since the principle application of this device is open water as used with a sailboat 4) further investigation of pressure differentials as the fluid moves from the pool through the turbine 5) in-depth investigation of frictional losses through the whole system.

13 DISCUSSION

During the investigation of the proposed closed convergent tidal energy system, we first conducted a proof of concept experiment using a small-scale physical model of the proposed tidal energy system. This allowed for testing the hypothesis that a fluid can be driven against gravity in a closed system. The experiment included using two closed compliant bladders with a simulated tide to force water back and forth through the system. Although this test was done on the small scale, all data pointed toward this posed hypothesis to be true. This test was limited by size and should be done on a larger scale to understand the frictional losses associated with the proposed system as it scales in size.

The results derived from the small-scale tests using a physical model to test the effect of convergent pipes and nozzles for optimizing fluid velocity through the proposed system showed that while using a nozzle for convergent flow, specific design is necessary to eliminate increases in frictional losses that overwhelm the fluid velocity increase within the system. In addition, although theoretical calculations suggest that the use of convergent pipes can be used to increase fluid velocity through the system, frictional losses tend to overwhelm this type of design and negate most if not all gains. Again, this test was limited by size an should be investigated either using a numerical model such as a computational fluid dynamics (CFD) model. This would allow further investigation of numerical analysis and data structure i.e. nozzle. Using this type of simulation will allow narrowing the scope of viable nozzle geometry that would be best suited for this specific application.

The development of a simplistic numerical model of the tidal system allowed for the estimation its behavior and investigation of theoretical fluid velocity and associated power

output. The results of this portion of research showed that, although directly related to volume, the amount of theoretical power generated by the system is on a level that indicated potential commercial scalability for energy production. This study was limited to a simplistic model and should include site-specific data i.e.: system volume, distance, elevation, tidal range and variability, and also consider frictional losses, and turbine efficiency.

The results from the economic study of the system that yielded an estimated Levelized Cost of Energy (LCOE) showed that at this preliminary analysis the proposed tidal energy system has the potential to comparable to other renewable energy systems as well as other current fossil fuel energy systems. Again, it is important to note that an economic analysis is site specific for a system such as the one proposed and a more robust LCOE would need to be conducted using system variable and site requirements. However, it is important to note that the proposed tidal system not only performs well economically but offers other intangible benefits when compared to other energy systems that cannot always be measured directly by monetary gains. Below is a chart that allows comparisons across the board of many available energy systems against the proposed tidal system. It is the hope that the continued research finds value not only in the economic potential but also some of the other attribute this technology has to offer, specifically the ability to generate electricity with a low carbon footprint and little environmental impact.

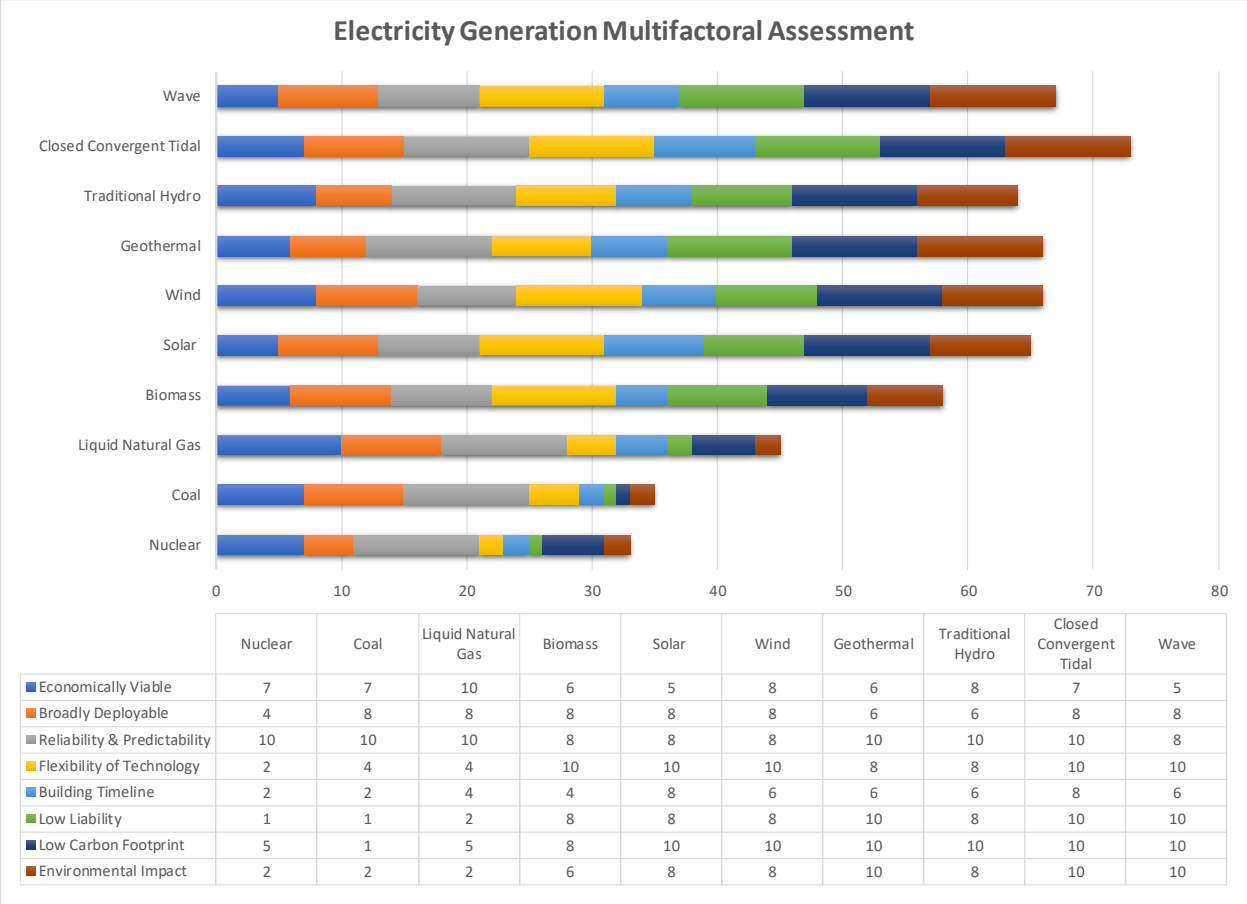

	Nuclear	Coal	Liquid Natural Gas	Biomass	Solar	Wind	Geothermal	Traditional Hydro	Closed Convergent Tidal	Wave
Economically Viable	7	7	10	6	5	8	6	8	7	5
Broadly Deployable	4	8	8	8	8	8	6	6	8	8
Reliability & Predictability	10	10	10	8	8	8	10	10	10	8
Flexibility of Technology	2	4	4	10	10	10	8	8	10	10
Building Timeline	2	2	4	4	8	6	6	6	8	6
Low Liability	1	1	2	8	8	8	10	8	10	10
Low Carbon Footprint	5	1	5	8	10	10	10	10	10	10
Environmental Impact	2	2	2	6	8	8	10	8	10	10

Figure 31: Multi factor assessment by electricity generation technologies

The final portion of hypothesis testing associated with this body of work included intermediate scale testing of the system with hopes of an eventual transition to an operational system. Again, the results point towards a viable system, but also shows that more robust testing of component parts of the tidal system require more in-depth research and testing.

14 CONCLUSIONS

The potential of generating electricity from the global tidal range is vast. This type of renewable energy has the potential to disrupt the current electricity generation portfolio due to its availability and predictability, especially because this form of energy is CO2 emission free. Add to the equation that fossil fuels have a limited abundance, and it is apparent that tidal energy has the potential to be a dominant contender in the energy markets as new technologies are researched and developed. With available potential energy being estimated at 15.6 Terawatt hours, this research into tidal energy system is immensely important.

After investigating the hypothesis that set out to determine the viability of a proposed closed convergent tidal energy capture system that utilizes convergent nozzles as the contained fluid approaches the turbine/turbines that set out to achieve: 1) tidal energy driven by the potential energy of the weight of the water column that is then converted to kinetic energy as the contained fluid is forced through a nozzle that optimizes fluid velocity; 2) a closed system that eliminates biofouling by avoiding exposure to water with high levels of salinity i.e. seawater; 3) a closed system that eliminates potential propeller impact on marine life; 4) on land turbine housing that allows for ease of operation and maintenance. It is the conclusion of this research that the initial investigations point to a system that has the potential to meet all of the above design criteria while also generating enough electricity to also be economically viable and competitive with existing energy sources, it has been determined through this research that the proposed system presents itself as viable and deserves further investigation to move it into a future operational system

15 FUTURE WORK

This exploratory work was just the beginning of demonstrating the viability of the proposed closed convergent tidal system. In order to continue research of the system the following future work is suggested: 1) In-depth modeling of the convergent flow between the closed compliant bladders through a convergent section with a subsequent physical model to validate the findings. 2) Research or development of turbine for this specific application to locate the most efficient working assembly. 3) Robust study of the potential environmental impacts created by installing a footprint of urethane compliant fabric bladder on the seafloor and associated hydrological changed in the installation area. 4) Research on the most viable fabrics and fittings for a system that is resistant to harsh environmental exposures. 5) Investigation of a mooring and protection system for the offshore portion of compliant bladders. 6) Modeling of proposed auxiliary bladder configuration to allow consistent generation of electricity or generation that meets at power demand curve. 7) In-depth study of LCOE that utilizes site-specific data. 8) Research on power transmission from the proposed system to the grid, storage system, home, or community.

As research on this proposed system continues, it is my hope that this initial work will eventually lead to large-scale commercial systems that can supply power to many cities.

REFERENCES

Chen, W. (2010, October). *Tidal Energy*. Retrieved from Stanford Edu: http://large.stanford.edu/courses/2010/ph240/chenw1/

Department of Oceanography, Naval Postgraduate School. (2017, June 5). *Basic Concepts in Physical Oceanography: Tides*. Retrieved from Navy Operational Ocean Cirulations and Tide Models: http://www.oc.nps.edu/nom/day1/partc.html

Department of Oceanography, Naval Postgraduate School. (2018). *Basic Concepts in Physical Oceanography: Tides*. Retrieved from Navy Operational Ocean Circulation and Tidal Models: http://www.oc.nps.edu/nom/day1/tidal_datums.gif

Egbert, G. a. (2002). *Global Inverse Tide Model.* Retrieved from ESR: http://www.esr.org/polar_tide_models/Model_TPXO62.html

Enerdata. (2018). *Global Energy Statistical Yearbook 2017*. Retrieved from Enerdata: https://yearbook.enerdata.net/renewables/renewable-in-electricity-production-share.html

Energy Efficiency & Renewable Energy. (2017). *Water Power Technologies Office*. Retrieved from How Hydro Power Works: https://www.energy.gov/eere/water/how-hydropower-works

Google. (2018, September 11). *Goggle Maps*. Retrieved from Google Maps: https://www.google.com/maps/

Institute for Energy Research. (2009). *Levelized Cost of New Electricity Generating Technologie.* Washington, D.C: Institute for Energy Research.

International Hydropower Association. (2017). *Key Trends in Hydropower.* Sutton, London: Chancery House. Retrieved from Key Trends in Hydropower:

https://www.hydropower.org/sites/default/files/publications-docs/2017 Key Trends in Hydropower_0.pdf

International Renewable Energy Agency. (2015). *Renewable Power Generation Cost 2015.* IRENA.

International Renewable Energy Agency. (2015). *Renewable Power Generation Cost 2015.* IRENA. Retrieved from http://www.irena.org/DocumentDownloads/Publications/IRENA_RE_Power_Costs_2014_report.pdf

Junqiang Xia1, R. A. (2015). *Estimation of annual energy output from a tidal barrage.* Wuhan, China: State Key Laboratory of Water Resources and Hydropower Engineering Science.

Kim Rutledge, M. M. (2011, June 14). *National Geographic Society*. Retrieved from Tidal Energy: https://www.nationalgeographic.org/encyclopedia/tidal-energy/

Kinetic Hydropower System (KHPS). (2017). Retrieved from Verdant Power: http://www.verdantpower.com/kinetic-hydropower-system.html

Kopp, D. B. (2018, June 25). Power Presentation. Jacksonville, FL: University of North Florida.

Lester Allan Pelton. (2012, June). Retrieved from ASME: https://www.asme.org/engineering-topics/articles/energy/lester-allan-pelton

Manhar Dhanak, A. D. (2016). *Springer Handbook Of Ocean Engineering.* New York: Springer Nature.

National Oceanic and Atmospheric Administration (NOAA). (2018, 09 11). *Tides and Currents*. Retrieved from National Oceanic and Atmospheric Administration (NOAA): https://tidesandcurrents.noaa.gov

NOAA. (2017, July 6). *Tides Education*. Retrieved from NOAA Ocean Service Education: https://oceanservice.noaa.gov/education/kits/tides/media/supp_tide07a.html

Office of Energy Efficiency and Renewable Energy. (2017). *History of Hydropower*. Retrieved from Energy Efficiency and Renewable Energy: https://www.energy.gov/eere/water/history-hydropower

Paul Lako, M. K. (2015). *Hydropower Technology Brief.* International Renewable Energy Agency.

Pelton Turbine. (2015). Retrieved from Mechanical Tutorial: http://www.mechanicaltutorial.com/pelton-turbine-or-pelton-wheel-turbine

Rance tidal power plant. (2017). Retrieved from WIKIMEDIA COMMONS: https://commons.wikimedia.org/wiki/File:Rance_tidal_power_plant.jpg

Ruud Kempener, F. N. (2014). *Tidal Energy Technology Brief.* International Renewable Energy Agency.

Sea Gen. (2017). Retrieved from Sea Generation: http://www.seageneration.co.uk/

Sean Petley, G. A. (2015, November 19). Swansea Bay tidal lagoon annual energy estimation. *Ocean Engineering*, 10.

Selin, N. E. (2010, September 9). *Tidal Power Energy*. Retrieved from Encyclopaedia Britannica: https://www.britannica.com/science/tidal-power

Selin, N. E. (2018, May 22). *Tidal Power*. Retrieved from Encyclopedia Britannica: https://www.britannica.com/science/tidal-power

Shere, J. (2013). *Renewable: the world-changing power of alernative energy.* New York: St. Martin's Press.

SunRun. (2018). *The price of residential solar power*. Retrieved from SunRun: https://www.sunrun.com/solar-lease/cost-of-solar

Tidal Power. (2017). Retrieved from Energy BC: http://energybc.ca/tidal.html

Turbine Selection. (n.d.). Retrieved from Oregan State Edu: http://rivers.bee.oregonstate.edu/book/export/html/35

U.S. Energy Information Administration. (2017, February 27). *Residential Energy Consumption Survey (RECS)*. Retrieved from U.S. Energy Information Administration: https://www.eia.gov/consumption/residential/data/2015/

U.S. Energy Information Association. (2017, September 21). *Florida State Profile and Energy Estimates*. Retrieved from U.S. Energy Information Association: https://www.eia.gov/state/analysis.php?sid=FL

Using the Power of Tidal Streams to Generate Electricity . (2017, March). Retrieved from Alternative Energy Tutorials: http://www.alternative-energy-tutorials.com/images/stories/tidal/alt93.gif

White, F. M. (2008). *Fluid Mechanics Sixth Edition.* New York: The McGraw-Hill Companies.

Windustry Resource Library. (2012). *How much do wind turbines cost?* Retrieved from Windustry: http://www.windustry.org/how_much_do_wind_turbines_cost

World-leading tidal energy system achieves 5GWh milestone. (n.d.). Retrieved from Marine Current Turbines: http://www.marineturbines.com/News/2012/09/05/world-leading-tidal-energy-system-achieves-5gwh-milestone

APPENDIX

Appendix 1: Analysis of Initial Experimental Results of Tidal System (Physical Model Closed Convergent Tidal System Test with 4.5" section without Turbine)

	4.5" Test without turbine					Simulated Head					Gravity Return			
Time Step	Weight	Adj Wt	Weight	Flow Rate	Time Step	Weight	Adj Wt	Weight	Flow Rate	Time Step	Weight	Adj Wt	Weight	Flow Rate
s	lb	lb	gal	gal/s	s	lb	lb	gal	gal/s	s	lb	lb	gal	gal/s
0.00	3668	0	0.00	0	0.00	2342	0	0.00	0	0.00	3386	0	0.00	0
0.02	3646	-22	2.64	1.32	0.02	2353	11	1.32	0.66	0.02	3372	-14	1.68	0.84
0.05	3585	-83	9.96	2.44	0.05	2386	44	5.28	1.32	0.05	3340	-46	5.52	1.28
0.07	3549	-119	14.29	2.16	0.07	2414	72	8.64	1.68	0.07	3321	-65	7.80	1.14
0.10	3491	-177	21.25	2.32	0.10	2454	112	13.45	1.60	0.10	3276	-110	13.21	1.80
0.12	3454	-214	25.69	2.22	0.12	2479	137	16.45	1.50	0.12	3261	-125	15.01	0.90
0.15	3415	-253	30.37	1.56	0.15	2507	165	19.81	1.12	0.15	3226	-160	19.21	1.40
0.17	3382	-286	34.33	1.98	0.17	2529	187	22.45	1.32	0.17	3208	-178	21.37	1.08
0.20	3340	-328	39.38	1.68	0.20	2557	215	25.81	1.12	0.20	3186	-200	24.01	0.88
0.22	3318	-350	42.02	1.32	0.22	2572	230	27.61	0.90	0.22	3157	-229	27.49	1.74
0.25	3277	-391	46.94	1.64	0.25	2593	251	30.13	0.84	0.25	3137	-249	29.89	0.80
0.27	3254	-414	49.70	1.38	0.27	2609	267	32.05	0.96	0.27	3117	-269	32.29	1.20
0.30	3218	-450	54.02	1.44	0.30	2630	288	34.57	0.84	0.30	3093	-293	35.17	0.96
0.32	3194	-474	56.90	1.44	0.32	2642	300	36.01	0.72	0.32	3077	-309	37.09	0.96
0.35	3177	-491	58.94	0.68	0.35	2656	314	37.70	0.56	0.35	3064	-322	38.66	0.52
0.37	3179	-489	58.70	-0.12	0.37	2663	321	38.54	0.42	0.37	3050	-336	40.34	0.84
0.40	3196	-472	56.66	-0.68	0.40	2676	334	40.10	0.52	0.40	3041	-345	41.42	0.36
0.42	3191	-477	57.26	0.30	0.42	2682	340	40.82	0.36	0.42	3037	-349	41.90	0.24
0.45	3161	-507	60.86	1.20	0.45	2691	349	41.90	0.36	0.45	3031	-355	42.62	0.24
0.47	3093	-575	69.03	4.08	0.47	2696	354	42.50	0.30	0.47	3026	-360	43.22	0.30
0.50	3084	-584	70.11	0.36	0.50	2697	355	42.62	0.04	0.50	3024	-362	43.46	0.08
0.52	3074	-594	71.31	0.60	0.52	2701	359	43.10	0.24	0.52	3027	-359	43.10	-0.18
0.55	3065	-603	72.39	0.36	0.55	2705	363	43.58	0.16	0.55	3028	-358	42.98	-0.04
0.57	3064	-604	72.51	0.06	0.57	2703	361	43.34	-0.12	0.57	3032	-354	42.50	-0.24
0.60	3058	-610	73.23	0.24	0.60	2701	359	43.10	-0.08	0.60	3035	-351	42.14	-0.12
0.62	3057	-611	73.35	0.06	0.62	2700	358	42.98	-0.06	0.62	3036	-350	42.02	-0.06
0.65	3057	-611	73.35	0.00	0.65	2695	353	42.38	-0.20	0.65	3033	-353	42.38	0.12
0.67	3059	-609	73.11	-0.12	0.67	2692	350	42.02	-0.18	0.67	3030	-356	42.74	0.18
0.70	3062	-606	72.75	-0.12	0.70	2689	347	41.66	-0.12	0.70	3022	-364	43.70	0.32
0.72	3065	-603	72.39	-0.18	0.72	2688	346	41.54	-0.06	0.72	3023	-363	43.58	-0.06
0.75	3067	-601	72.15	-0.08	0.75	2684	342	41.06	-0.16	0.75	3019	-367	44.06	0.16
0.77	3067	-601	72.15	0.00	0.77	2685	343	41.18	0.06	0.77	3021	-365	43.82	-0.12
						2686	344	41.30	0.00		3018	-368	44.18	0.00
											3016	-370	44.42	
											3024	-362	43.46	
											3032	-354	42.50	
											3036	-350	42.02	
											3036	-350	42.02	
											3032	-354	42.50	

Appendix 2: Analysis of Initial Experimental Results of Tidal System (Physical Model Closed Convergent Tidal System Test with 4.5" section without Turbine)

	Simulated Head					Gravity Return				Simulated Head	
Time Step	Weight	Adj Wt	Weight	Flow Rate	Time Step	Weight	Adj Wt	Weight	Flow Rate	Weight	Adj Wt
s	lb	lb	gal	gal/s	s	lb	lb	gal	gal/s	lb	lb
0.00	2289	0	0.00	0	0.00	3367	0	0.00	0	Corrupted Data	
0.02	2295	6	0.72	0.36	0.02	3358	-9	1.08	0.54	Corrupted Data	
0.05	2330	41	4.92	1.40	0.05	3309	-58	6.96	1.96	Corrupted Data	
0.07	2362	73	8.76	1.92	0.07	3284	-83	9.96	1.50	Corrupted Data	
0.10	2393	104	12.48	1.24	0.10	3244	-123	14.77	1.60	Corrupted Data	
0.12	2418	129	15.49	1.50	0.12	3209	-158	18.97	2.10	Corrupted Data	
0.15	2461	172	20.65	1.72	0.15	3180	-187	22.45	1.16	Corrupted Data	
0.17	2484	195	23.41	1.38	0.17	3156	-211	25.33	1.44	Corrupted Data	
0.20	2504	215	25.81	0.80	0.20	3128	-239	28.69	1.12	Corrupted Data	
0.22	2520	231	27.73	0.96	0.22	3108	-259	31.09	1.20	Corrupted Data	
0.25	2553	264	31.69	1.32	0.25	3092	-275	33.01	0.64	Corrupted Data	
0.27	2565	276	33.13	0.72	0.27	3078	-289	34.69	0.84	Corrupted Data	
0.30	2581	292	35.05	0.64	0.30	3055	-312	37.45	0.92	Corrupted Data	
0.32	2602	313	37.58	1.26	0.32	3044	-323	38.78	0.66	Corrupted Data	
0.35	2621	332	39.86	0.76	0.35	3031	-336	40.34	0.52	Corrupted Data	
0.37	2637	348	41.78	0.96	0.37	3022	-345	41.42	0.54	Corrupted Data	
0.40	2643	354	42.50	0.24	0.40	3015	-352	42.26	0.28	Corrupted Data	
0.42	2654	365	43.82	0.66	0.42	3009	-358	42.98	0.36	Corrupted Data	
0.45	2663	374	44.90	0.36	0.45	3004	-363	43.58	0.20	Corrupted Data	
0.47	2674	385	46.22	0.66	0.47	3001	-366	43.94	0.18	Corrupted Data	
0.50	2679	390	46.82	0.20	0.50	3001	-366	43.94	0.00	Corrupted Data	
0.52	2681	392	47.06	0.12	0.52	3003	-364	43.70	-0.12	Corrupted Data	
0.55	2682	393	47.18	0.04	0.55	3003	-364	43.70	0.00	Corrupted Data	
0.57	2685	396	47.54	0.18	0.57	3003	-364	43.70	0.00	Corrupted Data	
0.60	2679	390	46.82	-0.24	0.60	3005	-362	43.46	-0.08	Corrupted Data	
0.62	2678	389	46.70	-0.06	0.62	3005	-362	43.46	0.00	Corrupted Data	
0.65	2671	382	45.86	-0.28	0.65	3002	-365	43.82	0.12		
0.67	2665	376	45.14	-0.36	0.67						
0.70	2660	371	44.54	-0.20	0.70						
0.72	2656	367	44.06	-0.24	0.72						
0.75	2651	362	43.46	-0.20	0.75						
0.77	2649	360	43.22	-0.12	0.77						
	2645	356	42.74	0.01							
	2645	356	42.74	#DIV/0!							

Appendix 3: Analysis of Initial Experimental Results of Tidal System (Physical Model Closed Convergent Tidal System Test with 4.5" section without Turbine)

	Gravity Return					Simulated Head			
Time Step	Weight	Adj Wt	Weight	Flow Rate	Time Step	Weight	Adj Wt	Weight	Flow Rate
s	lb	lb	gal	gal/s	s	lb	lb	gal	gal/s
0.00	3290	0	0.00	0	0.00	2263	0	0.00	0
0.02	3276	-14	1.68	0.84	0.02	2284	21	2.52	1.26
0.05	3232	-58	6.96	1.76	0.05	2320	57	6.84	1.44
0.07	3202	-88	10.56	1.80	0.07	2348	85	10.20	1.68
0.10	3171	-119	14.29	1.24	0.10	2384	121	14.53	1.44
0.12	3142	-148	17.77	1.74	0.12	2408	145	17.41	1.44
0.15	3113	-177	21.25	1.16	0.15	2427	164	19.69	0.76
0.17	3095	-195	23.41	1.08	0.17	2444	181	21.73	1.02
0.20	3067	-223	26.77	1.12	0.20	2466	203	24.37	0.88
0.22	3050	-240	28.81	1.02	0.22	2480	217	26.05	0.84
0.25	3027	-263	31.57	0.92	0.25	2504	241	28.93	0.96
0.27	3012	-278	33.37	0.90	0.27	2512	249	29.89	0.48
0.30	2994	-296	35.53	0.72	0.30	2533	270	32.41	0.84
0.32	2980	-310	37.21	0.84	0.32	2538	275	33.01	0.30
0.35	2964	-326	39.14	0.64	0.35	2556	293	35.17	0.72
0.37	2953	-337	40.46	0.66	0.37	2567	304	36.49	0.66
0.40	2937	-353	42.38	0.64	0.40	2578	315	37.82	0.44
0.42	2935	-355	42.62	0.12	0.42	2584	321	38.54	0.36
0.45	2936	-354	42.50	-0.04	0.45	2592	329	39.50	0.32
0.47	2931	-359	43.10	0.30	0.47	2602	339	40.70	0.60
0.50	2937	-353	42.38	-0.24	0.50	2607	344	41.30	0.20
0.52	2940	-350	42.02	-0.18	0.52	2608	345	41.42	0.06
0.55	2939	-351	42.14	0.04	0.55	2608	345	41.42	0.00
0.57					0.57	2609	346	41.54	0.06
0.60					0.60				
0.62					0.62				
0.65					0.65				
0.67					0.67				
0.70					0.70				
0.72					0.72				
0.75					0.75				
0.77					0.77				

Appendix 4: Analysis of Initial Experimental Results of Tidal System (Physical Model Closed Convergent Tidal System Test with 4.5" section with Turbine)

	4.5" Test Segment w/ Turbine							Simulated Head					
Time Step	Weight	Adj Wt	Weight	Flow Rate	Power Reading	Power	Time Step	Weight	Adj Wt	Weight	Flow Rate	Power Reading	Power
s	lb	lb	gal	gal/s	Volts	Watts	s	lb	lb	gal	gal/s	Volts	Watts
0.00	3256	0	0.00	0.00	0	0	0.00	2171	0	0.00	0.00	0.0049	4.8E-06
0.02	3250	-6	0.72	0.36	2.096	0.87864	0.02	2189	18	2.16	1.08	1.596	0.50944
0.05	3218	-38	4.56	1.28	2.322	1.07834	0.05	2217	46	5.52	1.12	1.352	0.36558
0.07	3199	-57	6.84	1.14	2.276	1.03604	0.07	2234	63	7.56	1.02	1.361	0.37046
0.10	3162	-94	11.28	1.48	1.993	0.79441	0.10	2258	87	10.44	0.96	1.173	0.27519
0.12	3137	-119	14.29	1.50	1.793	0.64297	0.12	2274	103	12.36	0.96	1.028	0.21136
0.15	3102	-154	18.49	1.40	1.585	0.50245	0.15	3201	1030	14.50	0.71	0.0015	4.5E-07
0.17	3084	-172	20.65	1.08	1.704	0.58072	0.17	2329	158	18.97	2.23	0.0001	2E-09
0.20	3054	-202	24.25	1.20	1.344	0.36127	0.20	2345	174	20.89	0.64	0	
0.22	3036	-220	26.41	1.08	1.365	0.37265	0.22	2358	187	22.45	0.78	0	
0.25	3011	-245	29.41	1.00	0.922	0.17002	0.25	2375	204	24.49	0.68	0	
0.27	2998	-258	30.97	0.78	0.509	0.05182	0.27	2386	215	25.81	0.66	0	
0.30	2976	-280	33.61	0.88	0.0022	9.7E-07	0.30	2401	230	27.61	0.60	0	
0.32	2951	-305	36.61	1.50	0.003	1.8E-06	0.32	2414	243	29.17	0.78	0	
0.35	2945	-311	37.33	0.24	0	0	0.35	2429	258	30.97	0.60	0	
0.37	2937	-319	38.30	0.48	0	0	0.37	2436	265	31.81	0.42	0	
0.40	2923	-333	39.98	0.56	0	0	0.40	2451	280	33.61	0.60	0	
0.42	2914	-342	41.06	0.54	0	0	0.42	2460	289	34.69	0.54	0	
0.45	2901	-355	42.62	0.52	0	0	0.45	2472	301	36.13	0.48	0	
0.47	2894	-362	43.46	0.42	0	0	0.47	2477	306	36.73	0.30	0	
0.50	2886	-370	44.42	0.32	0	0	0.50	2484	313	37.58	0.28	0	
0.52	2882	-374	44.90	0.24	0	0	0.52	2487	316	37.94	0.18	0	
0.55	2875	-381	45.74	0.28	0	0	0.55	2494	323	38.78	0.28	0	
0.57	2874	-382	45.86	0.06	0	0	0.57	2498	327	39.26	0.24	0	
0.60	2878	-378	45.38	-0.16	0	0	0.60	2503	332	39.86	0.20	0	
0.62	2874	-382	45.86	0.24	0	0	0.62	2507	336	40.34	0.24	0	
0.65							0.65	2507	336	40.34	0.00	0	
0.67							0.67						
0.70							0.70						
0.72							0.72						
0.75							0.75						
0.77							0.77						

Appendix 5: Analysis of Initial Experimental Results of Tidal System (Physical Model Closed Convergent Tidal System Test with 4.5" section with Turbine)

	Gravity Return							Simulated Head					
Time Step	Weight	Adj Wt	Weight	Flow Rate	Power Reading	Power	Time Step	Weight	Adj Wt	Weight	Flow Rate	Power Reading	Power
s	lb	lb	gal	gal/s	Volts	Watts	s	lb	lb	gal	gal/s	Volts	Watts
0.00	3346	0	0.00	0.00	0.0231	0.00011	0.00	2150	0	0.00	0.00	0	0
0.02	3324	-22	2.64	1.32	3.104	1.92696	0.02	2163	13	1.56	0.78	1.163	0.27051
0.05	3291	-55	6.60	1.32	2.965	1.75825	0.05	2192	42	5.04	1.16	1.537	0.47247
0.07	3257	-89	10.68	2.04	2.868	1.64508	0.07	2204	54	6.48	0.72	1.528	0.46696
0.10	3219	-127	15.25	1.52	2.085	0.86945	0.10	2233	83	9.96	1.16	1.263	0.31903
0.12	3176	-170	20.41	2.58	1.596	0.50944	0.12	2254	104	12.48	1.26	1.072	0.22984
0.15	3159	-187	22.45	0.68	1.195	0.28561	0.15	2274	124	14.89	0.80	0.0012	2.9E-07
0.17	3140	-206	24.73	1.14	1.283	0.32922	0.17	2290	140	16.81	0.96	0.003	1.8E-06
0.20	3100	-246	29.53	1.60	0.926	0.1715	0.20	2311	161	19.33	0.84	0	0
0.22	3087	-259	31.09	0.78	1.578	0.49802	0.22	2322	172	20.65	0.66	0	0
0.25	3057	-289	34.69	1.20	1.689	0.57054	0.25	2343	193	23.17	0.84	0	0
0.27	3039	-307	36.85	1.08	1.482	0.43926	0.27	2352	202	24.25	0.54	0	0
0.30	3021	-325	39.02	0.72	1.072	0.22984	0.30	2369	219	26.29	0.68	0	0
0.32	3003	-343	41.18	1.08	0.75	0.1125	0.32	2383	233	27.97	0.84	0	0
0.35	3976	-362	43.46	0.76	1.247	0.311	0.35	2395	245	29.41	0.48	0	0
0.37	2962	-384	46.10	1.32	0.0019	7.2E-07	0.37	2406	256	30.73	0.66	0	0
0.40	2947	-399	47.90	0.60	0.001	2E-07	0.40	2419	269	32.29	0.52	0	0
0.42	2935	-411	49.34	0.72	0	0	0.42	2432	282	33.85	0.78	0	0
0.45	2918	-428	51.38	0.68	0	0	0.45	2442	292	35.05	0.40	0	0
0.47	2907	-439	52.70	0.66	0	0	0.47	2454	304	36.49	0.72	0	0
0.50	2897	-449	53.90	0.40	0	0	0.50	2459	309	37.09	0.20	0	0
0.52	2876	-470	56.42	1.26	0	0	0.52	2465	315	37.82	0.36	0	0
0.55	2867	-479	57.50	0.36	0	0	0.55	2469	319	38.30	0.16	0	0
0.57	2850	-496	59.54	1.02	0	0	0.57	2473	323	38.78	0.24	0	0
0.60	2857	-489	58.70	-0.28	0	0	0.60	2477	327	39.26	0.16	0	0
0.62	2851	-495	59.42	0.36	0	0	0.62	2481	331	39.74	0.24	0	0
0.65	2847	-499	59.90	0.16	0	0	0.65	2483	333	39.98	0.08	0	0
0.67	2843	-503	60.38	0.24	0	0	0.67	2491	341	40.94	0.48	0	0
0.70	2851	-495	59.42	-0.32	0	0	0.70	2498	348	41.78	0.28	0	0
0.72	2849	-497	59.66	0.12	0	0	0.72	2497	347	41.66	-0.06	0	0
0.75	2846	-500	60.02	0.12	0	0	0.75						
0.77	2841	-505	60.62	0.30	0	0	0.77						
	2841	-505	60.62	0.00	0	0							

Appendix 6: Analysis of Initial Experimental Results of Tidal System (Physical Model Closed Convergent Tidal System Test with 4.5" section with Turbine)

	Gravity Return							Simulated Head					
Time Step	Weight	Adj Wt	Weight	Flow Rate	Power Reading	Power	Time Step	Weight	Adj Wt	Weight	Flow Rate	Power Reading	Power
s	lb	lb	gal	gal/s	Volts	Watts	s	lb	lb	gal	gal/s	Volts	Watts
0.00	3311	0	0.00	0.00	0	0	0.00	2149	0	0.00	0.00	0.0205	8.4E-05
0.02	3296	-15	1.80	0.90	2.987	1.78443	0.02	2163	14	1.68	0.84	1.285	0.33025
0.05	3252	-59	7.08	1.76	2.872	1.64968	0.05	2190	41	4.92	1.08	1.365	0.37265
0.07	3224	-87	10.44	1.68	2.729	1.48949	0.07	2212	63	7.56	1.32	1.351	0.36504
0.10	3190	-121	14.53	1.36	2.294	1.05249	0.10	2237	88	10.56	1.00	1.099	0.24156
0.12	3161	-150	18.01	1.74	2.127	0.90483	0.12	2256	107	12.85	1.14	1.098	0.24112
0.15	3125	-186	22.33	1.44	2.055	0.84461	0.15	2281	132	15.85	1.00	0.0019	7.2E-07
0.17	3107	-204	24.49	1.08	1.768	0.62516	0.17	2295	146	17.53	0.84	0.0002	8E-09
0.20	3075	-236	28.33	1.28	1.79	0.64082	0.20	2321	172	20.65	1.04	0	0
0.22	3051	-260	31.21	1.44	1.495	0.44701	0.22	2335	186	22.33	0.84	0	0
0.25	3022	-289	34.69	1.16	1.015	0.20605	0.25	2357	208	24.97	0.88	0	0
0.27	3004	-307	36.85	1.08	0.0906	0.00164	0.27	2369	220	26.41	0.72	0	0
0.30	2981	-330	39.62	0.92	1.086	0.23588	0.30	2386	237	28.45	0.68	0	0
0.32	2968	-343	41.18	0.78	1.527	0.46635	0.32	2398	249	29.89	0.72	0	0
0.35	2943	-368	44.18	1.00	0.0011	2.4E-07	0.35	2408	259	31.09	0.40	0	0
0.37	2931	-380	45.62	0.72	0.002	8E-07	0.37	2418	269	32.29	0.60	0	0
0.40	2910	-401	48.14	0.84	0	0	0.40	2431	282	33.85	0.52	0	0
0.42	2905	-406	48.74	0.30	0	0	0.42	2442	293	35.17	0.66	0	0
0.45	2893	-418	50.18	0.48	0	0	0.45	2447	298	35.77	0.20	0	0
0.47	2885	-426	51.14	0.48	0	0	0.47	2456	307	36.85	0.54	0	0
0.50	2879	-432	51.86	0.24	0	0	0.50	2465	316	37.94	0.36	0	0
0.52	2872	-439	52.70	0.42	0	0	0.52	2470	321	38.54	0.30	0	0
0.55	2863	-448	53.78	0.36	0	0	0.55	2473	324	38.90	0.12	0	0
0.57	2858	-453	54.38	0.30	0	0	0.57	2476	327	39.26	0.18	0	0
0.60	2852	-459	55.10	0.24	0	0	0.60	2477	328	39.38	0.04	0	0
0.62	2846	-465	55.82	0.36	0	0	0.62	2477	328	39.38	0.00	0	0
0.65	2844	-467	56.06	0.08	0	0	0.65						
0.67	2843	-468	56.18	0.06	0	0	0.67						
0.70	2840	-471	56.54	0.12	0	0	0.70						
0.72	2840	-471	56.54	0.00	0	0	0.72						
0.75	2842	-469	56.30	-0.08	0	0	0.75						
0.77							0.77						

Appendix 7: Analysis of Initial Experimental Results of Tidal System (Physical Model Closed Convergent Tidal System Test with 4.5" section with Turbine)

	Gravity Return							Simulated Head					
Time Step	Weight	Adj Wt	Weight	Flow Rate	Power Reading	Power	Time Step	Weight	Adj Wt	Weight	Flow Rate	Power Reading	Power
s	lb	lb	gal	gal/s	Volts	Watts	s	lb	lb	gal	gal/s	Volts	Watts
0.00	3273	0	0.00	0.00	0.3785	0.02865	0.00	2113	0	0.00	0.00	0.1914	0.00733
0.02	3250	-23	2.76	1.38	2.944	1.73343	0.02	2130	17	2.04	1.02	1.963	0.77067
0.05	3211	-62	7.44	1.56	2.806	1.57473	0.05	2156	43	5.16	1.04	1.84	0.67712
0.07	3185	-88	10.56	1.56	2.54	1.29032	0.07	2176	63	7.56	1.20	1.674	0.56046
0.10	3148	-125	15.01	1.48	2.359	1.11298	0.10	2209	96	11.52	1.32	1.446	0.41818
0.12	3122	-151	18.13	1.56	2.055	0.84461	0.12	2227	114	13.69	1.08	0.852	0.14518
0.15	3089	-184	22.09	1.32	2.025	0.82013	0.15	2249	136	16.33	0.88	0.003	1.8E-06
0.17	3067	-206	24.73	1.32	1.709	0.58414	0.17	2267	154	18.49	1.08	0.001	2E-07
0.20	3044	-229	27.49	0.92	1.607	0.51649	0.20	2291	178	21.37	0.96	0	0
0.22	3018	-255	30.61	1.56	1.398	0.39088	0.22	2305	192	23.05	0.84	0	0
0.25	2992	-281	33.73	1.04	1.104	0.24376	0.25	2327	214	25.69	0.88	0	0
0.27	2974	-299	35.89	1.08	1.062	0.22557	0.27	2342	229	27.49	0.90	0	0
0.30	2950	-323	38.78	0.96	1.659	0.55046	0.30	2359	246	29.53	0.68	0	0
0.32	2934	-339	40.70	0.96	0.0045	4.1E-06	0.32	2370	257	30.85	0.66	0	0
0.35	2922	-351	42.14	0.48	0.001	2E-07	0.35	2387	274	32.89	0.68	0	0
0.37	2915	-358	42.98	0.42	0.001	2E-07	0.37	2393	280	33.61	0.36	0	0
0.40	2901	-372	44.66	0.56	0	0	0.40	2399	286	34.33	0.24	0	0
0.42	2889	-384	46.10	0.72	0	0	0.42	2403	290	34.81	0.24	0	0
0.45	2875	-398	47.78	0.56	0	0	0.45	2410	297	35.65	0.28	0	0
0.47	2862	-411	49.34	0.78	0	0	0.47	2416	303	36.37	0.36	0	0
0.50	2854	-419	50.30	0.32	0	0	0.50	2429	316	37.94	0.52	0	0
0.52	2847	-426	51.14	0.42	0	0	0.52	2434	321	38.54	0.30	0	0
0.55	2842	-431	51.74	0.20	0	0	0.55	2439	326	39.14	0.20	0	0
0.57	2835	-438	52.58	0.42	0	0	0.57	2443	330	39.62	0.24	0	0
0.60	2834	-439	52.70	0.04	0	0	0.60	2449	336	40.34	0.24	0	0
0.62	2831	-442	53.06	0.18	0	0	0.62	2452	339	40.70	0.18	0	0
0.65	2829	-444	53.30	0.08	0	0	0.65	2452	339	40.70	0.00	0	0
0.67	2825	-448	53.78	0.24	0	0	0.67	2452	339	40.70	0.00	0	0
0.70	2824	-449	53.90	0.04	0	0	0.70	2450	337	40.46	-0.08	0	0
0.72							0.72						
0.75							0.75						
0.77							0.77						

Appendix 8: Analysis and Results of Convergent Pipes and Nozzle for Amplified Fluid Velocity

	1 Pipe No Nozzle								
Time Step	$v_{average}$= ($\sum v$/)n	$Q_{average}$= ($\sum Q$/)n	$Q_{average}$= ($\sum Q$/)n	$W_{average}$= ($\sum W_2$/)n	W=W(gal/8.33lb)	$\Delta h_2=W_2/(Area_{TUB}\rho)$	$\Delta h=\Delta h(12in/ft)$	$\Delta h_{1=}h_{start}-\Delta h_2$	$\Delta h_{1=}h_{start}-\Delta h_2$
Seconds	m/s	in^3/s	m^3/s	Weight (lb)	gal	ft	in	in	m
0	0.00	0.00	0.00E+00	0.00	0.00	0.00	0.00	15.00	0.38
2	0.78	103.58	1.70E-03	14.94	1.79	0.06	0.77	14.23	0.36
4	1.63	215.19	3.53E-03	29.00	3.48	0.12	1.49	13.51	0.34
6	1.79	236.13	3.87E-03	46.96	5.64	0.20	2.42	12.58	0.32
8	1.85	244.45	4.01E-03	64.26	7.71	0.28	3.31	11.69	0.30
10	1.83	241.12	3.95E-03	81.74	9.81	0.35	4.21	10.79	0.27
12	1.74	230.17	3.77E-03	97.46	11.70	0.42	5.02	9.98	0.25
14	1.55	204.93	3.36E-03	111.30	13.36	0.48	5.73	9.27	0.24
16	1.48	195.37	3.20E-03	125.64	15.08	0.54	6.47	8.53	0.22
18	1.43	188.85	3.09E-03	138.54	16.63	0.59	7.14	7.86	0.20
20	1.26	166.53	2.73E-03	149.66	17.97	0.64	7.71	7.29	0.19
22	1.13	149.89	2.46E-03	160.16	19.23	0.69	8.25	6.75	0.17
24	1.11	146.14	2.39E-03	170.74	20.50	0.73	8.80	6.20	0.16
26	1.01	133.80	2.19E-03	179.46	21.54	0.77	9.25	5.75	0.15
28	0.93	122.85	2.01E-03	188.46	22.62	0.81	9.71	5.29	0.13
30	0.77	101.63	1.67E-03	194.12	23.30	0.83	10.00	5.00	0.13
32	0.56	73.35	1.20E-03	199.04	23.89	0.85	10.25	4.75	0.12
34	0.42	55.88	9.16E-04	202.18	24.27	0.87	10.42	4.58	0.12
36	0.28	37.30	6.11E-04	204.42	24.54	0.88	10.53	4.47	0.11
38	0.19	25.65	4.20E-04	205.88	24.72	0.88	10.61	4.39	0.11
40	0.16	21.35	3.50E-04	207.50	24.91	0.89	10.69	4.31	0.11
42	0.18	23.43	3.84E-04	209.26	25.12	0.90	10.78	4.22	0.11
44	0.14	18.30	3.00E-04	210.14	25.23	0.90	10.83	4.17	0.11
46	0.08	11.09	1.82E-04	210.86	25.31	0.91	10.86	4.14	0.11
48	0.06	8.32	1.36E-04	211.34	25.37	0.91	10.89	4.11	0.10
50	0.04	5.82	9.54E-05	211.70	25.41	0.91	10.91	4.09	0.10

Appendix 9: Analysis and Results of Convergent Pipes and Nozzle for Amplified Fluid Velocity

	2 Converging Pipes No Nozzle								
Time Step	$v_{average}$= ($\sum v$/)n	$Q_{average}$= ($\sum Q$/)n	$Q_{average}$= ($\sum Q$/)n	$W_{average}$= ($\sum W_2$/)n	W=W(gal/8.33lb)	$\Delta h_2=W_2/(Area_{TUB}\rho)$	$\Delta h=\Delta h$(12in/ft)	$\Delta h_{1=}h_{start}-\Delta h_2$	$\Delta h_{1=}h_{start}-\Delta h_2$
Seconds	m/s	in^3/s	m^3/s	Weight (lb)	gal	ft	in	in	m
0	0.00	0.00	0.00E+00	0.00	0.00	0.00	0.00	15.00	0.38
2	0.58	76.26	1.25E-03	11.60	1.39	0.05	0.60	14.40	0.37
4	1.43	189.54	3.11E-03	25.36	3.04	0.11	1.31	13.69	0.35
6	1.81	239.32	3.92E-03	43.54	5.23	0.19	2.24	12.76	0.32
8	1.83	241.54	3.96E-03	60.20	7.23	0.26	3.10	11.90	0.30
10	1.74	230.31	3.77E-03	76.76	9.21	0.33	3.95	11.05	0.28
12	1.66	218.66	3.58E-03	91.74	11.01	0.39	4.73	10.27	0.26
14	1.55	204.38	3.35E-03	106.24	12.75	0.46	5.47	9.53	0.24
16	1.48	195.37	3.20E-03	119.92	14.40	0.51	6.18	8.82	0.22
18	1.34	177.06	2.90E-03	131.78	15.82	0.57	6.79	8.21	0.21
20	1.15	152.11	2.49E-03	141.86	17.03	0.61	7.31	7.69	0.20
22	1.00	132.55	2.17E-03	150.90	18.12	0.65	7.77	7.23	0.18
24	0.93	123.13	2.02E-03	159.62	19.16	0.69	8.22	6.78	0.17
26	0.84	111.06	1.82E-03	166.92	20.04	0.72	8.60	6.40	0.16
28	0.67	88.88	1.46E-03	172.44	20.70	0.74	8.88	6.12	0.16
30	0.59	77.37	1.27E-03	178.08	21.38	0.76	9.17	5.83	0.15
32	0.55	72.66	1.19E-03	182.92	21.96	0.79	9.42	5.58	0.14
34	0.48	63.50	1.04E-03	187.24	22.48	0.80	9.65	5.35	0.14
36	0.41	53.80	8.82E-04	190.68	22.89	0.82	9.82	5.18	0.13
38	0.31	41.04	6.73E-04	193.16	23.19	0.83	9.95	5.05	0.13
40	0.22	28.70	4.70E-04	194.82	23.39	0.84	10.04	4.96	0.13
42	0.15	19.41	3.18E-04	195.96	23.52	0.84	10.10	4.90	0.12
44	0.09	11.79	1.93E-04	196.52	23.59	0.84	10.13	4.87	0.12

Appendix 10: Analysis and Results of Convergent Pipes and Nozzle for Amplified Fluid Velocity:

3 Converging Pipes No Nozzle								
$v_{average}$= (∑v/)n	$Q_{average}$= (∑Q/)n	$Q_{average}$= (∑Q/)n	$W_{average}$= ($\sum W_2$/)n	W=W(gal/8.33lb)	$\Delta h_2=W_2/(Area_{TUB}\rho)$	Δh=Δh(12in/ft)	$\Delta h_{1=}h_{start}-\Delta h_2$	$\Delta h_{1=}h_{start}-\Delta h_2$
m/s	in^3/s	m^3/s	Weight (lb)	gal	ft	in	in	m
0.00	0.00	0.00E+00	0.00	0.00	0.00	0.00	15.00	0.38
0.83	109.95	1.80E-03	17.16	2.06	0.07	0.88	14.12	0.36
1.76	231.97	3.80E-03	32.98	3.96	0.14	1.70	13.30	0.34
1.80	238.35	3.91E-03	49.76	5.97	0.21	2.56	12.44	0.32
1.77	234.33	3.84E-03	66.78	8.02	0.29	3.44	11.56	0.29
1.80	238.07	3.90E-03	84.10	10.10	0.36	4.33	10.67	0.27
1.68	222.40	3.64E-03	98.86	11.87	0.42	5.09	9.91	0.25
1.56	206.04	3.38E-03	113.82	13.66	0.49	5.86	9.14	0.23
1.44	190.37	3.12E-03	126.32	15.16	0.54	6.51	8.49	0.22
1.31	173.60	2.84E-03	138.86	16.67	0.60	7.15	7.85	0.20
1.23	163.06	2.67E-03	149.84	17.99	0.64	7.72	7.28	0.18
1.17	154.32	2.53E-03	161.12	19.34	0.69	8.30	6.70	0.17
1.15	152.52	2.50E-03	171.84	20.63	0.74	8.85	6.15	0.16
1.02	134.50	2.20E-03	180.52	21.67	0.78	9.30	5.70	0.14
0.84	111.48	1.83E-03	187.92	22.56	0.81	9.68	5.32	0.14
0.74	97.20	1.59E-03	194.54	23.35	0.84	10.02	4.98	0.13
0.65	85.55	1.40E-03	200.26	24.04	0.86	10.32	4.68	0.12
0.52	68.08	1.12E-03	204.36	24.53	0.88	10.53	4.47	0.11
0.36	47.84	7.84E-04	207.16	24.87	0.89	10.67	4.33	0.11
0.25	32.45	5.32E-04	209.04	25.09	0.90	10.77	4.23	0.11

Appendix 11: Analysis and Results of Convergent Pipes and Nozzle for Amplified Fluid Velocity

	4 Converging Pipes No Nozzle								
Time Step	$v_{average}$= ($\sum v$/)n	$Q_{average}$= ($\sum Q$/)n	$Q_{average}$= ($\sum Q$/)n	$W_{average}$= ($\sum W_2$/)n	W=W(gal/8.33lb)	Δh_2=W_2/ ($Area_{TUB}\rho$)	Δh=Δh(12in /ft)	$\Delta h_{1=}h_{start}$- Δh_2	$\Delta h_{1=}h_{start}$- Δh_2
Seconds	m/s	in^3/s	m^3/s	Weight (lb)	gal	ft	in	in	m
0	0.00	0.00	0.00E+00	0.00	0.00	0.00	0.00	15.00	0.38
2	0.86	113.00	1.85E-03	17.42	2.09	0.07	0.90	14.10	0.36
4	1.88	248.47	4.07E-03	36.02	4.32	0.15	1.86	13.14	0.33
6	2.04	269.55	4.42E-03	55.36	6.65	0.24	2.85	12.15	0.31
8	1.96	258.87	4.24E-03	73.36	8.81	0.31	3.78	11.22	0.28
10	1.83	241.68	3.96E-03	90.22	10.83	0.39	4.65	10.35	0.26
12	1.73	229.06	3.75E-03	106.40	12.77	0.46	5.48	9.52	0.24
14	1.67	220.46	3.61E-03	122.02	14.65	0.52	6.29	8.71	0.22
16	1.55	205.07	3.36E-03	135.98	16.32	0.58	7.01	7.99	0.20
18	1.39	183.44	3.01E-03	148.48	17.82	0.64	7.65	7.35	0.19
20	1.24	163.89	2.69E-03	159.62	19.16	0.69	8.22	6.78	0.17
22	1.08	142.12	2.33E-03	168.98	20.29	0.73	8.71	6.29	0.16
24	0.95	125.07	2.05E-03	177.66	21.33	0.76	9.15	5.85	0.15
26	0.89	117.86	1.93E-03	185.98	22.33	0.80	9.58	5.42	0.14
28	0.78	103.16	1.69E-03	192.54	23.11	0.83	9.92	5.08	0.13
30	0.61	81.11	1.33E-03	197.68	23.73	0.85	10.18	4.82	0.12
32	0.49	65.17	1.07E-03	201.94	24.24	0.87	10.40	4.60	0.12
34	0.38	50.47	8.27E-04	204.96	24.61	0.88	10.56	4.44	0.11
36	0.27	35.88	5.88E-04	207.00	24.85	0.89	10.66	4.34	0.11
38	0.15	19.41	3.18E-04	207.83	24.95	0.89	10.71	4.29	0.11
40	0.06	7.63	1.25E-04	208.73	25.06	0.90	10.75	4.25	0.11

Appendix 12: Analysis and Results of Convergent Pipes and Nozzle for Amplified Fluid Velocity

	1 Pipe With Nozzle								
Time Step	$v_{average}$= ($\sum v$/)n	$Q_{average}$= ($\sum Q$/)n	$Q_{average}$= ($\sum Q$/)n	$W_{average}$= ($\sum W_2$/)n	W=W(gal/8.33lb)	$\Delta h_2=W_2/(Area_{TUB}\rho)$	$\Delta h=\Delta h(12in/ft)$	$\Delta h_{1=}h_{start}-\Delta h_2$	$\Delta h_{1=}h_{start}-\Delta h_2$
Seconds	m/s	in^3/s	m^3/s	Weight (lb)	gal	ft	in	in	m
0	0.00	0.00	0.00E+00	0.00	0.00	0.00	0.00	15.00	0.38
2	2.23	69.05	1.13E-03	9.86	1.18	0.04	0.51	14.49	0.37
4	5.02	155.16	2.54E-03	18.58	2.23	0.08	0.96	14.04	0.36
6	5.01	155.02	2.54E-03	28.52	3.42	0.12	1.47	13.53	0.34
8	4.26	131.58	2.16E-03	37.56	4.51	0.16	1.94	13.06	0.33
10	4.07	125.76	2.06E-03	46.66	5.60	0.20	2.40	12.60	0.32
12	4.08	126.18	2.07E-03	55.76	6.69	0.24	2.87	12.13	0.31
14	4.03	124.51	2.04E-03	64.62	7.76	0.28	3.33	11.67	0.30
16	3.96	122.29	2.00E-03	73.40	8.81	0.32	3.78	11.22	0.28
18	3.65	113.00	1.85E-03	80.92	9.71	0.35	4.17	10.83	0.28
20	3.61	111.48	1.83E-03	89.48	10.74	0.38	4.61	10.39	0.26
22	3.72	115.08	1.89E-03	97.52	11.71	0.42	5.02	9.98	0.25
24	3.51	108.43	1.78E-03	105.12	12.62	0.45	5.42	9.58	0.24
26	3.39	104.68	1.72E-03	112.62	13.52	0.48	5.80	9.20	0.23
28	3.24	100.25	1.64E-03	119.58	14.36	0.51	6.16	8.84	0.22
30	3.09	95.67	1.57E-03	126.42	15.18	0.54	6.51	8.49	0.22
32	3.05	94.42	1.55E-03	133.20	15.99	0.57	6.86	8.14	0.21
34	3.00	92.62	1.52E-03	139.78	16.78	0.60	7.20	7.80	0.20
36	2.73	84.30	1.38E-03	145.36	17.45	0.62	7.49	7.51	0.19
38	2.63	81.25	1.33E-03	151.50	18.19	0.65	7.81	7.19	0.18
40	2.66	82.36	1.35E-03	157.24	18.88	0.68	8.10	6.90	0.18
42	2.49	77.09	1.26E-03	162.62	19.52	0.70	8.38	6.62	0.17
44	2.42	74.74	1.22E-03	168.02	20.17	0.72	8.66	6.34	0.16
46	2.26	70.02	1.15E-03	172.72	20.73	0.74	8.90	6.10	0.15
48	2.06	63.64	1.04E-03	177.20	21.27	0.76	9.13	5.87	0.15
50	1.79	55.32	9.07E-04	180.70	21.69	0.78	9.31	5.69	0.14
52	1.49	0.38	6.18E-06	183.84	22.07	0.79	9.47	5.53	0.14
54	1.36	0.35	5.78E-06	186.78	22.42	0.80	9.62	5.38	0.14
56	1.24	0.31	5.08E-06	189.36	22.73	0.81	9.76	5.24	0.13
58	1.10	0.28	4.60E-06	191.70	23.01	0.82	9.88	5.12	0.13
60	1.06	0.29	4.72E-06	194.10	23.30	0.83	10.00	5.00	0.13
62	1.02	0.26	4.21E-06	196.24	23.56	0.84	10.11	4.89	0.12
64	0.99	0.27	4.45E-06	198.50	23.83	0.85	10.23	4.77	0.12
66	0.98	0.25	4.17E-06	200.62	24.08	0.86	10.34	4.66	0.12
68	0.77	0.16	2.60E-06	201.94	24.24	0.87	10.40	4.60	0.12
70	0.58	0.15	2.48E-06	203.20	24.39	0.87	10.47	4.53	0.12
72	0.55	0.14	2.32E-06	204.38	24.54	0.88	10.53	4.47	0.11
74	0.46	0.11	1.73E-06	205.26	24.64	0.88	10.58	4.42	0.11
76	0.38	0.10	1.61E-06	206.08	24.74	0.88	10.62	4.38	0.11
78	0.39	0.10	1.57E-06	203.90	24.48	0.88	10.51	4.49	0.11

Appendix 13: Analysis and Results of Convergent Pipes and Nozzle for Amplified Fluid Velocity

	2 Converging Pipes with Nozzle								
Time Step	$v_{average}$= (∑v/)n	$Q_{average}$= (∑Q/)n	$Q_{average}$= (∑Q/)n	$W_{average}$= ($\sum W_2$/)n	W=W(gal/8.33lb)	$\Delta h_2=W_2/(Area_{TUB}\rho)$	Δh=Δh(12in/ft)	$\Delta h_{1=}h_{start}-\Delta h_2$	$\Delta h_{1=}h_{start}-\Delta h_2$
Seconds	m/s	in^3/s	m^3/s	Weight (lb)	gal	ft	in	in	m
0	0.00	0.00	0.00E+00	0.00	0.00	0.00	0.00	15.00	0.38
2	2.16	66.83	1.10E-03	9.64	1.16	0.04	0.50	14.50	0.37
4	3.96	122.57	2.01E-03	17.68	2.12	0.08	0.91	14.09	0.36
6	4.09	126.45	2.07E-03	27.88	3.35	0.12	1.44	13.56	0.34
8	4.19	129.50	2.12E-03	36.36	4.36	0.16	1.87	13.13	0.33
10	4.08	126.04	2.07E-03	46.06	5.53	0.20	2.37	12.63	0.32
12	4.27	132.14	2.17E-03	55.42	6.65	0.24	2.86	12.14	0.31
14	4.09	126.45	2.07E-03	64.30	7.72	0.28	3.31	11.69	0.30
16	3.93	121.46	1.99E-03	72.94	8.76	0.31	3.76	11.24	0.29
18	3.62	112.03	1.84E-03	80.46	9.66	0.35	4.15	10.85	0.28
20	3.56	110.23	1.81E-03	88.84	10.67	0.38	4.58	10.42	0.26
22	3.74	115.64	1.89E-03	97.14	11.66	0.42	5.00	10.00	0.25
24	3.53	109.26	1.79E-03	104.60	12.56	0.45	5.39	9.61	0.24
26	3.40	105.24	1.72E-03	112.32	13.48	0.48	5.79	9.21	0.23
28	3.27	101.08	1.66E-03	119.18	14.31	0.51	6.14	8.86	0.23
30	3.08	95.26	1.56E-03	126.06	15.13	0.54	6.49	8.51	0.22
32	3.07	94.98	1.56E-03	132.88	15.95	0.57	6.85	8.15	0.21
34	3.02	93.32	1.53E-03	139.52	16.75	0.60	7.19	7.81	0.20
36	2.82	87.21	1.43E-03	145.46	17.46	0.62	7.49	7.51	0.19
38	2.65	82.08	1.35E-03	151.36	18.17	0.65	7.80	7.20	0.18
40	2.60	80.28	1.32E-03	157.04	18.85	0.67	8.09	6.91	0.18
42	2.46	76.12	1.25E-03	162.34	19.49	0.70	8.36	6.64	0.17
44	2.50	77.23	1.27E-03	168.18	20.19	0.72	8.66	6.34	0.16
46	2.40	74.18	1.22E-03	173.04	20.77	0.74	8.92	6.08	0.15
48	2.03	62.67	1.03E-03	177.22	21.27	0.76	9.13	5.87	0.15
50	1.76	54.49	8.93E-04	180.90	21.72	0.78	9.32	5.68	0.14
52	1.56	48.11	7.88E-04	184.16	22.11	0.79	9.49	5.51	0.14
54	1.27	39.38	6.45E-04	186.58	22.40	0.80	9.61	5.39	0.14
56	1.06	32.72	5.36E-04	188.88	22.67	0.81	9.73	5.27	0.13
58	1.04	32.17	5.27E-04	191.22	22.96	0.82	9.85	5.15	0.13
60	1.04	32.03	5.25E-04	193.50	23.23	0.83	9.97	5.03	0.13
62	0.94	29.12	4.77E-04	195.42	23.46	0.84	10.07	4.93	0.13
64	0.88	27.32	4.48E-04	197.44	23.70	0.85	10.17	4.83	0.12
66	0.91	28.01	4.59E-04	199.46	23.94	0.86	10.28	4.72	0.12
68	0.77	23.71	3.89E-04	200.86	24.11	0.86	10.35	4.65	0.12
70	0.59	18.16	2.98E-04	202.08	24.26	0.87	10.41	4.59	0.12
72	0.55	16.92	2.77E-04	203.30	24.41	0.87	10.47	4.53	0.11
74	0.48	14.97	2.45E-04	204.24	24.52	0.88	10.52	4.48	0.11
76	0.42	12.89	2.11E-04	205.16	24.63	0.88	10.57	4.43	0.11
78	0.38	11.65	1.91E-04	205.92	24.72	0.88	10.61	4.39	0.11

Appendix 14: Analysis and Results of Convergent Pipes and Nozzle for Amplified Fluid Velocity

	3 Converging Pipes With Nozzle								
Time Step	$v_{average}$= (Σv/)n	$Q_{average}$= (ΣQ/)n	$Q_{average}$= (ΣQ/)n	$W_{average}$= (ΣW_2/)n	W=W(gal/8.33lb)	$\Delta h_2=W_2/(Area_{TUB}\rho)$	$\Delta h=\Delta h(12in/ft)$	$\Delta h_{1=}h_{start}-\Delta h_2$	$\Delta h_{1=}h_{start}-\Delta h_2$
Seconds	m/s	in^3/s	m^3/s	Weight (lb)	gal	ft	in	in	m
0	0.00	0.00	0.00E+00	0.00	0.00	0.00	0.00	15.00	0.38
2	2.32	71.82	1.18E-03	10.36	1.24	0.04	0.53	14.47	0.37
4	3.87	119.66	1.96E-03	17.26	2.07	0.07	0.89	14.11	0.36
6	3.68	113.84	1.87E-03	26.78	3.21	0.11	1.38	13.62	0.35
8	4.06	125.62	2.06E-03	35.38	4.25	0.15	1.82	13.18	0.33
10	3.68	113.70	1.86E-03	43.18	5.18	0.19	2.22	12.78	0.32
12	3.65	112.73	1.85E-03	51.64	6.20	0.22	2.66	12.34	0.31
14	3.78	117.03	1.92E-03	60.06	7.21	0.26	3.09	11.91	0.30
16	3.79	117.30	1.92E-03	68.56	8.23	0.29	3.53	11.47	0.29
18	3.59	110.92	1.82E-03	76.06	9.13	0.33	3.92	11.08	0.28
20	3.34	103.30	1.69E-03	83.46	10.02	0.36	4.30	10.70	0.27
22	3.34	103.30	1.69E-03	90.96	10.92	0.39	4.69	10.31	0.26
24	3.47	107.32	1.76E-03	98.94	11.88	0.42	5.10	9.90	0.25
26	3.33	102.88	1.69E-03	105.80	12.70	0.45	5.45	9.55	0.24
28	3.28	101.36	1.66E-03	113.56	13.63	0.49	5.85	9.15	0.23
30	3.14	97.20	1.59E-03	119.82	14.38	0.51	6.17	8.83	0.22
32	3.13	96.64	1.58E-03	127.50	15.31	0.55	6.57	8.43	0.21
34	3.23	99.97	1.64E-03	134.24	16.12	0.58	6.92	8.08	0.21
36	2.86	88.46	1.45E-03	140.26	16.84	0.60	7.23	7.77	0.20
38	2.75	85.13	1.40E-03	146.52	17.59	0.63	7.55	7.45	0.19
40	2.70	83.47	1.37E-03	152.30	18.28	0.65	7.85	7.15	0.18
42	2.54	78.62	1.29E-03	157.86	18.95	0.68	8.13	6.87	0.17
44	2.33	72.10	1.18E-03	162.70	19.53	0.70	8.38	6.62	0.17
46	2.45	75.71	1.24E-03	168.78	20.26	0.72	8.70	6.30	0.16
48	2.39	73.76	1.21E-03	173.34	20.81	0.74	8.93	6.07	0.15
50	1.96	60.45	9.91E-04	177.50	21.31	0.76	9.15	5.85	0.15
52	1.84	56.85	9.32E-04	181.54	21.79	0.78	9.35	5.65	0.14
54	1.75	54.08	8.86E-04	185.30	22.24	0.80	9.55	5.45	0.14
56	1.68	51.86	8.50E-04	189.02	22.69	0.81	9.74	5.26	0.13
58	1.63	50.33	8.25E-04	192.56	23.12	0.83	9.92	5.08	0.13
60	1.46	45.06	7.38E-04	195.52	23.47	0.84	10.07	4.93	0.13
62	1.29	39.93	6.54E-04	198.32	23.81	0.85	10.22	4.78	0.12
64	1.21	37.44	6.13E-04	200.92	24.12	0.86	10.35	4.65	0.12
66	1.13	34.94	5.73E-04	203.36	24.41	0.87	10.48	4.52	0.11
68	0.96	29.81	4.89E-04	205.22	24.64	0.88	10.57	4.43	0.11
70	0.82	25.37	4.16E-04	207.02	24.85	0.89	10.67	4.33	0.11
72	0.76	23.57	3.86E-04	208.62	25.04	0.90	10.75	4.25	0.11
74	0.66	20.38	3.34E-04	209.96	25.21	0.90	10.82	4.18	0.11
76	0.49	15.25	2.50E-04	210.82	25.31	0.91	10.86	4.14	0.11
78	0.36	11.23	1.84E-04	211.58	25.40	0.91	10.90	4.10	0.10
80	0.29	8.87	1.45E-04	212.10	25.46	0.91	10.93	4.07	0.10

Appendix 15: Analysis and Results of Convergent Pipes and Nozzle for Amplified Fluid Velocity

	4 Converging Pipes With Nozzle								
Time Step	$v_{average}$= (Σv/)n	$Q_{average}$= (ΣQ/)n	$Q_{average}$= (ΣQ/)n	$W_{average}$= (ΣW_2/)n	W=W(gal/8.33lb)	$\Delta h_2=W_2/(Area_{TUB}\rho)$	$\Delta h=\Delta h(12in/ft)$	$\Delta h_{1=}h_{start}-\Delta h_2$	$\Delta h_{1=}h_{start}-\Delta h_2$
Seconds	m/s	in^3/s	m^3/s	Weight (lb)	gal	ft	in	in	m
0	0.00	0.00	0.00E+00	0.00	0.00	0.00	0.00	15.00	0.38
2	2.45	75.71	1.24E-03	10.92	1.31	0.05	0.56	14.44	0.37
4	4.48	138.66	2.27E-03	20.00	2.40	0.09	1.03	13.97	0.35
6	4.16	128.53	2.11E-03	29.46	3.54	0.13	1.52	13.48	0.34
8	4.13	127.56	2.09E-03	38.40	4.61	0.16	1.98	13.02	0.33
10	4.11	127.01	2.08E-03	47.78	5.74	0.21	2.46	12.54	0.32
12	4.22	130.61	2.14E-03	57.24	6.87	0.25	2.95	12.05	0.31
14	4.09	126.45	2.07E-03	66.02	7.93	0.28	3.40	11.60	0.29
16	3.87	119.80	1.96E-03	74.52	8.95	0.32	3.84	11.16	0.28
18	3.96	122.29	2.00E-03	83.66	10.04	0.36	4.31	10.69	0.27
20	3.95	122.02	2.00E-03	92.12	11.06	0.40	4.75	10.25	0.26
22	3.66	113.14	1.85E-03	99.98	12.00	0.43	5.15	9.85	0.25
24	3.37	104.27	1.71E-03	107.16	12.86	0.46	5.52	9.48	0.24
26	3.19	98.72	1.62E-03	114.22	13.71	0.49	5.88	9.12	0.23
28	3.22	99.55	1.63E-03	121.52	14.59	0.52	6.26	8.74	0.22
30	3.07	94.84	1.55E-03	127.90	15.35	0.55	6.59	8.41	0.21
32	2.83	87.63	1.44E-03	134.16	16.11	0.58	6.91	8.09	0.21
34	2.95	91.24	1.50E-03	141.06	16.93	0.61	7.27	7.73	0.20
36	2.89	89.43	1.47E-03	147.06	17.65	0.63	7.58	7.42	0.19
38	2.48	76.54	1.25E-03	152.10	18.26	0.65	7.84	7.16	0.18
40	2.43	75.29	1.23E-03	157.92	18.96	0.68	8.14	6.86	0.17
42	2.39	73.76	1.21E-03	162.74	19.54	0.70	8.38	6.62	0.17
44	2.16	66.69	1.09E-03	167.54	20.11	0.72	8.63	6.37	0.16
46	2.11	65.31	1.07E-03	172.16	20.67	0.74	8.87	6.13	0.16
48	2.07	63.92	1.05E-03	176.76	21.22	0.76	9.11	5.89	0.15
50	1.89	58.51	9.59E-04	180.60	21.68	0.78	9.30	5.70	0.14
52	1.55	47.84	7.84E-04	184.70	22.17	0.79	9.52	5.48	0.14
54	1.35	41.87	6.86E-04	188.14	22.59	0.81	9.69	5.31	0.13
56	1.10	34.11	5.59E-04	190.82	22.91	0.82	9.83	5.17	0.13
58	1.01	31.34	5.14E-04	193.74	23.26	0.83	9.98	5.02	0.13
60	1.05	32.58	5.34E-04	196.64	23.61	0.84	10.13	4.87	0.12
62	1.04	32.17	5.27E-04	198.96	23.88	0.85	10.25	4.75	0.12
64	0.88	27.18	4.45E-04	201.00	24.13	0.86	10.36	4.64	0.12
66	0.70	21.63	3.54E-04	202.46	24.30	0.87	10.43	4.57	0.12
68	0.55	16.92	2.77E-04	203.70	24.45	0.87	10.49	4.51	0.11
70	0.45	13.87	2.27E-04	204.78	24.58	0.88	10.55	4.45	0.11
72	0.38	11.79	1.93E-04	205.66	24.69	0.88	10.60	4.40	0.11
74	0.27	8.46	1.39E-04	206.16	24.75	0.89	10.62	4.38	0.11
76	0.21	6.41	1.05E-04	205.75	24.70	0.88	10.60	4.40	0.11

Appendix 16: MATLAB script for simplistic numerical model (page 1)

```
%%%%%%%%%%%%%%%%%%%%%%%%%%%%%%%%%%%%%%%%%%%%%%%%%%%%%%%%%%%%%%%%%%%%%%%%%%%%
%%%%%%%%%%%%%%%%%%%%%%%%%%%%%%%%%%%%%%%%%%%%%%%%%%%%%%%%%%%%%%%%%%%%%%%%%%%%
% Convergent Closed System Tidal Renewable Energy
% System Modeling
% Power Calculations and Optimization
% Michelle Vieira
% 2017-2018
% University of North Florida
% Taylor Engineering Research Institute
%%%%%%%%%%%%%%%%%%%%%%%%%%%%%%%%%%%%%%%%%%%%%%%%%%%%%%%%%%%%%%%%%%%%%%%%%%%%
%%%%%%%%%%%%%%%%%%%%%%%%%%%%%%%%%%%%%%%%%%%%%%%%%%%%%%%%%%%%%%%%%%%%%%%%%%%%

clc; close all; clc;

% Program prompts user to input desired design variables to output the
% system power output

% Constants used in calculations (Metric Units)

p  = 1000;       % density of water (kg/m3)b
g  = 9.8;        % gravity constant (m/s2)
Cp = .593;       % betz limit turbine efficiency coefficient

% Design inputs from user
% Lb   = input('Enter the design length of bladder:')
% Wb   = input('Enter the design width of bladder:')
% Hb   = input('Enter the design height of bladder:')
% TAmp = input('Enter the location tidal amplitude:')
% rp   = input('Enter the design radius of pipe:')
% rn   = input('Enter the design radius of nozzle:')
% NT   = input('Enter the number of turbines:')

Lb   = 100.;
Wb   = 100.;
Hb   = 2;
TAmp = 1;
rp   =0.25;
rn   =0.15;
NT   = 10;

%set time interval 44676 seconds (full tidal cycle is seconds)
itime=[1:44676];

% Calculate area of bladder, pipes, and nozzle, and volume of bladder
```

Appendix 17: MATLAB script for simplistic numerical model (page 2)

```
Ab = Lb*Wb;      % area of bladder
Vb = Ab*Hb;      % volume of bladder
Ap = pi*rp^2;    % cross sectional area of pipe
An = pi*rn^2;    % cross sectional area of nozzle


%%%%%%%%%%%%%%%%%%%%%%%%%%%%%%%%%%%%%%%%%%%%%%%%%%%%%%%%%%%%%%%%%%%%%%%%%%%%%%%%
%%%%%%%%%%%%%%%%%%%%%%%%%%%%%%%%%%%%%%%%%%%%%%%%%%%%%%%%%%%%%%%%%%%%%%%%%%%%%%%%
%Time for bladder to empty seconds
SecondsToEmpty = (2*Ab*sqrt(Hb))/(An*NT*sqrt(2*g));
if SecondsToEmpty < 11169
    display('Empty time not optimized to tidal cycle')
end

%    if t > 11169
%        display ("""Run time exceeds tidal cycle:  Please change design
%                  specifications ie:  decrease badder size or increase
%                  pipe diameter""")
%    end
%     calculate emty time to check for optimums
%     TimeEmptyPipe=2.*ab*sqrt(hb)/ap*sqrt(2.*g)
%     TimeEmptyNozzle=2.*ab*sqrt(hb)/an*sqrt(2.*g)

%Begin calculation loop of onshore condition (bladder on land)
%Set initial conditions to zero
% power=0;
% volumebladderOFF=0; %volume of offshore bladder
% Vpt=0; %velocity in the pipe
% HbONSHORE=Hb; %set initial condition of onshore bladder height

%Tidal constituents to find height of tide adjusted by 1
htide=-TAmp*sin((itime-1)*2*pi/44676.);
extent = length(htide);

power=zeros(1,length(htide));
% power=(1:44676);
%%%%%%%%%%%%%%%%%%%%%%%%%%%%%%%%%%%%%%%%%%%%%%%%%%%%%%%%%%%%%%%%%%%%%%%%%%%%%%%%
%%%%%%%%%%%%%%%%%%%%%%%%%%%%%%%%%%%%%%%%%%%%%%%%%%%%%%%%%%%%%%%%%%%%%%%%%%%%%%%%

% Looping while considering all governing conditions
% 1.  Check SecondsToEmpty (this is the max amount of time the system can
%     run to empty the bladder)
% 2.  Check the tidal cycle time iteration (when itime equals 1-11169 the
%     tide is outgoing and the onshore bladder will be emptying.
% 3.  Check the tidal cycle time iteration (when itime equals 11170-22338
```

Appendix 18: MATLAB script for simplistic numerical model (page 3)

```
%     the tide is slack/incoming and the a holding cycle should take place
%     ie:  Hold volume and velocity until next cycle is reached.
% 4.  Check SecondsToEmpty (this is the max amount of time the system can
%     run to empty the bladder)
% 2.  Check the tidal cycle time iteration (when itime equals 22339-33507
%     the tide is incoming and the onshore bladder will be filling.
% 3.  Check the tidal cycle time iteration (when itime equals 33508-44676
%     the tide is slack/outgoing and the a holding cycle should take place
%     ie:  Hold volume and velocity until next cycle is reached.

% Save space for arrays and set values to zero;

Hbt(extent) = zeros;
Vpt(extent) = zeros;
Vnt(extent) = zeros;

for i=1:extent;
   disp(i);
   if (i >= 1) && (i <= 11169)
        Hbt(i)=Hb+htide(i);
        %Check system design empty time (Hbt is zero)
        if i>=SecondsToEmpty;
                Hbt(i)=0;
                display('Empty time not optimized to tidal cycle');
        end

        Vpt(i)=sqrt(2*g*Hbt(i));
        Vnt(i)=(Vpt(i)*rp^2)/rn^2;
        power(i)=(0.5*Cp*p*An*NT*Vnt(i)^3);

    elseif (i >= 11170) && (i <= 22338)
        Hbt(i)=Hb-htide(i);
%         Vpt(i)=sqrt(2*g*Hbt(i));
        Vnt(i)=(Vpt(i)*rp^2)/rn^2;
        power(i)=(0.5*Cp*p*An*NT*Vnt(i)^3);

    elseif (i >= 22339) && (i <= 33507)
    %Check system design empty time (Hbt is zero)
%         Hbt(i)=0;
        Hbt(i)=Hb-htide(i);
        if i>=SecondsToEmpty+22339;
                Hbt(i)=0;
                display('Empty time not optimized to tidal cycle');
        end
        Vpt(i)=sqrt(2*g*Hbt(i));
        Vnt(i)=(Vpt(i)*rp^2)/rn^2;
        power(i)=(0.5*Cp*p*An*NT*Vnt(i)^3);
```

Appendix 19: MATLAB script for simplistic numerical model (page 4)

```
  elseif (i >= 33508) && (i <= 44676)
        Hbt(i)=Hb+htide(i);
%         Vpt(i)=sqrt(2*g*Hbt(i));
        Vpt(i)=0;
        Vnt(i)=(Vpt(i)*rp^2)/rn^2;
        power(i)=(0.5*Cp*p*An*NT*Vnt(i)^3);

   end
   if Hbt(i)<0
       disp(i)
       disp('ERROR')
       break
   end
end

TidalEnergy = sum(power)/12.41;
KiloWattHrs=TidalEnergy/1000
MegaWattHrs=TidalEnergy/1000000

% Scaling for graphical display of Velocity
if mean(power) > 1000;
    MAG = 1000;
elseif mean(power) > 50;
    MAG = 100;
else MAG=10;
end

figure(1)
grid on
plot(itime,(htide*100000),'--b','linewidth',1); hold on;
plot(itime,(Vnt*MAG),'g','linewidth',2);
plot(itime,(power),'--r','linewidth',1); hold off;
xlabel('Tidal Cycle (seconds)')
% ylabel(P)
legend(['Tidal Cycle (sec)'],['Velocity (m/s) x ' num2str(MAG)],...
    ['Power (watts)'],'location','southeast')
grid minor
WORDS   = sprintf([ 'Available Tidal Energy (KWatthrs) =' ...
    num2str(KiloWattHrs) '\n'...
    'Design Constraints (m) = ' num2str(Wb),', ' num2str(Lb),...
    ',' num2str(Hb),', ' num2str(rp),', ' num2str(rn)]);

% WORDS3  = [ 'Power(Watthrs) = ' num2str(TidalEnergy)]
%     dx = 10;
Pmax = max(power);
dy= Pmax*.98;
title([WORDS])
% text(50,dy,WORDS);
% text(10,255,WORDS3);
t(1).Fontsize = 8;
```

Appendix 20: HUSKY brand bladder part number and specifications

Part No.	Capacity US Gal./ Imp Gal./ Liters	Approx. Filled Size STD / Metric	Approx. Folded Size STD / Metric	Empty Weight lbs. / kg.	Shipping Weight lbs. / kg.
BT-25V30	25 / 21 / 95	24" x 36" x 8" / .6m x .9m x .2m	14" x 18" x 6" / .4m x .5m x .15m	10 lbs. / 4.5 kg	14 lbs. / 6.4 kg *
BT-50V30	50 / 42 / 189	36" x 52" x 9" / .9m x 1.3m x .2m	15" x 21" x 7" / .4m x .5m x .15m	14 lbs. / 6.4 kg	18 lbs. / 8.2 kg *
BT-75V30	75 / 63 / 284	42" x 54" x 9" / 1m x 1.4m x .2m	20" x 22" x 7" / .5m x .6m x 1.5m	16 lbs. / 7.3 kg	20 lbs. / 9 kg *
BT-100V30	100 / 83 / 376	48" x 66" x 9" / 1.2m x 1.7m x .2m	22" x 25" x 7" / .6m x .6m x 1.5m	19 lbs. / 8.6 kg	23 lbs. / 10.4 kg *
BT-150V30	150 / 125 / 568	60" x 60" x 12" / 1.5m x 1.5m x .3m	22" x 26" x 8" / .6m x .7m x .2m	22 lbs. / 10 kg	26 lbs. / 11.8 kg *
BT-250V30	250 / 208 / 946	60" x 84" x 14" / 1.5m x 2.1m x .4m	22" x 32" x 8" / .6m x .8m x .2m	27 lbs. / 12.3 kg	31 lbs. / 14 kg *
BT-500V30	500 / 416 / 1892	84" x 108" x 16" / 2.1m x 2.7m x .4m	25" x 32" x 9" / .6m x .8m x .2m	33 lbs. / 15 kg	37 lbs. / 16.8 kg *
BT-750V30	750 / 625 / 2839	99" x 114" x 16" / 2.5m x 2.9m x .4m	25" x 35" x 9" / .6m x .9m x .2m	49 lbs. / 22.2 kg	53 lbs. / 24 kg *
BT-1000V30	1000 / 833 / 3785	9' x 11' x 16" / 2.7m x 3.4m x .4m	40" x 48" x 14" / 1m x 1.2m x .4m	60 lbs. / 27.2 kg	95 lbs. / 43 kg
BT-1250V30	1250 / 1041 / 4731	9'6" x 12'4" x 18" / 2.9m x 3.8m x .5m	40" x 48" x 14" / 1m x 1.2m x .4m	68 lbs. / 30.9 kg	103 lbs. / 46.7 kg
BT-1500V30	1500 / 1249 / 5678	10' x 14' x 18" / 3m x 4.3m x .5m	40" x 48" x 15" / 1m x 1.2m x .4m	78 lbs. / 35.4 kg	113 lbs. / 51.3 kg
BT-2000V30	2000 / 1666 / 7570	10'6" x 14'6" x 22" / 3.2m x 4.4m x .6m	40" x 48" x 18" / 1m x 1.2m x .5m	82 lbs. / 37.2 kg	117 lbs. / 53 kg
BT-2500V30	2500 / 2082 / 9463	12' x 14'6" x 24" / 3.7m x 4.4m x .6m	40" x 48" x 18" / 1m x 1.2m x .5m	91 lbs. / 41.3 kg	126 lbs. / 3.2 kg
BT-3000V30	3000 / 2498 / 11355	13'6" x 15' x 24" / 4.1m x 4.6m x .6m	40" x 48" x 22" / 1m x 1.2m x .6m	105 lbs. / 47.6 kg	140 lbs. / 63.5 kg
BT-4000V30	4000 / 3330 / 15140	14' x 18' x 27" / 4.3m x 5.5m x .7m	40" x 48" x 24" / 1m x 1.2m x .6m	128 lbs. / 58.1 kg	162 lbs. / 73.5 kg
BT-5000V30	5000 / 4164 / 18925	15'6" x 19'6" x 27" / 4.7m x 5.9m x .7m	40" x 48" x 26" / 1m x 1.2m x .7m	159 lbs. / 72.1 kg	194 lbs. / 88 kg
BT-6000XR30	6000 / 4996 / 22710	16'6" x 20' x 30" / 5m x 6m x .8m	40" x 48" x 28" / 1m x 1.2m x .7m	197 lbs. / 89.4 kg	232 lbs. / 105.2 kg
BT-10000XR30	10000 / 8327 / 37850	20' x 24' x 36" / 6m x 7.3m x .9m	40" x 48" x 30" / 1m x 1.2m x .8m	284 lbs. / 128.8 kg	324 lbs. / 147 kg
BT-20000U40	20000 / 16654 / 75700	22' x 31' x 48" / 6.7m x 9.5m x 1.2m	42" x 48" x 48" / 1.1m x 1.2m x 1.2m	551 lbs. / 250 kg	626 lbs. / 284 kg
BT50000U40	50000 / 41635 / 189250	30' x 46' x 60" / 9.1m x 14m x 1.5m	48" x 72" x 56" / 1.2m x 1.8m x 1.4m	1017 lbs. / 461 kg	1092 lbs. / 495 kg

PATENT COOPERATION TREATY

From the RECEIVING OFFICE

PCT

To:
PAUL MURTY
SMITH & HOPEN, P.A.
180 PINE AVE, NORTH
OLDSMAR, FLORIDA 34677

Confirmation No: 6858

NOTIFICATION OF THE INTERNATIONAL APPLICATION NUMBER AND OF THE INTERNATIONAL FILING DATE

(PCT Rule 20.2(c))

Date of mailing (day/month/year)	06 Sep 2018
Applicant's or agent's file reference: 2908-37-PRWO	IMPORTANT NOTIFICATION

International application No.	International filing date (day/month/year)	Priority date (day/month/year)
PCT/US2018/000147	15 Aug 2018	15 Aug 2017

Applicant
UNIVERSITY OF NORTH FLORIDA BOARD OF TRUSTEES

Title of the invention
INTEGRATED SYSTEM FOR OPTIMAL EXTRACTION OF HEAD-DRIVEN TIDAL ENERGY WITH MINIMAL OR NO ADVERSE

1. The applicant is hereby notified that the international application has been accorded the international application number and the international filing date indicated above.

2. The applicant is further notified that the record copy of the international application:

☒ was transmitted to the International Bureau on 06 Sep 2018

☐ has not yet been transmitted to the International Bureau for the reason indicated below and a copy of this notification has been sent to the International Bureau*:

☐ because the necessary national security clearance has not yet been obtained.

☐ because (reason to be specified):

* The International Bureau monitors the transmittal of the record copy by the receiving Office and will notify the applicant (with Form PCT/IB/301) of its receipt. Should the record copy not have been received by the expiration of 14 months from the priority date, the International Bureau will notify the applicant (Rule 22.1(c)).

3. FOREIGN TRANSMITTAL LICENSE INFORMATION Completed by: VM

☐ Additional license for foreign transmittal not required. This subject matter is covered by a license already granted or the equivalent U.S. national application. Refer to that license for information concerning its scope.

☐ License for foreign transmittal not required. 37 CFR 5.11(e)(1) or 37 CFR 5.11(e)(2). However, a license may be required for additional subject matter. See 37 CFR 5.15(b).

☒ Foreign transmittal license granted. 35 U.S.C. 184; 37 CFR 5.11 on 05 Sep 2018 (date)

☐ 37 CFR 5.15(a) ☒ 37 CFR 5.15(b)

Name and mailing address of the receiving Office	Authorized officer
Mail Stop PCT, Commissioner for Patents P.O. Box 1450, Alexandria, VA 22313-1450	Vanessa Moore
Facsimile No. 571-273-8300	Telephone No. 571-272-0445

Form PCT/RO/105 (July 2008)

Appendix 21: Notification of the international application number and of the international filing date

MICHELLE A. VIEIRA

| Jacksonville, FL

PROFESSIONAL SUMMARY

Passionate and innovative engineer with an eagerness to learn and adaptability to new environments. Interdisciplinary education in mechanical engineering and coastal engineering, with a focus on renewable energy systems and interest in coastal resilience planning and ecology. Exhibited internal motivation with the initiative to follow through on projects with proven time management capabilities. Over ten years of experience demonstrating leadership capabilities, working collaboratively to tackle complex problems, and reaching for creative solutions.

PROFESSIONAL EXPERIENCE

Graduate Research Assistant, Taylor Engineering Research Institute……..*Spring 2017-Present*

-Hand selected by Dr. Don Resio, the director of TERI, to conduct innovative renewable tidal energy research.

-Simulation and numerical modeling of proposed tidal system using FORTRAN and MATLAB.

-Field data collection of small and intermediate scale physical models.

-Technical writing in the form of submission of provisional, utility, and international patents for the proposed tidal system.

-Collaborative work to establish system design and testing procedure and implementation.

Engineering Intern, Neptune Fire Protection Engineering…… …August *2018-Present*

-Preparation of fire engineering plan drawings in AutoCAD.

-Attending site visits with senior engineers to assess the project requirements and work with clients to determine project goals.

-Establish project requirement from scope of work to assist in writing and drafting final reports for over 15 projects.

-Creating and editing calculation tools in EXCEL to increase areas of use and efficiency.

Owner, Operator, Restoration Projects……..….*May 2010-January 2017*

-Through an established connection with local nonprofits with global reach was able to provide hundreds of meals and days of
clean water to children in Uganda.

-Grew business from start up into online distribution and over 10 retail distributors.

-Created marketing strategies that ranged from grass roots person to person contact to social media platforms.

-Responsible for budgeting, financial planning, and daily bookkeeping.

Manager, Black Creek Outfitters……*October 2005-April 2015*

-Coordinated, trained, and assisted in hiring a staff of over 30 employees.

-Served as a liaison between outfitter and local environmental nonprofits with a goal of increasing public awareness and
fundraising.

-Planned and coordinated in-store and off-site events, community education, and environmental outreach events.

-Executed annual planning, budgeting, and design for marketing. Decreased marketing budget by 25%.

Lift Operator & Mechanic / Breckenridge Ski Resort……..*November 2004-August 2005*

-Engaged customers at ski lift points and assured proper and safe entrance and exit onto lift and mountain.

-Apprenticed under senior mechanics on lift maintenance and trouble shooting.

Engineering Intern Johnson & Johnson Vision Care / Vistakon……...*Summer 2002*

-Researched production line weaknesses to create a plan of action to design a more efficient process.

-Conducted economic losses calculations to determine the value of addressing each point of production line weakness.

-Interacted with production line technicians to understand their role in establishing a more efficient line.

ACADEMIC INFORMATION

Master of Science in Coastal and Port Engineering, University of North Florida……..….*December 2018*

-Focus of interdisciplinary research that incorporates a holistic perspective on the interaction of ecology, biology, and coastal engineering.

-Worked alongside Dr. Don Resio, the director of the Coastal Engineering program, to design, test and patent an innovative tidal energy system.

-Collaborated with a team awarded a $15,000 grant from the UNF Office of Research and Sponsored Programs for our work on both a tidal and wave energy system.

Certificate of Architectural Restoration of Historical Heritage, University of Perugia, Italy….*Summer 2018*

-Received technical training on restoration techniques applicable to historical buildings in order to preserve its integrity.

-Hands on restoration of a 1,000-year-old castle that utilized state of the art techniques for wall stabilization.

Bachelor of Science in Mechanical Engineering, University of North Florida……..*May 2003*

-Graduated with Summa Cum Laude honors.

-Senior design project focused on clean and renewable energies with a specific concentration on photovoltaic cells.

-Co-led engineering summer camps for local elementary aged students to introduce them to the basic concepts of engineering and encourage them to pursue STEM fields.

ADDITIONAL INFORMATION

Skills

-Experience with data analysis tools: MATLAB, FORTRAN, Python, and R studio.

-American Heart Association Heartsaver First Aid CPR AED Certified, Child DPR AED, and Infant CPR

One Spark Crowd Sourcing Festival Presenter

Selected as a technology presenter for the 2018 One Spark Festival to showcase my master's thesis work on a proposed tidal energy system.

Student Affairs International Learning Scholarship

Selected as a recipient of the Student Affairs International Learning Scholarship from the University of North Florida for a study abroad course focused on the restoration of historic structures in Italy.

Society of Women Engineers Scholarship

Selected out of over 1800 applicants to receive the 2017 Olive Lynn Salembier Memorial Reentry scholarship that is awarded to individuals that have demonstrated outstanding academic achievement as well as strong engineering potential.

Poster Presenter for The American Shore and Beach Preservation Association

-Accepted as a poster presenter at the ASBPA 2018 Resilience Shore Lines for Rising Tides National Coastal Conference

Volunteering

-Field research for the Guana Tolomato Matanzas National Estuarine Research Reserve conducting water sampling for their
Site Wide System Monitoring program.

-Set up and technical writing for the University of North Florida Fluid Dynamics Laboratory.

-Mentor and leader to middle, high, and college aged students for Young Life, with over 15 years of leadership experience in groups reaching over 100 participants.

-Served on the Greenspace and Health and Wellness committees at Seaside Community Charter School.

-Led multiple group trips abroad that collaborated with local humanitarian relief efforts established in country.

Professional Affiliations

-Society of Women Engineers, Southeastern Estuarine Research Society, Coastal Ocean and Ports Research Institute, American
Society of Civil Engineers, United States Society of Dams.

Personal Interests

-Sustainability and resilience planning, ocean and beach clean ups, renewable energy and energy policy, climate science, surfing, long distance running, and the outdoors.